



National Library  
of Canada

Bibliothèque nationale  
du Canada

Canadian Theses Service

Services des thèses canadiennes

Ottawa, Canada  
K1A 0N4

## CANADIAN THESES

## THÈSES CANADIENNES

### NOTICE

The quality of this microfiche is heavily dependent upon the quality of the original thesis submitted for microfilming. Every effort has been made to ensure the highest quality of reproduction possible.

If pages are missing, contact the university which granted the degree.

Some pages may have indistinct print especially if the original pages were typed with a poor typewriter ribbon or if the university sent us an inferior photocopy.

Previously copyrighted materials (journal articles, published tests, etc.) are not filmed.

Reproduction in full or in part of this film is governed by the Canadian Copyright Act, R.S.C. 1970, c. C-30. Please read the authorization forms which accompany this thesis.

**THIS DISSERTATION  
HAS BEEN MICROFILMED  
EXACTLY AS RECEIVED**

### AVIS

La qualité de cette microfiche dépend grandement de la qualité de la thèse soumise au microfilmage. Nous avons tout fait pour assurer une qualité supérieure de reproduction.

S'il manque des pages, veuillez communiquer avec l'université qui a conféré le grade.

La qualité d'impression de certaines pages peut laisser à désirer, surtout si les pages originales ont été dactylographiées à l'aide d'un ruban usé ou si l'université nous a fait parvenir une photocopie de qualité inférieure.

Les documents qui font déjà l'objet d'un droit d'auteur (articles de revue, examens publiés, etc.) ne sont pas microfilmés.

La reproduction, même partielle, de ce microfilm est soumise à la Loi canadienne sur le droit d'auteur, SRC 1970, c. C-30. Veuillez prendre connaissance des formules d'autorisation qui accompagnent cette thèse.

**LA THÈSE A ÉTÉ  
MICROFILMÉE TELLE QUE  
NOUS L'AVONS REÇUE**



National Library of Canada

Bibliothèque nationale du Canada

0-315-24849-1

Canadian Theses Division

Division des thèses canadiennes

Ottawa, Canada  
K1A 0N4

### PERMISSION TO MICROFILM — AUTORISATION DE MICROFILMER

• Please print or type — Écrire en lettres moulées ou dactylographier

Full Name of Author — Nom complet de l'auteur

ANDREA OLGA WAYWANKO

Date of Birth — Date de naissance

AUGUST 14 / 1951

Country of Birth — Lieu de naissance

CANADA

Permanent Address — Résidence fixe

10335 - 140 ST,  
Edmonton, Alta.  
T5N 2L7

Title of Thesis — Titre de la thèse

Sedimentology and Geophysical Well Log Analysis  
of the Clearwater Formation (Lower Cretaceous),  
Cold Lake, Alberta.

University — Université

UNIVERSITY OF ALBERTA

Degree for which thesis was presented — Grade pour lequel cette thèse fut présentée

MASTER OF SCIENCE

Year this degree conferred — Année d'obtention de ce grade

1984

Name of Supervisor — Nom du directeur de thèse

FRANCES J. HEIN

Permission is hereby granted to the NATIONAL LIBRARY OF CANADA to microfilm this thesis and to lend or sell copies of the film.

The author reserves other publication rights, and neither the thesis nor extensive extracts from it may be printed or otherwise reproduced without the author's written permission.

L'autorisation est, par la présente, accordée à la BIBLIOTHÈQUE NATIONALE DU CANADA de microfilmer cette thèse et de prêter ou de vendre des exemplaires du film.

L'auteur se réserve les autres droits de publication; ni la thèse ni de longs extraits de celle-ci ne doivent être imprimés ou autrement reproduits sans l'autorisation écrite de l'auteur.

Date

OCTOBER 15 / 84

Signature

THE UNIVERSITY OF ALBERTA

Sedimentology and Geophysical Well Log Analysis of the Clearwater Formation (Lower  
Cretaceous), Cold Lake, Alberta

by

Andréa O. Waywanko

A THESIS

SUBMITTED TO THE FACULTY OF GRADUATE STUDIES AND RESEARCH  
IN PARTIAL FULFILMENT OF THE REQUIREMENTS FOR THE DEGREE  
OF Master of Science

Department of Geology

EDMONTON, ALBERTA

© Fall, 1984

THE UNIVERSITY OF ALBERTA

RELEASE FORM

NAME OF AUTHOR Andrea O. Wawanko  
TITLE OF THESIS Sedimentology and Geophysical Well Log Analysis of the  
Clearwater Formation (Lower Cretaceous), Cold Lake, Alberta  
DEGREE FOR WHICH THESIS WAS PRESENTED Master of Science  
YEAR THIS DEGREE GRANTED Fall, 1984

Permission is hereby granted to THE UNIVERSITY OF ALBERTA LIBRARY to reproduce single copies of this thesis and to lend or sell such copies for private, scholarly or scientific research purposes only.

The author reserves other publication rights, and neither the thesis nor extensive extracts from it may be printed or otherwise reproduced without the author's written permission.

(SIGNED)

*A. Wawanko*

PERMANENT ADDRESS:

*10335-14051*

*Edmonton, Alberta*

*TSN 247*

DATED *October 14* 19 *84*

THE UNIVERSITY OF ALBERTA  
FACULTY OF GRADUATE STUDIES AND RESEARCH

The undersigned certify that they have read, and recommend to the Faculty of Graduate Studies and Research, for acceptance, a thesis entitled Sedimentology and Geophysical Well Log Analysis of the Clearwater Formation (Lower Cretaceous), Cold Lake, Alberta submitted by Andrea O. Waywanko in partial fulfilment of the requirements for the degree of Master of Science.

.....  
Francis J. Hein

Supervisor

.....  
N. W. Rutter

.....  
W. J. G. Spence

.....  
J. F. Hillier

.....  
D. J. Krystoffel FOR

N.W. RUTTER

Date... October 14, 1984 .....

## Abstract

The Clearwater Formation in the Cold Lake oil sands area of east-central Alberta contains the most continuous reserves with the highest hydrocarbon saturation in the Cold Lake oil sands area of east-central Alberta. The Clearwater Formation in the detailed study area, located at the site of the British Petroleum Pilot Plant (Township 6 Range 5W4), has an average thickness of 40 m (120 ft) and is overlain by approximately 430 m (1400 ft) of overburden.

The Clearwater Formation can be informally divided into ten stratigraphic units. Six facies associations have been recognized in the interbedded stratigraphic units: heavily bioturbated silty shale; heavily bioturbated silty shale to silt and sand; moderately to heavily bioturbated sand with silt and silty shale; sand, silt and silty shale; graded sand, silt and shale with Bouma sequences; and sand and carbonaceous sand. Two coarsening-upward sequences are present in the Clearwater Formation. The facies associations represent offshore and nearshore sedimentation in a shallow epeiric sea which received detritus from a source situated to the southeast of the study area. Poorly developed very fine-grained sand bars and ridges were constructed on top of a muddy shelf and are the best potential reservoirs in this area.

The very fine-grained sands are feldspathic litharenites to litharenites. The sediments consist of a complex suite of minerals, including quartz, chert, feldspar, igneous rock fragments, metamorphic rock fragments, sedimentary rock fragments, volcanic rock fragments, clastic carbonates and glauconite. A dual provenance from the Cordillera to the west and the Shield area to the northeast is indicated. The clay mineralogy is also complex and consists of varying amounts of kaolinite, illite and smectite with minor chlorite.

The study of the relationship between geophysical well logs and core data indicates that correlation of these parameters is difficult. The corrected sonic porosity is the best indicator of total porosity and correlates best with the core porosity which also detects total porosity. The core and sonic porosity values are overly-optimistic because clay-bound water is detected as porosity.

A shaly sand cross-plot of corrected bulk density versus sandstone neutron porosity gives the most realistic values for volume of shale and effective porosity. In the

least shaly sands, effective porosity is approximately 12 porosity units lower than the porosity indicated by core analysis. The cleanest sands contain 25 percent shale in dispersed, structural and laminated forms. Effective porosity is as high as 31 percent. Only a small portion of stratigraphic unit F is producible in well 10-17-6-14.

## Acknowledgements

The writer wishes to express her gratitude to the Late Dr. Hans Steiner for his support as thesis supervisor during the early stages of this project. Sincere thanks are also expressed to Dr. Fran Hein for her support as thesis supervisor in the completion and critical reading of the thesis. Thanks are also expressed to Mr. Frank Bosworth for his invaluable advice on, and critical reading of, the section on geophysical well log analysis. Dr. Grant Mossop, Dr. John Kramers, Dr. Daryl Wightman, Brian Rottenfusser and Dr. Donald Scafe of the Alberta Geological Survey are thanked for their advice at various stages of the project. Gratitude is also expressed to Dr. Chaitanya Singh for his interpretation of the micropaleontologic samples and Dr. George Pemberton for his aid in the identification of trace fossils.

Funding is gratefully acknowledged from British Petroleum Exploration Canada Limited, the Alberta Oil Sands Technology and Research Authority and the Petroleum Aid to Education Fund. The writer also expresses her thanks to the staff of British Petroleum Exploration Canada Limited for their technical advice and access to confidential information.

I would like to express my gratitude to the many people at the Alberta Geological Survey who provided technical support. Thin sectioning and grain size analysis were performed by Max Baaske, Tim Beresniuk, Campbell Kidston and Lavorka Swenson. Susan Putz performed the X-ray diffraction analysis and Bruno Untergasser processed the micropaleontologic samples.

I would also like to express my deep appreciation for the support given by my companion, Gregory and the co-operation given by Meghan and Damien.



## Table of Contents

Chapter	Page
I. Introduction .....	1
A. Purposes of Study .....	1
B. Location and Geological Setting of Study Area .....	2
C. Methods of Investigation .....	2
Geophysical Well Log Analysis .....	5
Laboratory Analyses .....	7
II. Stratigraphy .....	9
A. Previous Work .....	9
B. Correlations derived from the Present Study .....	11
III. Sedimentology .....	14
A. Previous Work .....	14
Provenance and Tectonic Framework .....	16
B. Introduction to Sedimentology .....	17
Definition of Facies Associations .....	17
C. Facies Associations .....	19
Facies Association 1. Heavily Bioturbated Silty Shale .....	19
Facies Association 2. Heavily Bioturbated Silty Shale to Silt and Sand .....	19
Facies Association 3. Moderately to Heavily Bioturbated Sand with Silt and Silty Shale .....	23
Facies Association 4. Sand, Silt and Silty Shale .....	24
Facies Association 5: Graded Sand, Silt and Shale with Bouma Sequences .....	25
Facies Association 6. Sand and Carbonaceous Sand .....	26
D. Stratigraphic Units .....	26
E. Micropaleontology .....	30
F. Sedimentary Textures .....	32
G. Isopach and Structural Mapping .....	37
Structural Maps .....	37
Isopach Maps .....	39
H. Facies Association Interpretation .....	47
Introduction .....	47

Coarsening-upward Sequence: Stratigraphic Units J to F .....	53
Coarsening-upward Sequence: Stratigraphic Units E to B .....	58
Summary .....	62
IV. Mineralogy .....	63
A. Bulk Mineralogy .....	63
Quartz .....	66
Chert .....	66
Feldspar .....	66
Rock Fragments .....	67
Glauconite .....	68
Calcareous Cement .....	69
Organic Debris .....	69
Accessories .....	70
B. Clay Mineralogy .....	70
Sand Samples .....	72
Argillaceous Sand Samples .....	72
Mixed Sand and Clay Samples .....	73
Shale Samples .....	73
V. Geophysical Well Log Response in Shaly Sands .....	74
A. Previous Work .....	74
B. Introduction to Geophysical Well Log Study .....	75
Function of Well Logging Tools .....	76
The Effects of Clays on Geophysical Well Log Response .....	80
Summary .....	82
C. Shaly Sand Plots .....	82
Sources of Error in the Determination of Core-derived Parameters .....	83
M-N Plot .....	84
Corrected Sonic Porosity versus Neutron Porosity .....	84
Shaliness Indicators .....	86
Relationships between Log- and Core-derived Parameters .....	95
VI. Conclusions .....	103

A. Sedimentologic Implications ..... 103

B. Geophysical Well Logging Implications ..... 104

Bibliography ..... 121

Appendices ..... 133

### List of Tables

Table	Page
1. Sedimentary Types .....	18
2. Partial analogues used in facies association interpretation .....	51
3. Comparative Mineralogy .....	64
4. Relative percentages of clay minerals by X-ray diffraction .....	71

## List of Figures

Figure	Page
1. Location of study area .....	3
2. Location of detailed study: structural cross-sections indicated by lines A—B and A—C .....	4
3. Location of oil sands, shale and micropaleontologic samples from well 10-17-66-5W4 .....	6
4. Stratigraphic correlation chart .....	12
5. Legend for structural cross-sections .....	20
6. Northwest-southeast structural cross-section, showing the distribution of facies associations, stratigraphic units and micropaleontologic results .....	21
7. North-south structural cross-section, showing the distribution of facies associations, stratigraphic units and micropaleontologic results .....	22
8. Standard deviation (sorting) versus mean grain size, showing relationship of facies to grain size parameters .....	33
9. Representative grain size histogram for sand samples .....	34
10. Representative grain size histogram for argillaceous sand samples .....	35
11. Representative grain size histogram for mixed sand and clay samples .....	36
12. Regional well control for structural and isopach maps .....	38
13. Structural map of pre-Cretaceous unconformity .....	38
14. Stratigraphic unit F structural map .....	40
15. Stratigraphic unit J isopach map .....	40
16. Stratigraphic unit I isopach map .....	41
17. Stratigraphic unit H isopach map .....	41
18. Stratigraphic unit G isopach map .....	43
19. Stratigraphic unit F isopach map .....	43
20. Stratigraphic subunit F <sub>2</sub> isopach map .....	44
21. Stratigraphic subunit F <sub>2</sub> sand / shale ratio map .....	44
22. Stratigraphic unit D isopach map .....	46
23. Stratigraphic unit C isopach map .....	46
24. Stratigraphic unit B isopach map .....	48
25. Stratigraphic unit A isopach map .....	48

Figure	Page
26. Local summary sequence of sedimentary facies associations, showing two coarsening-upward sequences .....	49
27. Ternary plot of point-counted thin sections from well 10-17-66-5W4, showing classification of sands as feldspathic litharenites and litharenites .....	65
28. Selected geophysical well logs for well 10-17-66-5W4 .....	77
29. M versus N lithoplot, showing the effect of shale on the lithology of Clearwater sediments .....	85
30. Corrected sonic porosity versus neutron porosity, showing the difference in the response of the acoustic and neutron tools .....	85
31. Corrected bulk density versus neutron porosity, showing the construction of the shaly sand plot .....	87
32. Detail of shaly sand plot, showing relationship of points to volume of shale and effective porosity .....	87
33. Effect of various minerals on the corrected bulk density versus neutron (CNL) porosity plot .....	89
34. Volume of shale versus effective porosity, showing good inverse relationship .....	91
35. Sandstone density porosity versus effective porosity, showing good direct relationship .....	91
36. Density porosity versus neutron porosity, illustrating the construction of the shaly sand plot .....	93
37. Detail of shaly sand plot, showing relationship of points to volume of shale and effective porosity .....	93
38. Gamma ray index versus volume of shale, showing consistently larger percentage of shale indicated by gamma ray index .....	94
39. Bulk volume clay fraction versus volume of shale, illustrating a good direct relationship .....	94
40. Volume of dispersed shale versus volume of shale, illustrating a direct relationship and the presence of laminar and structural shales .....	96
41. Calculated effective porosity versus effective porosity, illustrating discrepancies .....	96
42. Volume of dispersed shale versus effective porosity, showing decrease in porosity with increase in dispersed shales .....	98
43. Core porosity versus density porosity, illustrating poor relationship between log- and core derived porosities .....	98
44. Core porosity versus corrected sonic porosity, illustrating a good relationship between log- and core-derived parameters .....	100

Figure	Page
45. Core porosity versus effective porosity, illustrating discrepancies .....	100
46. Effective porosity versus bulk volume water, showing a poor relationship and reflecting an increased amount of bound water in shalier sands .....	102

## List of Plates

Plate	Page
Core photographs for stratigraphic units J to H .....	108
2. Core photographs for stratigraphic units G to E .....	110
3. Core photographs for stratigraphic units D to B .....	112
4. Mineralogy .....	114
5. Mineralogy .....	116
6. Mineralogy and Textures .....	118
7. Mineralogy .....	120



## I. Introduction

Due to their economic potential, the oil sands and heavy oil deposits of Alberta and western Saskatchewan have received increased attention over the past decade.

Until recently, most studies have concentrated on the Athabasca oil sands deposit because a small part of it can be mined using surface mining methods and the oil can be extracted using proven techniques. However, the oil in the vast majority of the Athabasca deposit and in all other oil sands deposits is found under hundreds of metres of overburden and must be extracted using in situ methods.

In the case of the present study of the Clearwater Formation in the Cold Lake oil sands deposit, in situ extraction requires the use of subsurface techniques based on the study of core and the interpretation of geophysical well logs. With the exception of a mineralogic study by Putnam and Pedskalny (1983), no detailed mineralogic study has been carried out on the Cold Lake Clearwater Formation deposit. To date, there has been no detailed work done on the relationship of lithology and mineralogy to geophysical well log response.

An insight into Clearwater Formation sedimentology and petrology is needed in order to satisfactorily deal with a one-dimensional subsurface view of the deposit. The vertically, and to a lesser extent laterally, discontinuous reservoir sands, as well as the complex mineralogy, reflect intricate facies associations which must be understood so that oil extraction techniques can be optimally designed and applied.

### A. Purposes of Study

One purpose of this study is to define the facies associations in the Clearwater Formation by conducting a site-specific analysis of the deposit. From the lateral and vertical relationships of facies associations, an environmental reconstruction can be made. The patterns discerned from the examination of lithologies and the geophysical well log response will then be applied on a regional scale. Comparisons with sedimentary models can be applied to the deposit.

The second purpose of this study is to define the relationship between geophysical log response and the lithology of the shaly sand of the Clearwater Formation. In cases where the Clearwater Formation has been cored, lithologic analysis is relatively simple.

However, when wells are not cored or core is missing, one must rely only on geophysical logs; and, the analysis is much more complex.

The geophysical well logging tools respond to the bound water in hydrous phyllosilicates, such as clays, mica and glauconite, as effective porosity. This results in anomalously high porosity readings. In order to minimize the need for logging core, predictive modelling for the Clearwater Formation in this area is imperative.

### **B. Location and Geological Setting of Study Area**

The Cold Lake oil sands area in east-central Alberta is located from Townships 52 to 70, Ranges 1 to 10 west of the 4th meridian (Figure 1). It contains heavy oil reservoirs in all formations of the Lower Cretaceous Mannville Group. In the northern part of the deposit, the best, most laterally continuous reservoir is found in the Clearwater Formation.

The site of the present study is the British Petroleum Marguerite Lake Pilot Plant area and vicinity, located in Township 66, Range 5W4M (Figure 2). The Clearwater Formation here has an average thickness of 40 m (120 ft) and is overlain by approximately 430 m (1400 ft) of overburden. Five non-confidential wells with useable core are located in this area: 6-3-66-5W4, 6-5-66-5W4, 10-7-66-5W4, 10-17-66-5W4, and 2-19-66-5W4. The core from these wells was examined, sampled and photographed at the Energy Resources Conservation Board Core Laboratory located in Calgary, Alberta.

### **C. Methods of Investigation**

Each core was examined bed-by-bed in conjunction with an analysis of the geophysical logs. The parameters described were lithology, texture, sedimentary structures and macrofossil content. A photographic record was made of each core.

This formed the sedimentologic basis for stratigraphic correlations and facies association analysis. Stratigraphic units and facies associations were defined and correlated between these wells. Then a regional study of these facies associations in 54 wells was undertaken on the basis of well log evaluation. Isopach and structural maps were generated for the various stratigraphic units and the underlying pre-Cretaceous unconformity to discern regional trends in a ten township area.

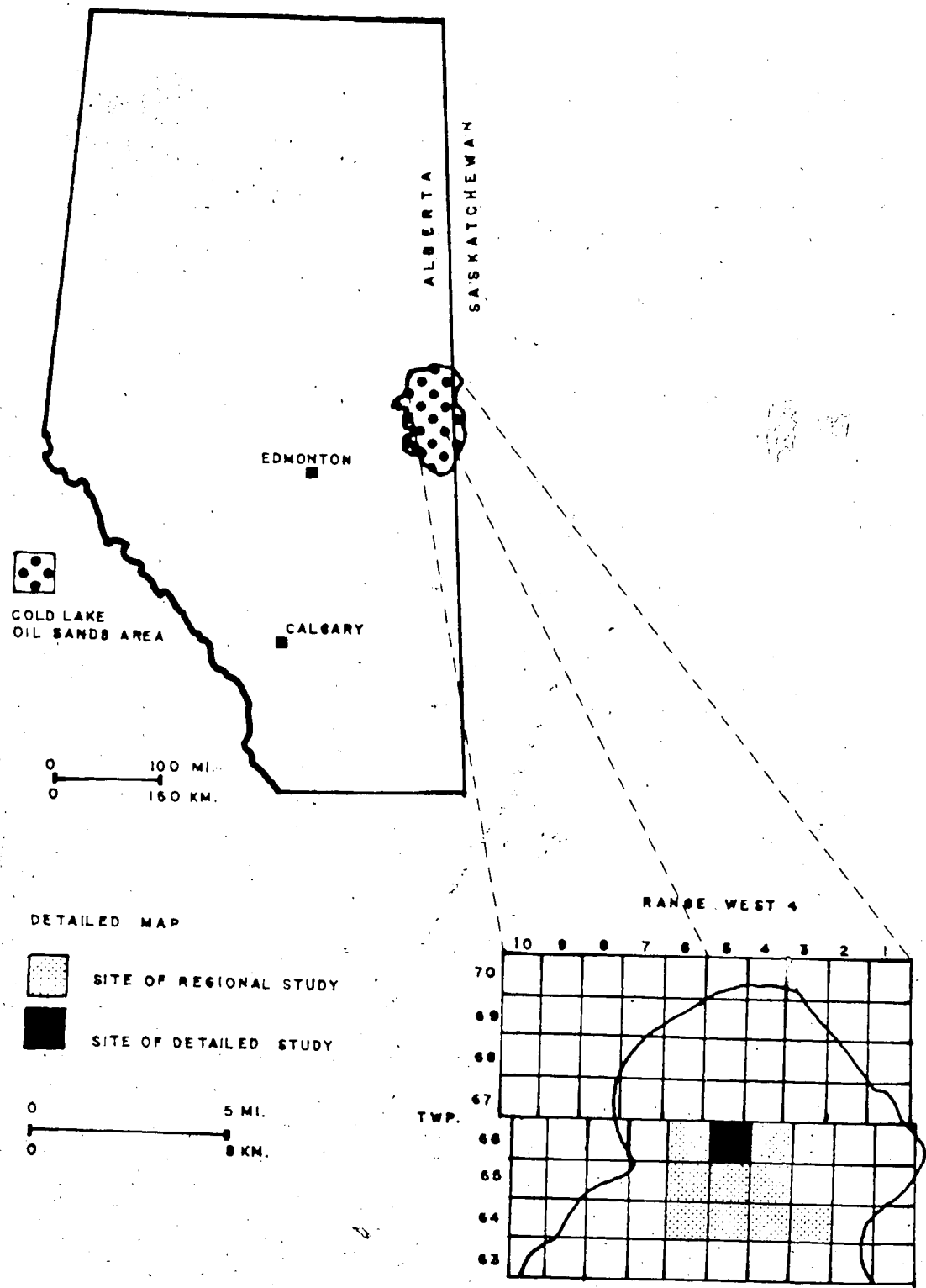


FIGURE 1. Location of study area.

TWP. 66, RGE. 5W4M.

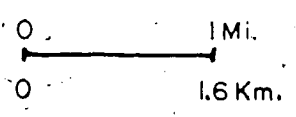
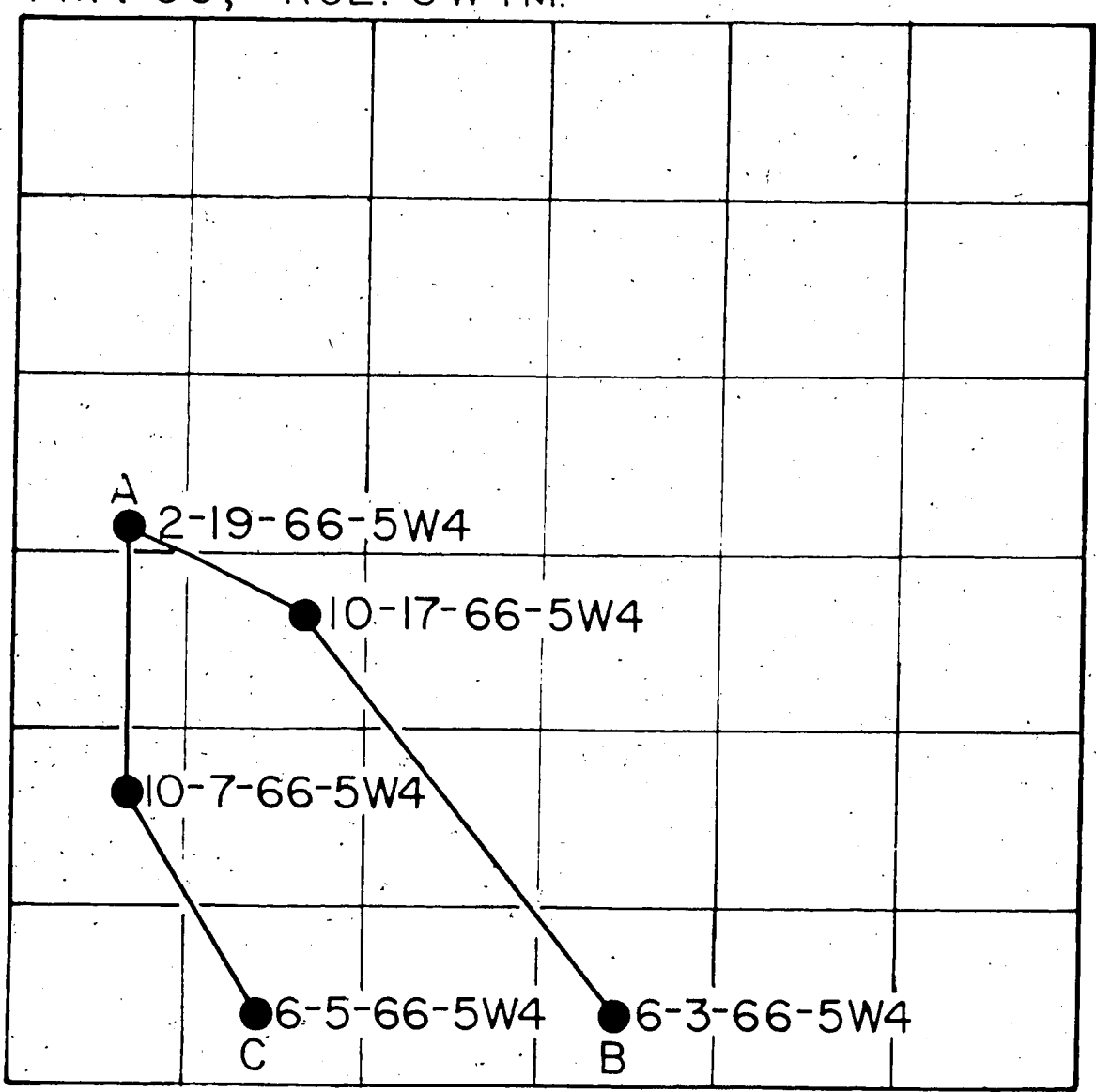


FIGURE 2. Location of detailed study: structural cross-sections indicated by lines A-B and A-C.

After the initial examination, one well (10-17-66-5W4) was chosen for detailed study. Factors such as completeness of core, presence of representative lithologies, good geophysical log control and location near the centre of the B.P. pilot plant area were used in choosing this core.

A total of 43 lithologic samples of 10-17-66-5W4 core were taken. The location of samples is given in Figure 3. At least one lithologic sample was taken at the top, bottom, and within each major lithology. Maximum spacing of samples was 2.5 m (8 ft), with an average spacing over the entire length of the core of 0.85 m (2.8 ft). Where sand beds were separated by thin silt and shale partings, separate samples were taken for oil sands and micropaleontologic analysis.

#### Geophysical Well Log Analysis

All wells were studied in conjunction with an examination of geophysical well logs.

Logs available for each well are as follows:

- 6-3-66-5W4: Dual Induction Laterolog  
Compensated Neutron Formation Density
- 6-5-66-5W4: Induction Electrical Log  
Compensated Neutron Formation Density
- 10-7-66-5W4: Dual Induction Laterolog  
Compensated Neutron Formation Density  
Borehole Compensated Sonic Log
- 10-17-66-5W4: Dual Induction Laterolog  
Compensated Neutron Formation Density  
Borehole Compensated Sonic Log
- 2-19-66-5W4: Induction Electrical Log  
Compensated Neutron Formation Density

The geophysical logs were correlated with the core and were used to detect core that had expanded after the release of overburden pressure. In the detailed study of well

10-17-66-5W4, all logs were digitized using a Tektronix graphic terminal. However, the digitizing procedure gave readings that were up to 0.5 m (1.5 ft) away from the actual depth indicated by the geophysical well log. These inaccuracies were a result of limitations of scale on the Tektronix graphic terminal and variations in the geophysical well logs.

Readings were made every six inches and at every sample point manually. The data were analyzed using shaly sand cross-plotting techniques with the scattergram computer program developed by Nie *et al* (1975). The geophysical well log parameters were then

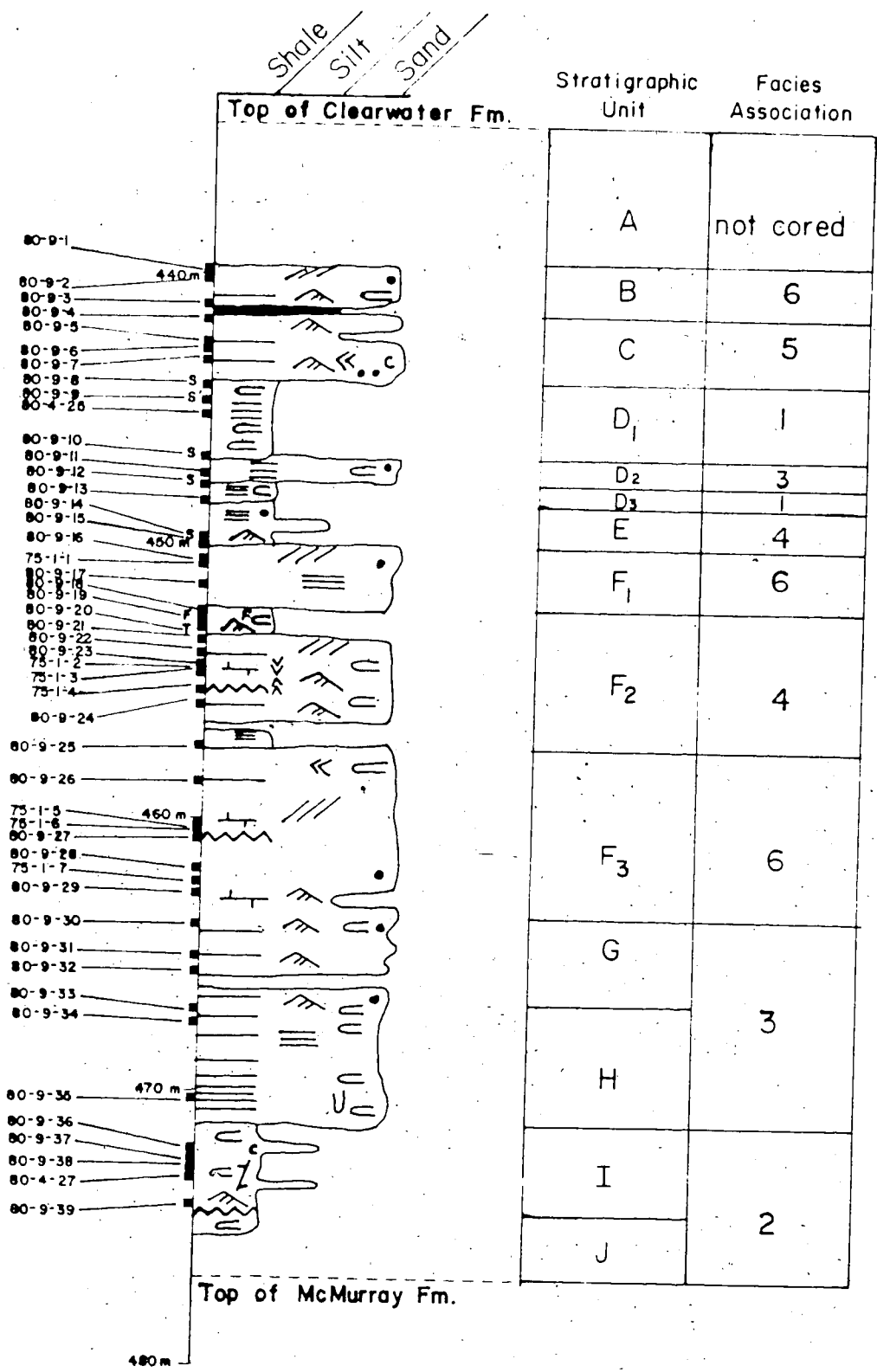


FIGURE 3. Location of oil sands, shale (S), trace fossil (T) and macropaleontologic (F) samples.

related to core analysis parameters.

### Laboratory Analyses

Thirty-four of the 43 samples taken from well 10-17-66-5W4 core were submitted for oil sands analysis. The analysis consisted of a calculation of weight percentages of oil and water saturation by the use of the Dean-Stark separation technique (Kidston, personal communication). The method involves the extraction of the bitumen by refluxing hot toluene, measuring the amount of water extracted through condensation and obtaining the weight percent bitumen by calculating the difference between the weight of the original sample and the dry sample plus water (Eade, 1975). The grain size distribution was studied through both dry and wet sieving. Dry sieving was performed using a series of sieves ranging from -4.0 phi to +11.0 phi, graduated in 0.5 phi intervals. The mean, median, standard deviation (sorting), skewness and kurtosis were determined graphically (Folk, 1968). Histograms and cumulative curves were generated for each sample.

Thirty-four samples were thin-sectioned, impregnated with blue epoxy and stained with sodium cobaltinitrite for the identification of feldspars. Along with seven thin sections on loan from British Petroleum, they formed the basis of a petrographic study of the Clearwater Formation, in which 300 point counts were made of each slide.

X-ray diffraction analyses were conducted on the less than 2 micron smear slides of 36 samples to study clay mineralogy and to obtain relative percentages of clay types.

Fourteen samples, 3 from 6-3-66-5W4, 6 from 10-17-66-5W4 and 5 from 2-19-66-5W4 were submitted for micropaleontologic study by Dr. C. Singh. Dinoflagellate assemblages were studied to discern the geologic age of desposition and to aid in the analysis of paleoenvironmental conditions at the time of Clearwater deposition.

Macropaleontologic identification was made of the one complete shell fragment found and one sample was taken for trace fossil analysis. Other trace fossils were identified through core analysis. In the heavily bioturbated deposits, trace fossil identification was impossible.

A series of parameters were obtained using the equations listed in Appendix III. These parameters were then used in the shaly sand analysis. Cross-plots were used to

examine and demonstrate the complex relationship between petrography, core analysis and geophysical well log response.



## II. Stratigraphy

### A. Previous Work

The "Clearwater shale" was first recognized in the Athabasca area by McConnell (1891) and was later elevated to formational status (McLearn, 1917). The Clearwater Formation was placed in the Lower Cretaceous Group (McLearn, 1918) along with the McMurray and Grand Rapids Formations. Subsequently, the Lower Cretaceous Group was correlated throughout Alberta (McLearn, 1931 and 1932).

The Lower Cretaceous Group in the Vermilion-Wainwright area was divided into six members on the basis of lithology and named the Mannville Formation (Nauss, 1945). In the Lloydminster area, which is in essentially the same geographic location as Vermilion-Wainwright, the Mannville Formation was divided into three units (Wickenden, 1948). The middle unit is roughly correlative with the Clearwater Formation in the Athabasca area and with Nauss's (1945) Cummings, Islay, Tovell and part of the Borradaile Members.

The Mannville Formation was elevated to group status (Badgley, 1952) and correlations were extended into the subsurface (Badgley, 1952; Williams, 1963). A glauconitic sandstone found at the base of the Clearwater Formation was named the Wabiskaw Member of the Clearwater Formation (Badgley, 1952).

The Mannville Group was subdivided into two units (Glaister, 1957 and 1959; Rudkin, 1964). Glaister (1957 and 1959) included the Wabiskaw Member with the upper unit, whereas Rudkin (1964) included it with the lower unit.

The Blairmore Group of western Alberta was correlated with the Mannville Group on the basis of lithology, flora and fauna (Mellon and Wall, 1963). Correlations between the Athabasca and Lloydminster areas were made (Rudkin, 1964) and further stratigraphic work was undertaken by Mellon (1967) who commented on the difficulties in establishing the lower stratigraphic boundary of the Clearwater Formation on the basis of faunal changes.

In the first geologic study of the Cold Lake area, correlations were made between the Cold Lake and Athabasca deposits (Webber, 1967). Correlations between all oil sand and heavy oil deposits were then made (Vigrass, 1968). In the Lloydminster area, tongues

of marine sedimentary rock in the lower Upper Mannville Group were correlated to the Clearwater Formation. In the Cold Lake area, the Mannville Group was divided into informal 'A', 'B', 'C', and 'D' units (Vigrass, 1968) which were correlated approximately with the Upper Grand Rapids, Lower Grand Rapids, Clearwater, and McMurray Formations in the Athabasca area. The 'C' unit top was placed slightly lower than the Clearwater Formation top in Athabasca.

On the basis of three cores in the northeastern part of the Cold Lake area, Vigrass's (1968) informal 'A' and 'B' units were correlated with the Grand Rapids Formation, the 'C' unit with the Clearwater Formation and the 'D' unit with the McMurray Formation (Clack, 1968).

Further refinements of correlation between all oil sand and heavy oil deposits were attempted (Kramers, 1974; Kendall, 1977; Mossop *et al.*, 1981). These latter correlations underline the continuing problems with delimiting the upper and lower boundaries of the Clearwater Formation in the Cold Lake area, which will be discussed further below.

The base of the Mannville Group is marked by an unconformity, while the Mannville Group-Colorado Group contact is considered unconformable (Mossop *et al.*, 1981) or a diastem (Mossop, personal communication).

The contact between the Clearwater Formation and the overlying Grand Rapids Formation has been described as a gradational interfingering facies boundary (Williams, 1963) caused by time transgressive (Mellon and Wall, 1956 and 1963) or diachronous (Mellon, 1967; Mossop *et al.*, 1981) deposition.

The basal Clearwater contact with the underlying McMurray Formation is considered interfingering (Mellon and Wall, 1956; Carrigy, 1963) or gradational (Mellon, 1967). In northeast Alberta the change in the sandstone composition at the top of the McMurray Formation is still evident even though the sediments are faunally and lithologically gradational (Mellon, 1967).

Petrographic criteria for differentiating between the McMurray and Clearwater Formations in the absence of fossils have been recognized (Carrigy, 1963). The Clearwater Formation can be recognized by the presence of glauconite pellets, euhedral biotite flakes, montmorillonite, and euhedral plagioclase grains.

## B. Correlations derived from the Present Study

Correlating the Clearwater Formation in the Cold Lake area is complicated by the fact that this area is transitional between the northeastern Alberta oil sands deposits and the Lloydminster heavy oil deposit. Sedimentation is significantly different in these areas. To the north, the Clearwater Formation is interpreted as an open marine shale, whereas in the south, its equivalent is interpreted as a complex mixture of marine shales, shelf and nearshore deposits, with some continental deposits.

Previous attempts to correlate the Clearwater Formation in the Cold Lake area have adopted the stratigraphic nomenclature of the northeastern deposits (Figure 4). One notable exclusion is that the Wabiskaw Member is not included in the Cold Lake deposit since it cannot be distinguished here.

The main correlation problem in the Clearwater Formation is the placement of the basal and upper shales. Previous studies (Kramers, 1974) placed the upper shale in the Lower Grand Rapids Formation and the basal shale with the McMurray Formation. More recently (Mossop, 1984), the upper shale has been included within the Clearwater Formation.

To be stratigraphically and sedimentologically consistent, both the upper and basal shales should be included within the Clearwater Formation. In both the Athabasca and Wabasca oil sands areas, the McMurray / Clearwater and Clearwater / Lower Grand Rapids correlations are based on, in part, a lithologic change from the shale of the Clearwater Formation to the sands of the other two formations. In addition, there is no basis to exclude these shales from the Clearwater Formation in Cold Lake with respect to correlation with the Lloydminster area. The only micropaleontologic sample taken from the basal shale in the present study was poorly preserved, but was assigned on the basis of its dinoflagellate assemblage to the early Albian Age. Taking into account Mellon's (1967) comments on the difficulty of defining the base of the Clearwater Formation on faunal changes, the micropaleontologic results of the present study tend to confirm the placement of the basal shale within the Clearwater Formation.

One basis for placing the basal shale within the McMurray Formation is that its contact with the Clearwater Formation is erosional. However, an erosional surface is often associated with the deposition of coarser-grained sediment. In addition, the nature of the

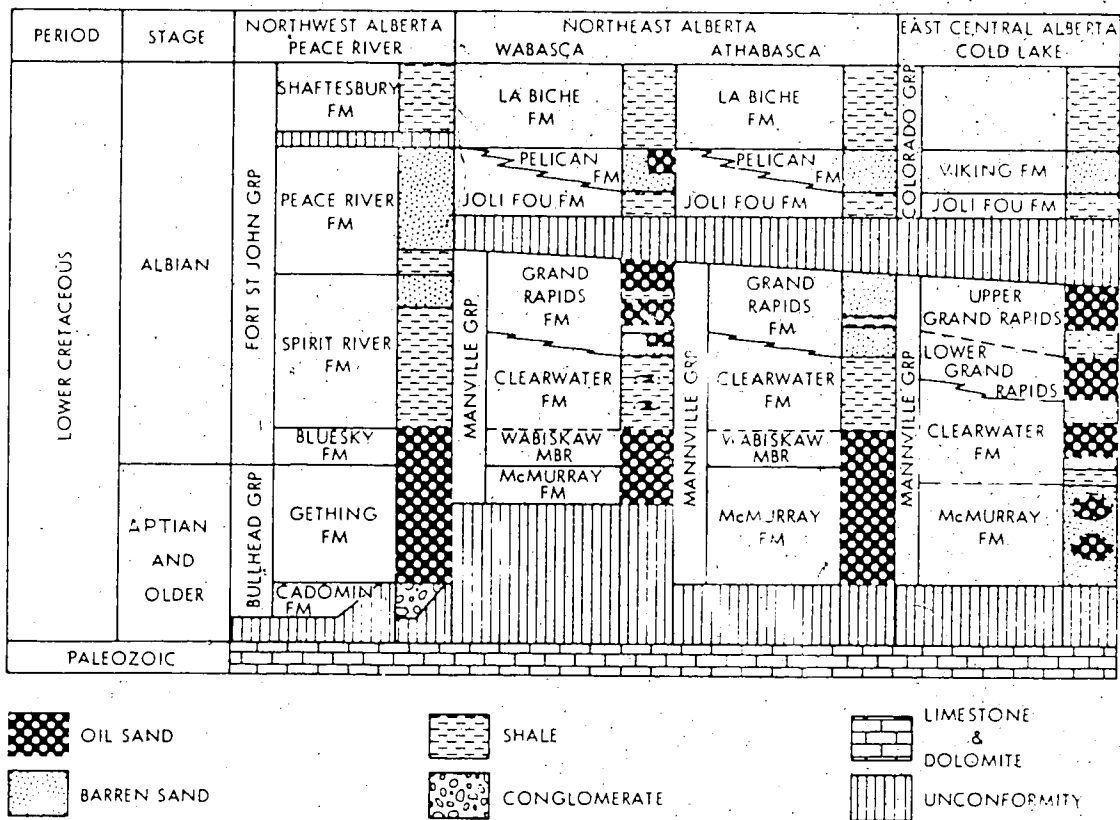


FIGURE 4. Stratigraphic correlation chart (modified from Kramers, 1975)

contact between the shale and the McMurray Formation is not known since no core was recovered from this depth. If the basal contact of the shale is proven to be conformable with the McMurray Formation the proposed correlation could be incorrect.

Further core and micropaleontologic work would help resolve this problem with stratigraphic correlations.

### III. Sedimentology

#### A. Previous Work

The sedimentology of the oil sands and heavy oil deposits is highly complex and a knowledge of facies is important to oil exploration (Mossco *et al.*, 1981).

Rudkin (1964) wrote extensively on the stratigraphy and depositional history of both the Athabasca and Lloydminster areas. In his schema, the Lower Mannville Group included the McMurray Formation and the Wabiskaw Member of the Clearwater Formation and consisted of nonmarine basal fill deposits. The Upper Mannville Group included the Clearwater and Grand Rapids Formations and consisted of time transgressive marine units. The Clearwater Formation was considered to be a deltaic deposit, modified by periodic marine advances of a boreal sea whose axis trended southeast and lay close to the present Shield edge in northeastern Alberta. Marine conditions prevailed in the north (Athabasca area), mixed marine / non-marine conditions in the central area (Cold Lake and Lloydminster areas), and non-marine conditions in the south.

The first description of the Clearwater Formation was made at the Athabasca outcrop area. The Clearwater Formation was described as interbedded sands and shales (McConnell, 1891) or as "soft grey shales, black shales, and grey and green sandstone with some hard concretionary layers" (McLearn, 1917). The first paleogeographic map (McLearn, 1932) depicted the Clearwater Formation as marine in origin.

After further study, the Clearwater Formation was described as glauconitic sandstone basally, overlain by dark grey shales grading up into sandstone of marine origin (Mellon, 1967). Gallup (1974) studied the geologic history of McMurray-Clearwater deposition in the Athabasca oil sand area and characterized the environment of deposition as lagoonal and deltaic.

A study of the chemical composition of the Mannville Group shales in central Alberta (Campbell and Williams, 1965) showed that Clearwater depositional environments were generally marine in the lower part and brackish in the upper part.

A lithological description of the Mannville Formation in the Vermilion-Wainwright area was based upon the presence or absence of dark minerals, the distribution of marine fossils and the occurrence of coal seams (Nauss, 1945). The strata which are

approximately equivalent to the Clearwater Formation were described as: 88 feet of dark shales interbedded with silts and "salt and pepper" sandstone of marine origin; overlain by 10 feet of quartz beach sandstone; overlain by 78 feet of deltaic "salt and pepper" sandstone, grey shale and siltstone with a few plant remains; overlain by 29 feet of beach reworked quartz sands, shale and siltstone. Overall, a nearshore to upper shoreface environment was indicated for the Vermilion-Wainwright area.

Clearwater equivalent strata in the Lloydminster area (Wickenden, 1948) were described as composed of well-rounded fine-grained quartz with glauconite grains of probable delta front origin. Vigrass (1977) conducted a detailed study of the Lloydminster area and characterized the deposit as lithologically similar in all its nine members. The Clearwater Formation approximate equivalent Cummings to Sparky Members were considered marine in origin. Channel deposits in Clearwater equivalent Lloydminster strata (MacCallum, 1981) and nearshore marine deposits (Tilley and Last, 1980) were recognized.

The 205 m (600 ft) of Mannville Group sediment in Cold Lake was described (Webber, 1967) as interbedded sand, silt and shale with minor stringers of coal. In a detailed sedimentologic review of the Cold Lake area (Minken, 1974), the Clearwater Formation was characterized as a "salt and pepper" sandstone with glauconite, grading to shale southward.

Cold Lake area sedimentology has been generally characterized as non-marine in the McMurray Formation, marine in the Clearwater Formation, and non-marine in the Grand Rapids Formation (Outtrim and Evans, 1977).

The Clearwater Formation in the Cold Lake area has been generally described as a laterally extensive nearshore marine sand deposit with associated marine shales (Mossop *et al.*, 1981).

A general geologic report on the Clearwater Formation in the Cold Lake area (Carrigy and Kramers, 1974) revealed that marine conditions prevailed and that the Cold Lake deposit could be placed close to the southern limits of a boreal sea. Consequently, nearshore, transitional, and deltaic environments predominated. The Wabiskaw Member of the Clearwater Formation was described as shallow sea reworked McMurray Formation sands (Kramers, 1975).

The depositional environment of the Clearwater Formation at Cold Lake has been variously characterized as nearshore deltaic (Jardine, 1974; Esso Resources, 1978), nearshore tidal (Wenneker *et al.*, 1979), or an Arctic boreal sea transgressive marine bar and interbar sand wedge (Minken, 1974).

In a site-specific study, Harrison *et al.* (1981) examined over sixty wells in a three township area in the northeastern portion of the Cold Lake oil sands deposit. They concluded that the Clearwater Formation consisted of delta-fringe silts and shales, lower delta front sands and shales, and upper delta front stream mouth bar and beach sands in this area.

### **Provenance and Tectonic Framework**

Two source areas for Lower Cretaceous sediment have been proposed (Glaister, 1959; Mellon, 1967; Carrigy and Kramers, 1974; Jardine, 1974; Keeler, 1980; Harrison *et al.*, 1981). The major source area was in the Cassiar-Omineca and Nelson uplift areas of south-central British Columbia, while minor contributions of sediment came from positive areas of the emergent Shield of Saskatchewan and Manitoba. The latter had a local significance in eastern Alberta, including the Cold Lake area.

The hypothesis of dual provenance was reinforced by a geochemical study of Lower Cretaceous strata (Cameron, 1965) which found that the sediments could be divided into low, medium and high soda content groups which reflect different source areas. In the Athabasca, Cold Lake, and Lloydminster areas, tongues of low soda level sediment showed that some detritus came from the east, in addition to the major sediment source from the west. The Pre-Cambrian Shield to the northeast of the Lloydminster heavy oil deposit was cited as the source area for sediments deposited here by a southward transgressing Clearwater Sea (Putnam, 1979). However, in a recent paper, Putnam and Pedskalny (1983) contend that the source rocks for the Clearwater Formation at Cold Lake are only to the west and that there is no northeasterly Shield component.

Relief on the Paleozoic erosion surface, which controlled Mannville Group deposition, was reported to be from 94 m (300 ft) to 120 m (400 ft) and locally up to 150 m (500 ft) (Williams, 1963). An isopach and a paleogeologic map of the Lower Cretaceous strata in central Alberta north of the present area of study shows that rivers



flowed in a northwesterly direction in large channels etched into the pre-Cretaceous surface. The deposition of Mannville sediment was also controlled by a series of pre-Cretaceous islands trending in a northwest-southeast direction (Jardine, 1974). Mannville Group thickness was stated to be between 550 and 880 feet depending upon the sub-Cretaceous erosional relief (Clack, 1968). Two erosional pre-Cretaceous fluvial channels with northerly drainage were recognized here.

Williams and Stelck (1975) provided an overview of the depositional history and paleogeography throughout Mannville time in Alberta. A study of basement controls on Lower Cretaceous deposition (Stelck, 1975) showed that the Peace River and Sweetgrass arches controlled Lower Cretaceous sedimentation in Alberta.

In the Cold Lake area, salt solution in late Mannville time, as well as subsequent to Mannville deposition, resulted in a discontinuity of facies (Energy Resources Conservation Board, 1973). Carbonate ridges and channels in the underlying Devonian strata also controlled sedimentation.

Beaumont (1981) cites subsidence, caused by a combination of loading of thrust plates and erosion of these plates, as the major control on sea level and deposition in the Cretaceous Period.

## **B. Introduction to Sedimentology**

Clearwater Formation is characterized by finely interbedded lithofacies. Consequently, it is most practical to describe the deposit with respect to facies associations. A facies association is a group of lithofacies which tend to occur together and are considered to be genetically or environmentally related (Reading, 1978).

It is beyond the scope of the present study to perform a strict facies analysis of the cores. The main purpose of the study is to relate general sedimentological features and the geophysical well log response.

### **Definition of Facies Associations**

The cores were studied bed-by-bed and sedimentary types were defined (See Table 1 for the range of features observed in core).

Table 1.

<u>SEDIMENTARY TYPES</u>		
Bed-by-bed Total Counts	Lithology	Structures
112	Silty Shale	horizontal laminae; stringers; structureless
220	Silty Shale Argillaceous Silt	laminated (horizontal, curved, inclined, undulating); load casts; wedges and lenses
151	Carbonaceous Sand, Silt and Shale Coal	laminated (horizontal, curved, inclined, undulating); lenses; minor bioturbation
307	Silty Shale, Shale, Argillaceous Silt	heavily bioturbated
140	Shale	laminated (horizontal, curved, inclined, undulating); load casts; stringers
211	Silt	laminated (horizontal); stringers
107	Silt	laminated (curved, inclined, undulating, contorted); lenses
391	Sand Calcareous Cement	laminated (horizontal); cone-in-cone carbonate
105	Sand Calcareous Cement	laminated (inclined); stringers
275	Sand Calcareous Cement	laminated (undulating and curved); lenses and wedges
426	Sand Calcareous Cement	apparently structureless
119	Sand Silt	heavily bioturbated remnant structures
50	All Lithologies	scoured surface
63	All Lithologies	silty shale rip-up clasts
<hr/> Total	2677	

The dominant lithologies in the Clearwater Formation are unconsolidated sand, unconsolidated silts to siltstone, silty shale, shale and calcareous cemented material. Silt-sized sediment is commonly oil saturated and unconsolidated and will be termed a silt. In the case of stratigraphic unit F, some silt-sized sediment is indurated and will be termed a siltstone.

The major criteria for defining facies associations were grain size and the amount of bioturbation present. Heavy oil saturation in the sands and silts often obscures primary sedimentary structures and bioturbation often destroys these structures.

The geophysical well log response was also used to help define the stratigraphic units and facies associations. It was the sole criterion used in situations where no core was available. The geophysical well log response is given in Appendix I.

### C. Facies Associations

The Clearwater Formation is made up of six facies associations: heavily bioturbated silty shale; heavily bioturbated silty shale to silt and sand; moderately to heavily bioturbated sand with silt and silty shale; sand, silt and silty shale; graded sand, silt and shale with Bouma sequences; and sand and carbonaceous sand.

The facies associations have been related to the stratigraphic units in the structural cross-sections A—B and A—C (Figure 5 to Figure 7).

#### Facies Association 1. Heavily Bioturbated Silty Shale

Facies Association 1 consists of a heavily bioturbated fissile silty shale (Plate 3-1). Some remnant horizontal laminae were preserved, although most primary sedimentary structures are destroyed by bioturbation. The silty shale is bioturbated by organisms, including those which produce Planolites nicholson (1873).

#### Facies Association 2. Heavily Bioturbated Silty Shale to Silt and Sand

Facies Association 2 consists of a grey shale with oil stained argillaceous silt and very fine-grained sand interbeds (Plates 1-1 and 1-2). The facies association becomes more shaley to the northwest. Silty shale thicknesses range from individual laminae to beds 0.45 m (1.5 ft) thick. Silt and sand range from individual laminae to beds up to 20 cm

## LEGEND

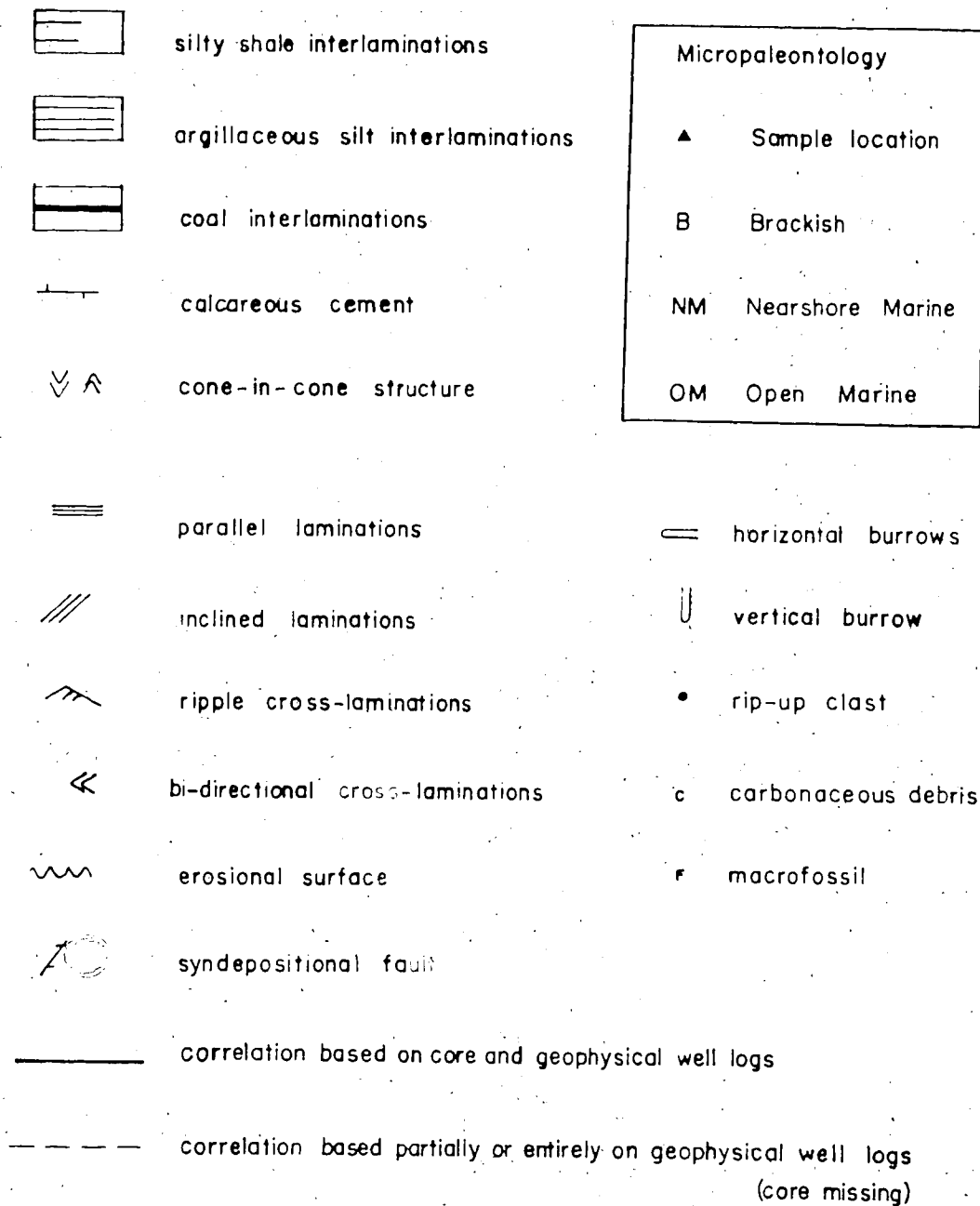


FIGURE 5. Legend for structural cross-sections.

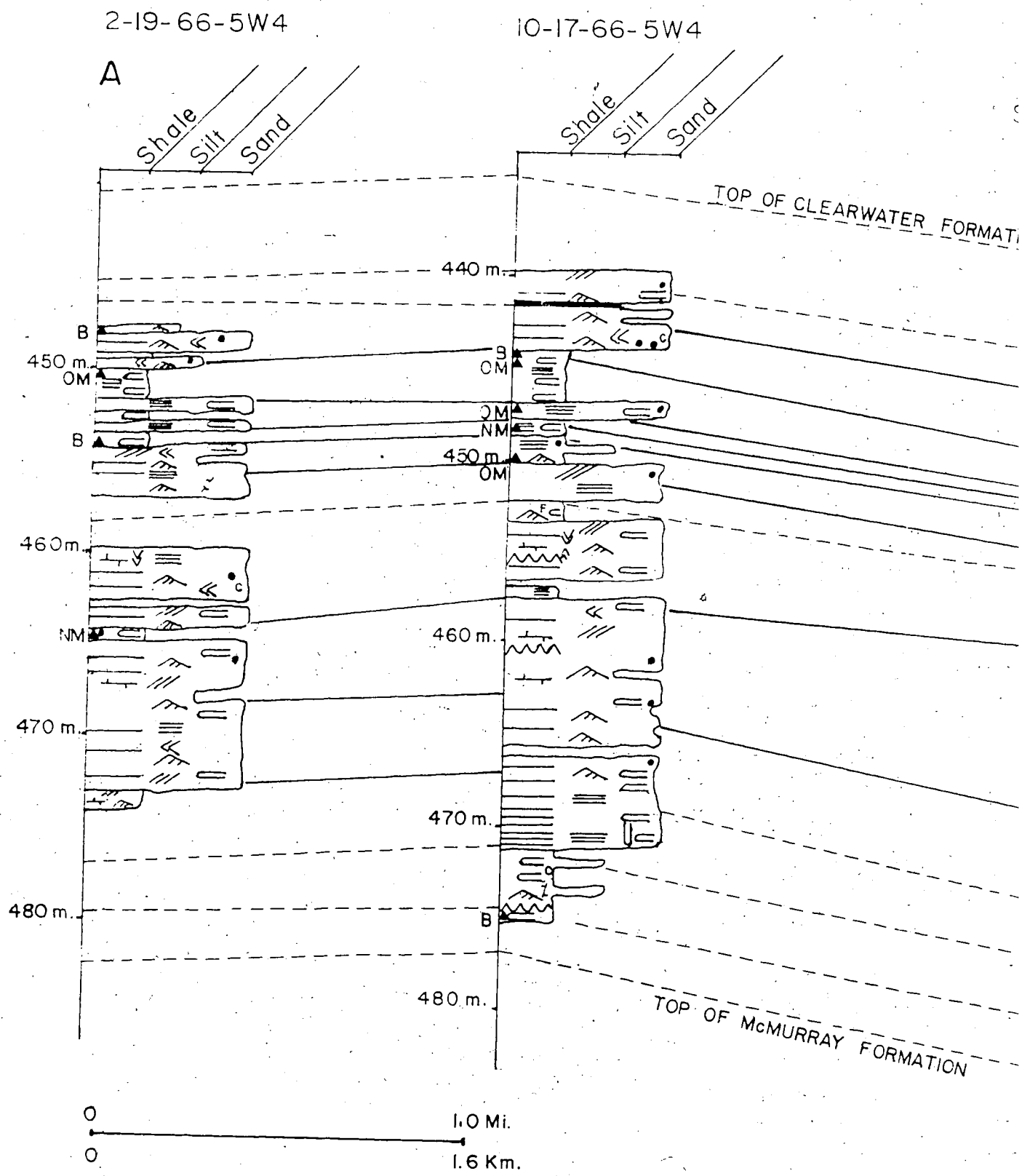


FIGURE 6. Northwest-southeast structural cross-section, showing the distribution facies associations and stratigraphic units and micropaleontologic results.

6-3-66-5W4

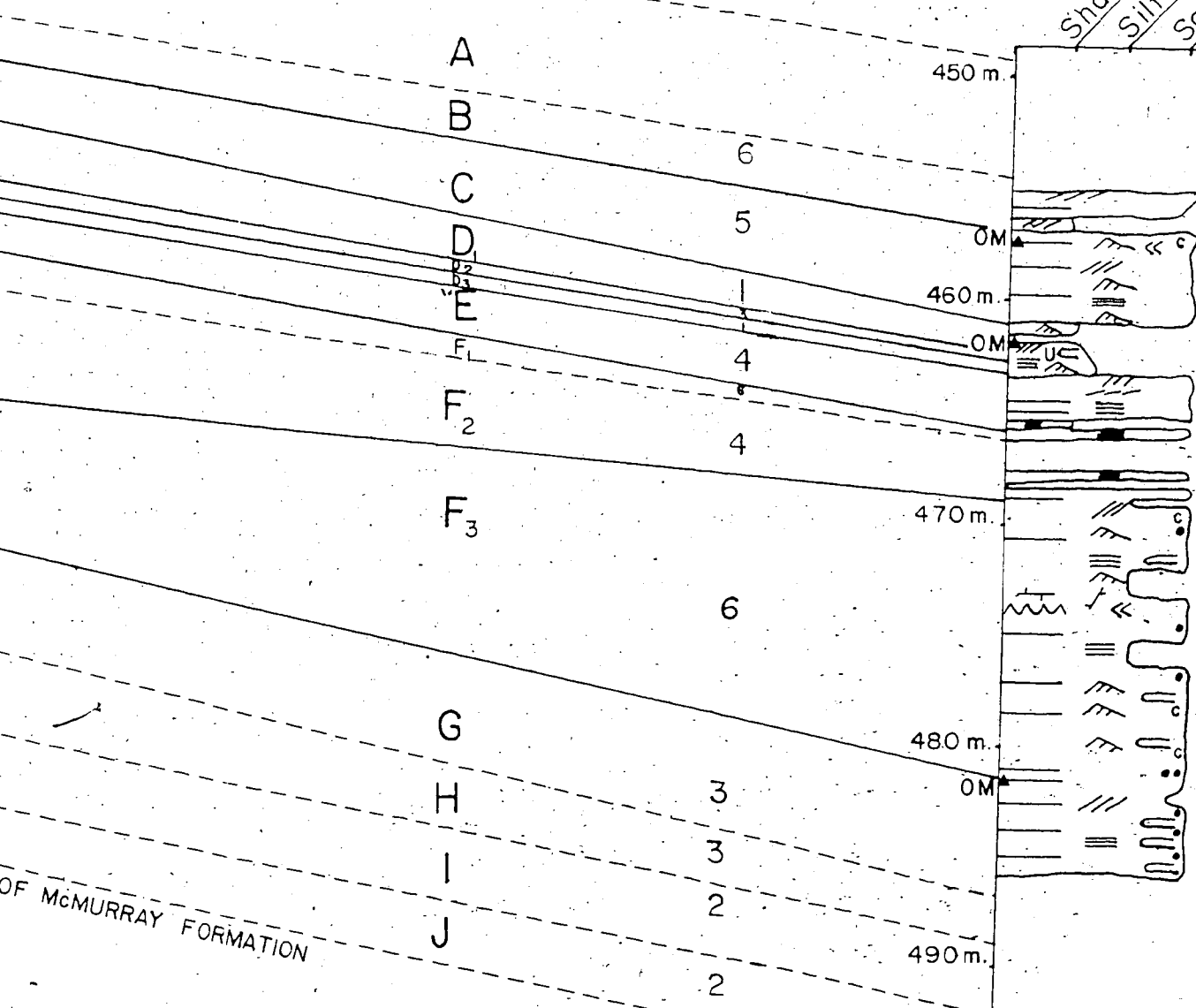
B

STRATIGRAPHIC UNIT

FACIES ASSOCIATION

TOP OF CLEARWATER FORMATION

Shale  
Silt  
Sand



, showing the distribution of and micropaleontologic results.

20/2

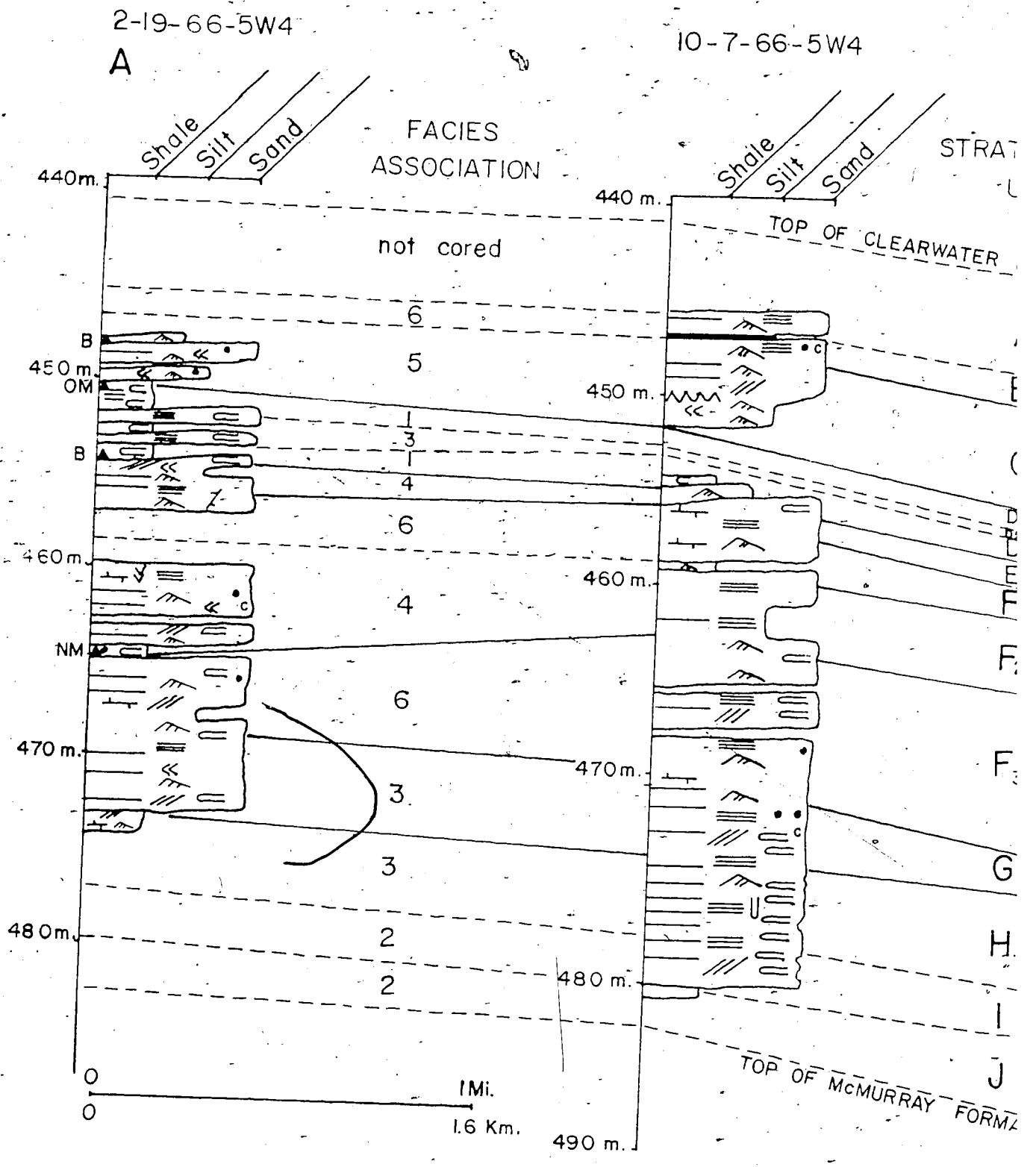
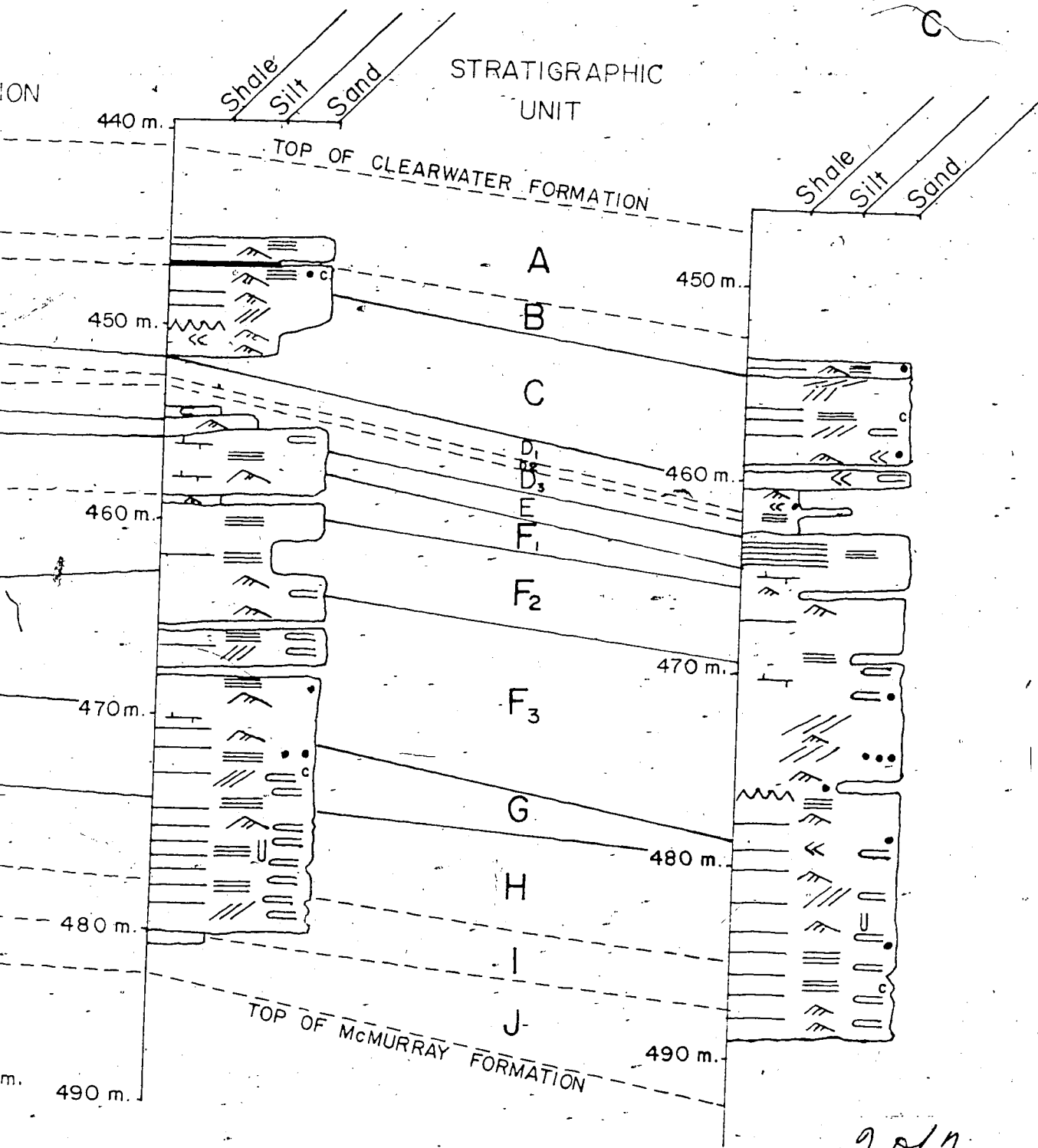


FIGURE 7. North-south structural cross-section, showing the distribution of facies associations and stratigraphic units and micropaleontologic results.

10-7-66-5W4

6-5-66 5W4



cross-section, showing the distribution of facies  
stratigraphic units and micropaleontologic results.



(8 in) thick. The thickness of sand and silt interbeds increases upwards within stratigraphic units J to I.

The beds typically consist of horizontal and undulating laminae with rare inclined cross-laminae dipping at a low angle of  $4^\circ$ . Some bi-directional low-angle cross-laminae dipping at  $8^\circ$  were observed in the basal portion of the facies association in well 10-7-66-5W4. Small silty shale clasts of less than 1 cm diameter "float" in some of the oil saturated silt and sand beds. Synsedimentary normal faults were observed in well 10-17-66-5W4. They are not coring artifacts because they occur within the core and do not extend to the core edge.

The shales and silty shales are highly bioturbated by traces of Planolites nicholson (1873). The location of bioturbation is given in Figures 5 to 7. The degree of bioturbation decreases upwards within stratigraphic units J to I.

### **Facies Association 3. Moderately to Heavily Bioturbated Sand with Silty and Silty Shale**

Facies Association 3 consists of interbedded to interlaminated very fine-grained sand to silt and silty shale (Plates 1-3, 2-1 and 3-1). Sand units range from individual laminae to beds 0.9 m (3 ft) thick in well 6-3-66-5W4. Silty shale is found as individual laminae to beds 25 cm (10 in) thick. The proportion of silty shale increases towards the northwest. Carbonaceous debris is found in a 10 cm (4 in) thick interbed of laminated silt in well 6-3-66-5W4. In stratigraphic unit G, carbonaceous debris is found in silty shale beds up to 4 cm (1.5 in) thick.

Structures are obscured in the heavily oil saturated sands and in stratigraphic subunit D<sub>2</sub> where bioturbation has destroyed primary sedimentary structures. Where observed, structures in the sands and silts are dominantly horizontal laminae. Undulating and ripple cross-laminae are also commonly found. Some sequences (up to 25 cm thick in stratigraphic unit H in well 6-3-66-5W4) of interbedded and interlaminated sand and silty shale are inclined up to  $15^\circ$  and are probably accretion surfaces. Bi-directional low-angle inclined laminae were noted in stratigraphic unit G in well 2-19-66-5W4 and bi-directional ripple cross-laminae were noted in stratigraphic unit G in well 6-5-66-5W4.

The silty shale exhibits horizontal and inclined laminae. The low-angle inclined laminae dip at angles between 3° and 10°. The silty shale laminae often exhibit scoured surfaces.

Silty shale intraclasts (0.1 cm to 2 cm in diameter) are numerous in some parts of the core "floating" within the oil saturated sands. The silty shale intraclasts are most likely derived from silty shales which have undergone scouring.

Bioturbation of the sands, silts and silty shales is extensive in stratigraphic unit D<sub>2</sub> and the basal portion of stratigraphic unit H. The degree of bioturbation in the silty shales decreases upwards through stratigraphic units H and G. Bioturbation consists of 1 cm diameter traces of Planolites nicholson (1873) and simple vertical traces of Skolithos linearis haldeman (1840). The latter are found in association with Planolites nicholson (1873) at equivalent depths of stratigraphic unit H in wells 6-5-66-5W4, 10-7-66-5W4 and 10-17-66-5W4. This trace varies between 1 cm and 2 cm in diameter and cuts across sedimentary types, attaining a maximum length of 22 cm in well 10-17-66-5W4.

#### **Facies Association 4. Sand, Silt and Silty Shale**

Facies Association 4 consists of very fine-grained, moderately poorly sorted to poorly sorted sand, interlaminated or interbedded with poorly sorted silty shale, argillaceous silt and silt (Plates 2-2 and 2-3). The proportion of silty shale laminae and beds increases to the northwest in stratigraphic subunit F<sub>2</sub>.

Sand and silt are found primarily as horizontal laminae, but beds can attain thicknesses of up to 20 cm (6 in). The silty shale is also usually finely interlaminated with the coarser units, although silty shale beds up to 15 cm (6 in) thick occur. Minor portions of the sands and siltstones in stratigraphic subunit F<sub>2</sub> exhibit low-angle cross-laminae inclined up to 7°. To the northwest, some small (up to 0.5 cm diameter) silty shale intraclasts were noted in this facies association. A small syndepositional normal microfault was noted in stratigraphic unit E in well 2-19-66-5W4. The fault does not extend to the core edge and the core does not exhibit features suggestive of breakage.

Bioturbation is rare and consists of small (up to 0.5 cm diameter) isolated traces of Planolites nicholson (1873) in the silty shales. In the upper silty shale bed of stratigraphic

subunit F<sub>2</sub> in well 10-17-66-5W4, a shell specimen of Psilyma peterpondia and a trace of Muensteria von Sternberg (1883) were found.

Calcareous cemented siltstones with associated cone-in-cone structures were observed in stratigraphic subunit F<sub>2</sub> in wells 2-19-66-5W4 and 10-17-66-5W4. The cone-in-cone structures suggest that high pressure levels existed during dewatering of the sediment.

#### **Facies Association 5. Graded Sand, Silt and Shale with Bouma Sequences**

Facies Association 5 consists of interbedded to interlaminated sand, silt and silty shale.

The sand is found as individual laminae and as beds up to 0.6 m (2 ft) thick (Plate 3-2). Silty shale is found as individual laminae and in beds of laminated silty shale up to 13 cm (5 in) thick.

Major structures include undulating, horizontal and low-angle inclined (up to 10°) laminae. Bi-directional low-angle cross-laminae were observed in all wells. The silty shale is commonly scoured. Silty shale intraclasts are commonly found. These clasts are subangular and average 1.5 cm in diameter. Sequences in well 10-17-66-5W4 between 443.5 m (1454 ft) and 444.5 m (1457.5 ft) exhibit graded beds with Bouma Sequences (Plate 3-2). These deposits consist of a very fine-grained, heavily oil saturated, massive sand (Bouma Ta subdivision), grading upwards into a lightly oil stained, plane parallel laminated silt (Bouma Tb subdivision). Intraclasts are incorporated into either the sand or silt beds. The sequence is capped by ripple cross-laminated sands, draped by undulating silty shale laminae (Bouma Tc subdivision) and parallel silty shale laminae (Bouma Td subdivision). Some of the horizontally laminated silty shale represent interturbidite deposits (Bouma Te subdivision). The topmost laminae of shale is usually scoured, marking the commencement of the next turbidity current deposit. Rare Planolites nicholson (1873) traces were noted.

### **Facies Association 6. Sand and Carbonaceous Sand**

Facies Association 6 consists of very fine-grained, poorly sorted sand with rare silty shale laminae and silty shale stringers. Carbonaceous debris is concentrated in some silty shale laminae (Plates 2-2 and 3-3).

Sand is found as individual laminae or as large beds of laminated sand up to 12 m (40 ft) thickness in stratigraphic subunit F<sub>3</sub>. Silty shale is found as individual laminae or as beds of laminae up to 5 cm (2 in) thick in stratigraphic unit B. Carbonaceous debris and a coal lamina 2 cm (0.8 in) thick were observed in the basal portion of stratigraphic unit B in well 10-17-66-5W4.

Sedimentary structures within this facies association are predominately horizontal laminae, inclined low-angle cross-laminae (up to 12°) and ripple cross-laminae. The ripple cross-laminae are commonly draped by undulating silty shale laminae. Bi-directional low-angle cross-laminae were observed in stratigraphic subunit F<sub>3</sub> in well 10-17-66-5W4. Scoured surfaces were seen in stratigraphic subunit F<sub>3</sub> in most wells. Usually the scouring is associated with individual or groups of silty shale intraclasts up to 2 cm in diameter. A small synsedimentary normal microfault is associated with an erosional surface in stratigraphic subunit F<sub>3</sub> in well 6-3-66-5W4. The fault does not extend to the core edge and is not a coring artifact. Rare individual traces of Planolites nicholson (1873) occur in Facies Association 4.

Small portions (up to 15 cm (6 in) thick) of stratigraphic subunits F<sub>1</sub> and F<sub>3</sub> are altered by calcareous cementation, but some remnant ripple cross-laminae and horizontal laminae are preserved.

### **D. Stratigraphic Units**

The Clearwater Formation was divided into ten informal stratigraphic units on the basis of lithology and geophysical well log response (Figures 5 to 7 and Appendix I). The stratigraphic units were defined to describe groups of facies associations which could be combined into higher order assemblages. The informal stratigraphic units were also used in the mapping and delineation of large scale vertical sequences to define regional sedimentation patterns. This required an ordering of the system at a level higher than that of facies associations.

Stratigraphic unit J (Facies Association 2) overlies the McMurray Formation sediments. The nature of the contact between the McMurray and Clearwater Formations in this area is unknown since no core was available. The thickness of stratigraphic unit J ranges from 2.5 m (8 ft) to 5.5 m (18 ft). Core from this unit is available from only three of five wells, with a maximum length of 1.5 m (5 ft) cored in well 6-5-66-5W4. Stratigraphic unit H exhibits a gamma ray response of 128 API units and a deep induction log response of 2 ohms  $m^2/m$ .

Stratigraphic unit I (Facies Association 2) overlies stratigraphic unit J with either a sharp or erosional contact. In wells 6-5-66-5W4 and 10-7-66-5W4 the contact is sharp, but cannot be conclusively identified as erosional. However, well 10-17-66-5W4 has an erosional contact. The thickness of this stratigraphic unit is fairly uniform, ranging from 2.3 m (7.5 ft) in the southeast to 3.8 m (12.5 ft) in the northwest. Complete core from this stratigraphic unit was available in three out of five wells (6-5-66-5W4, 10-7-66-5W4 and 10-17-66-5W4). Stratigraphic unit I was recognized from the geophysical well logs by an abrupt shift in the gamma ray log from 128 API units to 95 API units at the top of stratigraphic unit I. The deep induction log value for this stratigraphic unit is 3.5 ohms  $m^2/m$ .

Stratigraphic unit I is overlain by stratigraphic unit H (Facies Association 3). The nature of the contact is usually gradational, but in the case of well 10-17-66-5W4 it is sharp. The differentiation of stratigraphic units I and H is based upon a change in the lithology and in the degree of bioturbation. In the case of a gradational contact, the degree of bioturbation in the silty shales is similar between stratigraphic units I and H and the contact must be picked from geophysical well logs. Stratigraphic unit H has a variable thickness, ranging from 3.7 m (12.5 ft) in the northwest and 5.2 m (17.5 ft) in the southeast to 6 m (20 ft) at well 10-7-66-5W4. Complete core was available from three out of five wells. In addition, well 6-3-66-5W4 is missing only the basal 0.8 m (2.5 ft) and well 2-19-66-5W4 has only the upper 0.6 m (2 ft) cored. The base of stratigraphic unit H was picked at the 95 API unit level on the gamma ray log. The deep induction log response increases uniformly upward from 3.5 ohms  $m^2/m$  at the base to 8 ohms  $m^2/m$  at the top of this stratigraphic unit.

Stratigraphic unit G (Facies Association 3) gradationally overlies stratigraphic unit H. The contact must be picked with the aid of geophysical well logs. In well 6-5-66-5W4, stratigraphic unit G is less well developed, but the contact with stratigraphic unit H is more apparent. Thickness of stratigraphic unit G sediments is variable, ranging from 0.75 m (2.5 ft) in well 6-5-66-5W4 to 3 m (10 ft) in well 6-3-66-5W4 to 4.5 m (15 ft) in the other three wells. Core recovery is good with only small parts of core missing. The contact between stratigraphic units G and H is marked by a deflection of the gamma ray log value from 90 API units to 83 API units. The deep induction log displays a sharp increase from 8 ohms  $m^2/m$  to 12 ohms  $m^2/m$ .

Stratigraphic unit F sharply overlies stratigraphic unit G. It is the thickest unit in the Clearwater Formation, averaging 13.75 m (45 ft) in the five wells studied. Core recovery is fair with minor portions missing. Stratigraphic unit F has been divided into three subunits, primarily on the basis of lithology. Stratigraphic subunit  $F_3$  (Facies Association 6), the basal portion of stratigraphic unit F, ranges in thickness from 4.2 m (14 ft) in the northwest to 13 m (42 ft) in the southeast. The contact between stratigraphic subunit  $F_3$  and the underlying stratigraphic unit G is marked by a deflection of the gamma ray from 87 API units at the top of stratigraphic unit G to 75 API units at the base of stratigraphic subunit  $F_3$ . The deep induction log registers an increase from 11 ohms  $m^2/m$  at the top of stratigraphic unit G to 13 ohms  $m^2/m$  in stratigraphic subunit  $F_3$ . Stratigraphic subunit  $F_2$  (Facies Association 4) thickens to the northwest. It ranges in thickness from 6.4 m (21 ft) in well 2-19-66-5W4 to 2.4 m (8 ft) in well 6-3-66-5W4. Core recovery was good in the sands, but only fair in the shales. Some shale core was destroyed during coring and correlations had to be established through an examination of the geophysical well logs. Stratigraphic subunit  $F_1$  is distinguished from stratigraphic subunit  $F_3$  by an increase in the gamma 75 API units to 90 API units. The deep induction log decreases abruptly from 13 ohms  $m^2/m$  to 6 ohms  $m^2/m$ . The thickness of stratigraphic subunit  $F_1$  (Facies Association 6) is highly variable. The thickest section is 3 m (10 ft) and is found in well 10-7-66-5W4. The thinnest section is 0.75 m (2.5 ft) and is found in well 6-3-66-5W4. Core recovery is poor. Stratigraphic subunit  $F_1$  is distinguished from stratigraphic subunit  $F_2$  by a deflection of the gamma ray log value from 97 API units at the top of stratigraphic subunit  $F_2$  to 77 API units near the base of stratigraphic subunit  $F_1$ . The

deep induction log increases rapidly to 30 ohms  $m^2/m$  in stratigraphic subunit  $F_1$  from 9 ohms  $m^2/m$  at the top of stratigraphic subunit  $F_2$ .

Stratigraphic unit E (Facies Association 4) sharply overlies stratigraphic unit F. It has a variable thickness, ranging from 3.4 m (11 ft) in well 6-3-66-5W4 to 0.9 m (3 ft) in well 10-7-66-5W4. The base of stratigraphic unit E is marked by a gamma ray value of 98 API units and a rapid decrease in the deep induction log to 11 ohms  $m^2/m$ .

Stratigraphic unit D sharply overlies stratigraphic unit E. This stratigraphic unit thickens to the northwest. Thicknesses range from 2.1 m (7 ft) in well 6-3-66-5W4 to 4.5 m (15 ft) in well 2-19-66-5W4. Core recovery was poor. Wells had to be correlated using geophysical well logs. Stratigraphic unit D is made up of three subunits. It consists of a very fine-grained, poorly sorted sand unit (stratigraphic subunit  $D_2$ ) enclosed by fissile silty shales (stratigraphic subunits  $D_3$  and  $D_1$ ). Stratigraphic subunit  $D_3$  (Facies Association 1) ranges in thickness from 0.5 m (1.7 ft) to 1.75 m (5.8 ft) in well 10-17-66-5W4. It is distinguished from stratigraphic unit E by a deflection of the gamma ray log to 108 API units and a decrease in the deep induction log response from 11 ohms  $m^2/m$  to 8.5 ohms  $m^2/m$ . Stratigraphic subunit  $D_2$  (Facies Association 3) ranges in thickness from 0.5 m (1.7 ft) in the southeast to 2 m (6 ft) in the northwest. The gamma ray log value shifts slightly from 108 API units to 102 API units and the deep induction log exhibits a sharp increase from 8.5 ohms  $m^2/m$  to 13.5 ohms  $m^2/m$ . Stratigraphic subunit  $D_1$  (Facies Association 1) ranges in thickness from 1 m (3.3 ft) to 2.75 m (9.1 ft) in well 10-17-66-5W4. It is distinguished from stratigraphic subunit  $D_2$  by an increase in the gamma ray log value from 102 API units to 108 API units and by a deep induction log response decreasing from 11 ohms  $m^2/m$  to 7 ohms  $m^2/m$ .

Stratigraphic unit C (Facies Association 5) sharply overlies stratigraphic unit D. The thickness of this stratigraphic unit is highly variable, ranging from 2.7 m (9 ft) in well 10-17-66-5W4 to 6.2 m (21 ft) in well 6-5-66-5W4. In general, this stratigraphic unit thickens to the southeast. Core recovery is good except in well 2-19-66-5W4, where only 2.1 m (7 ft) out of 3.7 m (12 ft) was cored. Stratigraphic unit C was recognized on the gamma ray log by a sharp decrease from 108 API units to 87 API units and on the deep induction log by an increase from 9 ohms  $m^2/m$  to 13 ohms  $m^2/m$ .

Stratigraphic unit B (Facies Association 6) sharply overlies stratigraphic unit C. It is fairly uniform in thickness, averaging 1.5 m (5 ft). Core recovery is poor. Well 10-17-66-5W4 was the only well from which complete core was recovered. Stratigraphic unit B is characterized by a gamma ray response of 82 API units and a rapid increase in the deep induction log from 12 ohms  $m^2/m$  to 25 ohms  $m^2/m$ .

There was no core recovery from stratigraphic unit A. It is recognized by an increase in the gamma ray response from 101 API units to 117 API units and a marked decrease in the deep induction log from 12 ohms  $m^2/m$  to 4 ohms  $m^2/m$ . These responses suggest that stratigraphic unit A is a shale. The thickness of this stratigraphic unit ranges from 4.5 m (15 ft) in the northwest to 6 m (20 ft) in the southeast.

#### **E. Micropaleontology**

A total of fourteen samples were submitted to Dr. Singh (Alberta Geological Survey) for analysis of dinoflagellate and megaspore assemblages. The location of the samples is given in the structural cross-sections (Figure 6 and Figure 7).

Eighteen dinoflagellate species were identified. Four samples were poorly preserved and must be interpreted with caution. The moderately preserved samples contained up to 20 specimens. There were no well preserved samples.

Dinoflagellate populations are useful in stratigraphic studies of the Cretaceous since they give highly accurate stratigraphic results (Sarjeant, 1974). All samples submitted were assigned to the early Albian Age.

The use of dinoflagellate assemblages in paleoenvironmental reconstruction is less conclusive since microfossils are easily transported in shallow marine environments (Heckel, 1972). Paleoenvironmental interpretation of dinoflagellate assemblages is based on population diversity (C. Singh, personal communication), species morphology, and absolute frequency (Sarjeant, 1974). The presence of few species suggests low salinity brackish conditions. Thin-walled, less ornamented cysts are found in shallow, more turbid environments, while more delicate specimens denote deeper, less turbid conditions. An increase in cyst density indicates open marine conditions. But as the proportion of land-derived material declines, total numbers drop. Thus fewer specimens can be indicative of either nearshore or deep-water conditions. The seaward extension of river



deltas can create conditions which change the dinoflagellate assemblage. The large amounts of detritus in the water column would decrease the light supply (Sarjeant, 1974) and the assemblage would reflect a brackish environment.

An examination of samples for the five wells in this study confirms the complexity of sedimentation in a shallow epeiric sea.

Stratigraphic unit J was sampled in well 10-17-66-5W4. Recovery and preservation were poor, but the presence of one specimen of Mudergonia assymetrica (Brideaux, 1977) and another specimen of Mudergonia sp. suggests brackish conditions. The specimen in stratigraphic unit J is from the basal shale. The existence of brackish conditions at the time this shale was deposited suggests that fully open marine conditions did not exist in this area of the shallow sea. Further investigation is recommended to confirm this interpretation, especially because the interpretation is based on only two specimens. The poor preservation of these specimens suggests that they may have been transported rather than part of the "living community".

The number of samples examined is too low for regional interpretations to be made, but a general trend toward open marine and nearshore marine environments is reinforced by paleoenvironmental interpretations of stratigraphic units H and F. The assemblage in stratigraphic unit F (well 2-19-66-5W4) is consistent with a more saline environment. However, the presence of nine specimens of megaspores, comprising Bacutrilletes, Erlansonisporites, and Minerisporites suggests proximity to a shoreline which was not recognized in core.

Examination of specimens in Facies D suggest that brackish conditions prevailed towards the northwest and open marine conditions prevailed towards the southeast portion of the study area. However, in an area of subsidence such as this, low salinity brackish conditions can prevail just before open marine conditions are established (Singh, personal communication). These species then die out when open marine conditions are fully established and are replaced by a suite of open marine assemblages. Stratigraphic unit D in wells 2-19-66-5W4 and 10-17-66-5W4 reflects this pattern. Samples taken at the base of stratigraphic unit D are brackish. Preservation was poor in this sample. However, 9 dinoflagellate specimens were identified along with thirteen megaspore specimens, comprising Erlanisporites and Bacutrilletes. Further upsection, at 448.9 m

(1459.5 ft) in well 10-17-66-5W4, open marine assemblages are found. Samples taken from the top of stratigraphic unit D and from the overlying stratigraphic unit C contain poorly preserved brackish and nearshore suites, suggesting a return to more less saline conditions. Once again, no actual evidence for emergence was found. This would suggest that the shoreline shifted rapidly and was subjected to reworking in this shallow sea environment.

Micropaleontologic data reflect deposition in a "shelfal" to nearshore environment. More detailed sampling, along with sedimentologic study is required to confirm interpretations in a complex environment such as this.

#### F. Sedimentary Textures

The textures of the sediments in the Clearwater Formation were analyzed using standard sieve analysis procedure. Results are given in Appendix II.

A plot of standard deviation (sorting) versus mean grain size (Figure 8) shows that the sands are uniformly very fine-grained (between 3 and 4 phi) and predominantly poorly sorted (between 1 and 2 phi standard deviation according to Folk's (1968) classification) (Plates 6-1 and 6-2). An excellent direct relationship ( $r=0.94$ ) is exhibited between the standard deviation and the mean grain size. The coarsest samples are the best sorted, whereas the finer-grained samples are the most poorly sorted.

General features of sand, argillaceous sand and matrix-supported samples are shown in representative histograms. Relatively clean sands (Figure 9) are unimodal and show a pronounced peak at the 4 phi level. There are relatively few fines in these samples. Argillaceous oil sands (Figure 10) display the same unimodal peak as the oil sands samples, but there is a more pronounced skewness towards the fines (higher phi values). Matrix-supported samples exhibit bimodality (Figure 11). The major peak is found at the 3.5 to 4 phi level which is similar to previously-mentioned sample types. In addition, a more diffuse peak is located between 9 phi and 10.5 phi. This reflects what is seen in thin section as discrete grains "floating" in a fine matrix.

Two coarsening-upward sequences can be discerned within the very fine-grained sands, one from stratigraphic unit I to the top of stratigraphic unit F and the other from stratigraphic unit E to stratigraphic unit B (Figure 8). The sands in this latter

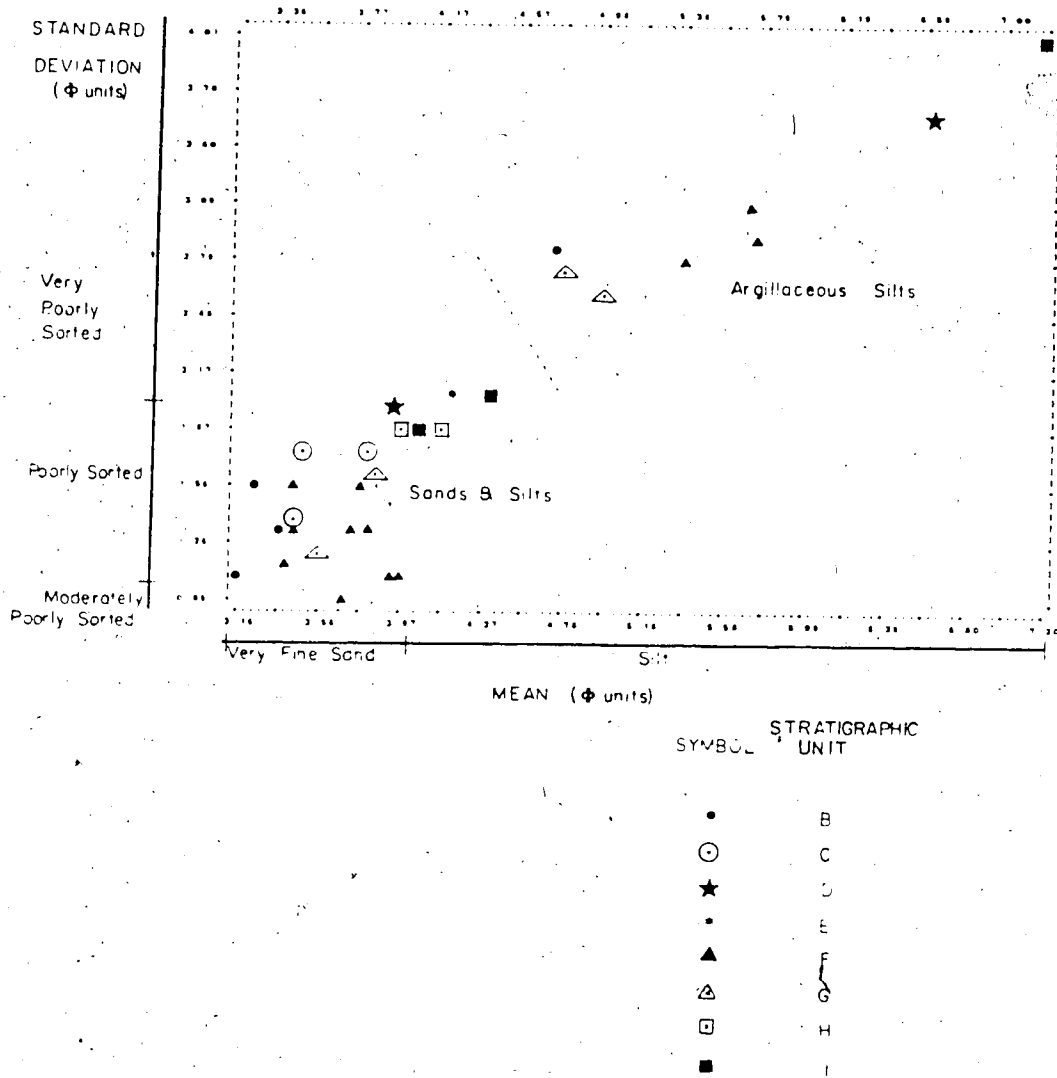


FIGURE 8. Standard deviation (sorting) versus mean grain size, showing relationship of stratigraphic units to grain size parameters. ( $r = 0.94$ )

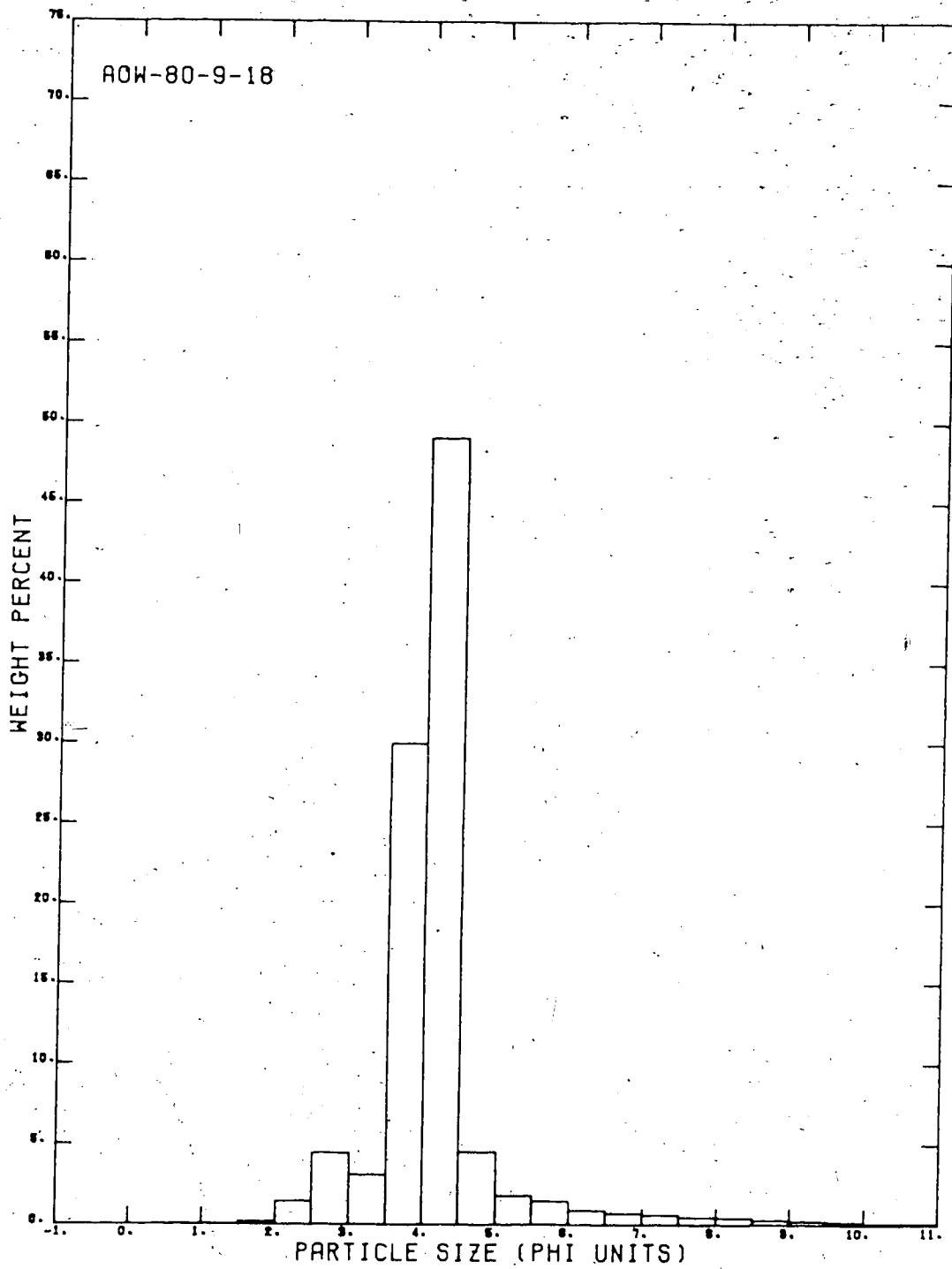


FIGURE 9. Representative grain size histogram for sand samples.

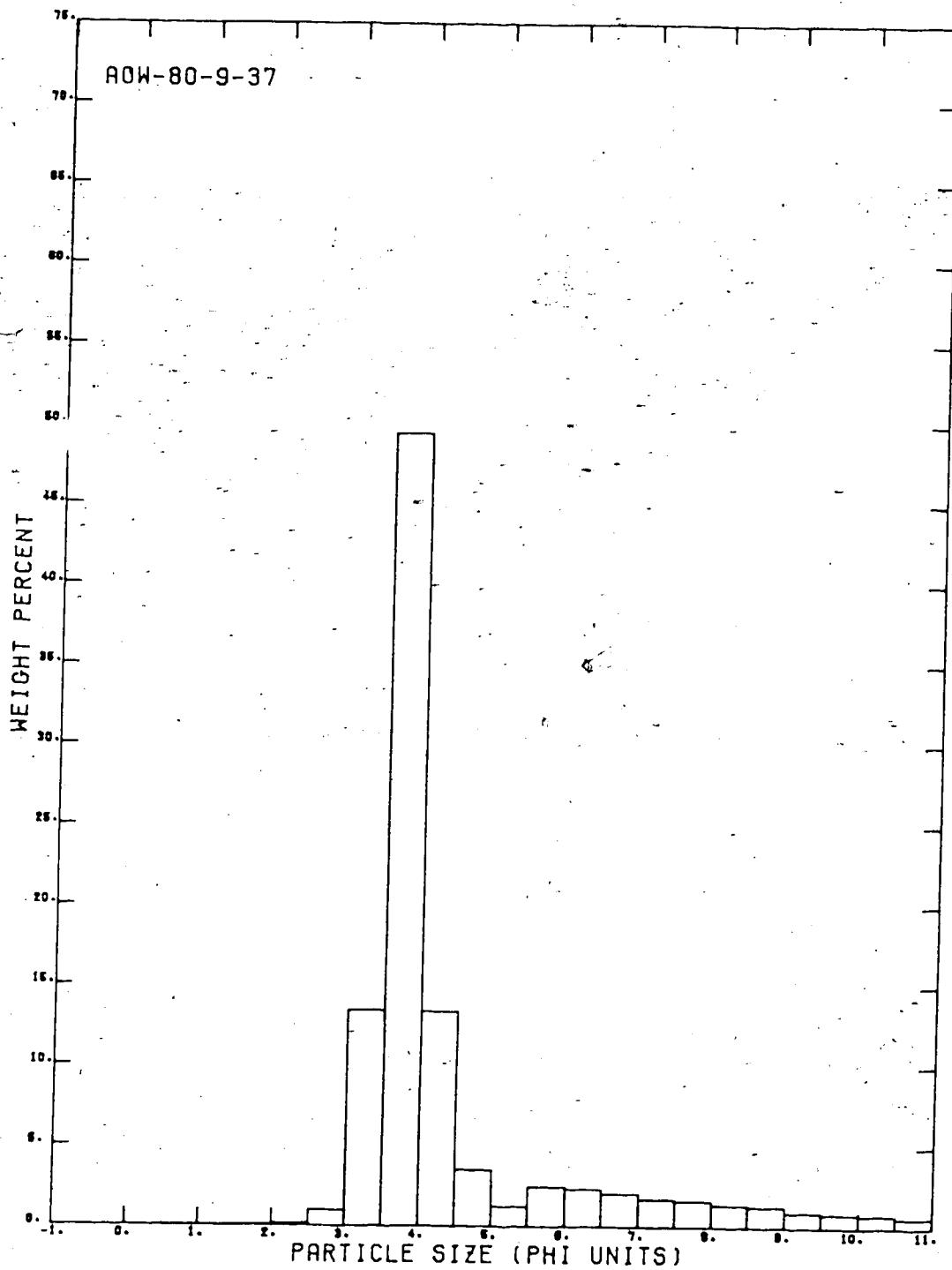


FIGURE 10. Representative grain size histogram for argillaceous sand samples.

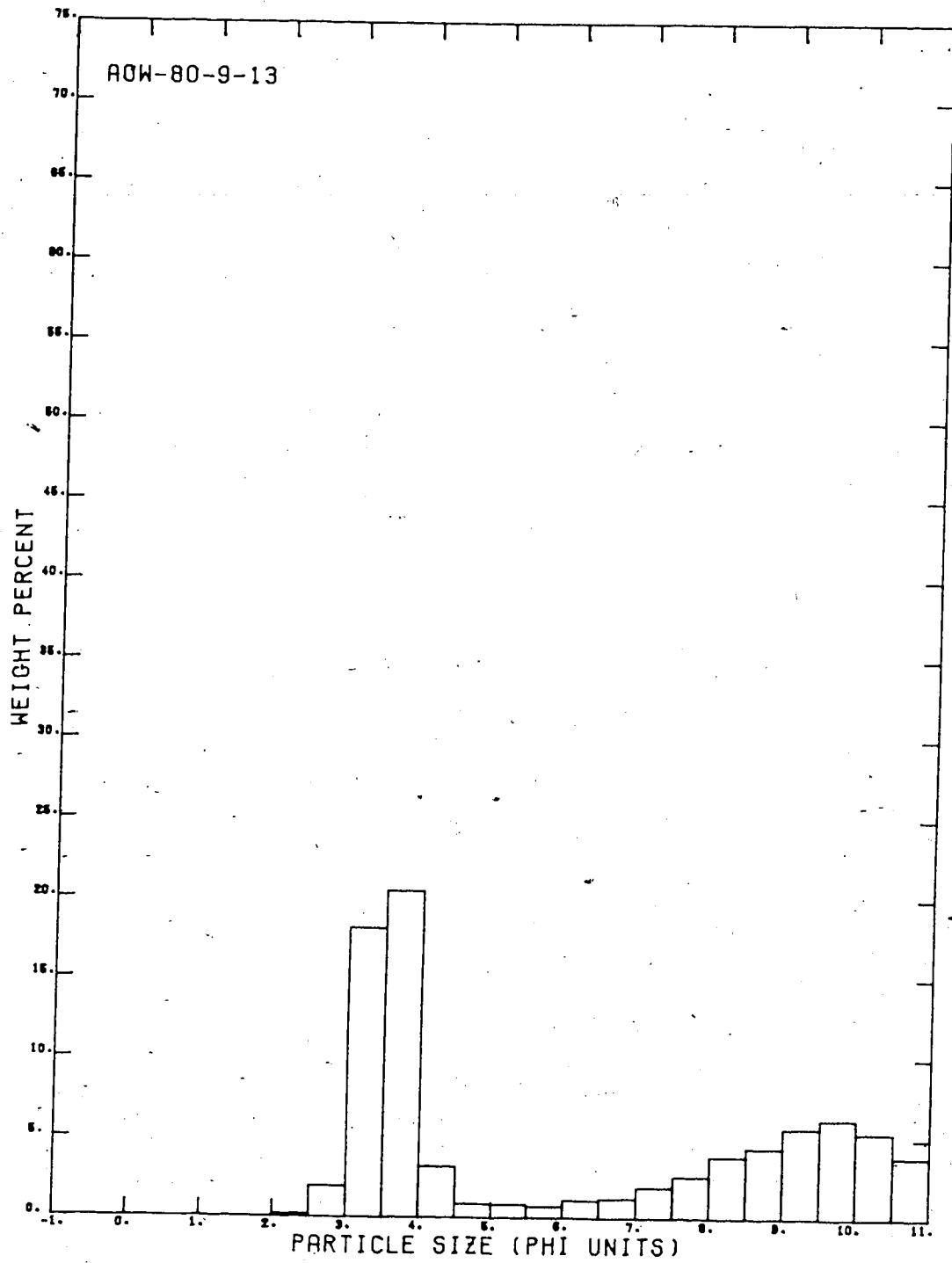


FIGURE 11. Representative grain size histogram for mixed sand and clay samples.

coarsening-upward sequence are slightly coarser-grained, although they are still within the very fine-grained classification.

### **G. Isopach and Structural Mapping**

The geophysical well log response for each stratigraphic unit (Appendix I) was used to correlate facies regionally. Fifty-four wells (Figure 12) were examined in a ten township area (Townships 64 to 66, Ranges 4W4 to 6W4 and Township Range 3W4). Structural maps were generated for the pre-Cretaceous unconformity and the tops of stratigraphic units F, G, H and A to discern the regional dip of these features. Isopach maps were generated for all stratigraphic units to delineate regional sedimentation trends and to examine the effects of the structure of the pre-Cretaceous unconformity on subsequent sedimentation.

#### **Structural Maps**

The structural maps of the pre-Cretaceous unconformity (Figure 13) agrees well with the structural map of the pre-Cretaceous unconformity constructed by Martin and Jamin (1963) and Kramers (1975). The pre-Cretaceous surface dips to the south-southeast at a rate of about 5 metres per kilometre. A local high of the pre-Cretaceous unconformity trending northwest-southeast is found in the western part of Township 66-5W4, the eastern part of Township 66-6W4 and the northeastern part of Township 65-6W4. Another local high trending northeast-southwest is located in Township 64-6W4. A local low is found in the southern part of Townships 65-5W4 and 64-5W4.

The structural maps of the tops of stratigraphic units F, G, H and the top of the Clearwater Formation (stratigraphic unit A) depart from that of the pre-Cretaceous unconformity, but are similar to one another. This indicates tectonic movement prior to Clearwater Formation deposition and a uniform response to tectonic movement during the deposition of Clearwater sediments.

The deposits of the Clearwater Formation dip from north to south at a rate of 2.5 metres per kilometre. In the central part of the area there is a structural high trending northwest-southeast. A structural low trending northeast-southwest is located in Township 64-5W4. These features are found in all facies examined, but are best

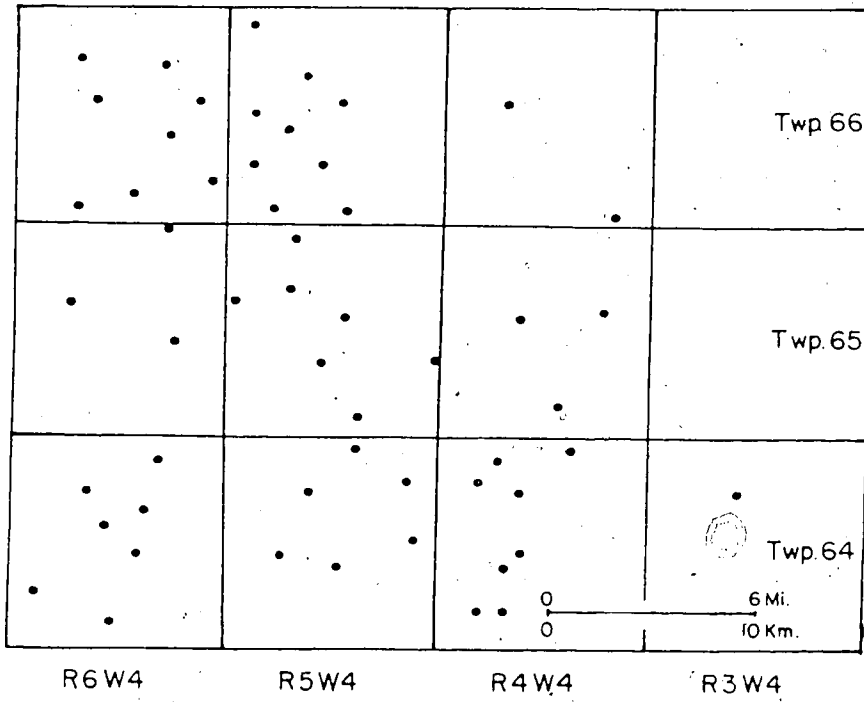


FIGURE 12. Regional well control for structural and isopach maps.

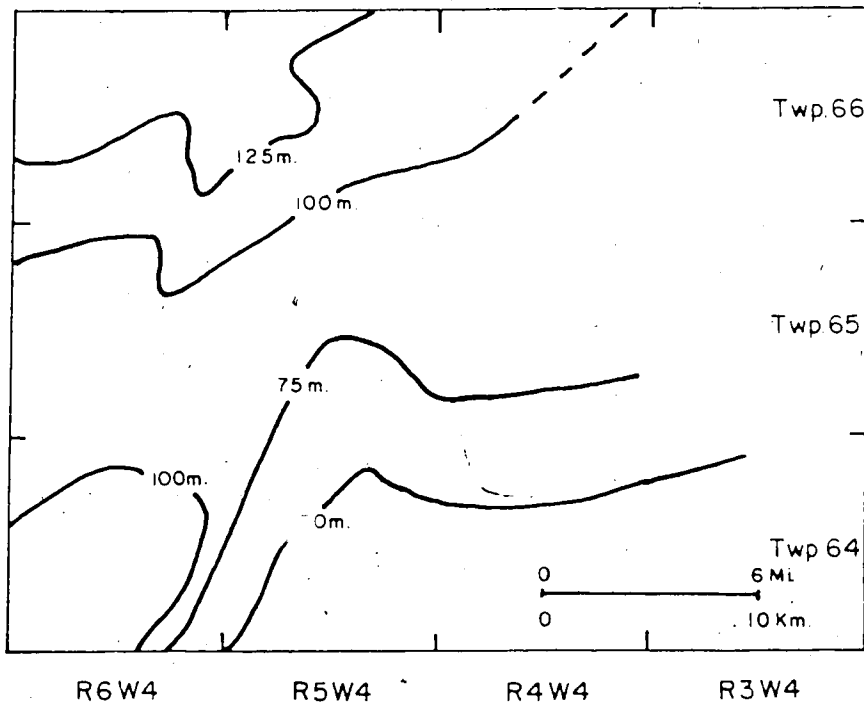


FIGURE 13. Structural map of pre-Cretaceous unconformity.



expressed in the structural map of the top of stratigraphic unit F (Figure 14).

### Isopach Maps

#### Stratigraphic Unit J

The isopach of stratigraphic unit J (Figure 15) shows a blanket shale which attains a maximum thickness of 6 m (20 ft). A north-south trending thinning is located in the central part of the region where thicknesses are of the order of 0.9 m (3 ft) to 2 m (7 ft). The distribution of thicknesses is very dissimilar from other stratigraphic units in the Clearwater Formation. This is further evidence for the placement of an erosional surface between stratigraphic units J and I. In stratigraphic unit J there is a small area of thickening in the northwest corner of Township 65-5W4 situated over one of the local pre-Cretaceous highs. Here the stratigraphic unit reaches a thickness of 6 m (20 ft). This represents the most complete section of this stratigraphic unit in the area. It may have been protected from erosion by its location on the local pre-Cretaceous high, above the general level of erosion.

#### Stratigraphic Unit I

Stratigraphic unit I (Figure 16) is thickest in a line trending northeast-southwest where it is up to 7.2 m (24 ft) thick. The pre-Cretaceous high in Township 64-6W4 has some control on the development of a thicker deposit here, but the other highs do not have an effect on sedimentation. The thinnest accumulations of stratigraphic unit I are between 1.5 m (5 ft) and 2.1 m (7 ft) and are found in the extreme northwest and southeast of the area.

#### Stratigraphic Unit H

Stratigraphic unit H (Figure 17) is almost the mirror image of stratigraphic unit I. The sediments of stratigraphic unit H are up to 10.5 m (34 ft) thick in the northwestern and southeastern parts of the area and thinnest in an area trending northeast to southwest through the centre of the region. Here the stratigraphic unit is as thin as 1.8 m (6 ft). The local high in Township 64-6W4 still exerts control on sedimentation and a thickening of the stratigraphic unit to 8.2 m (27 ft) is seen here.

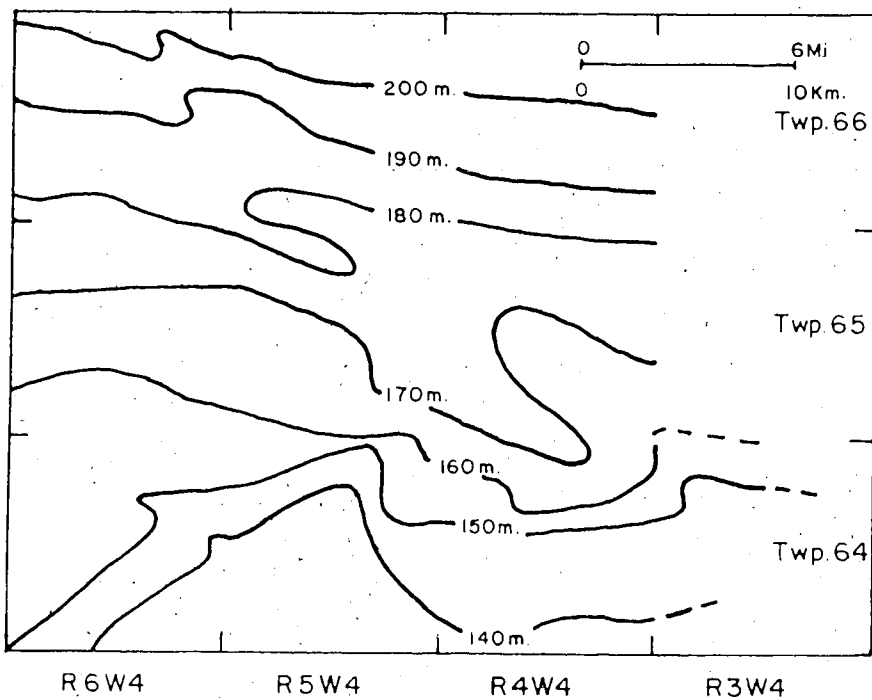


FIGURE 14. Stratigraphic unit F structural map.

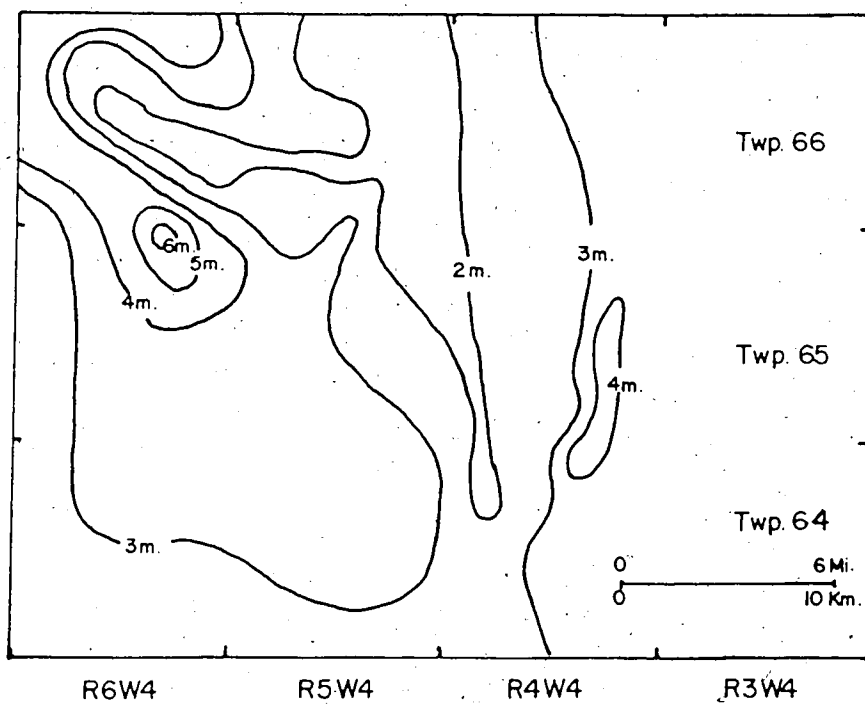


FIGURE 15. Stratigraphic unit J isopach map.

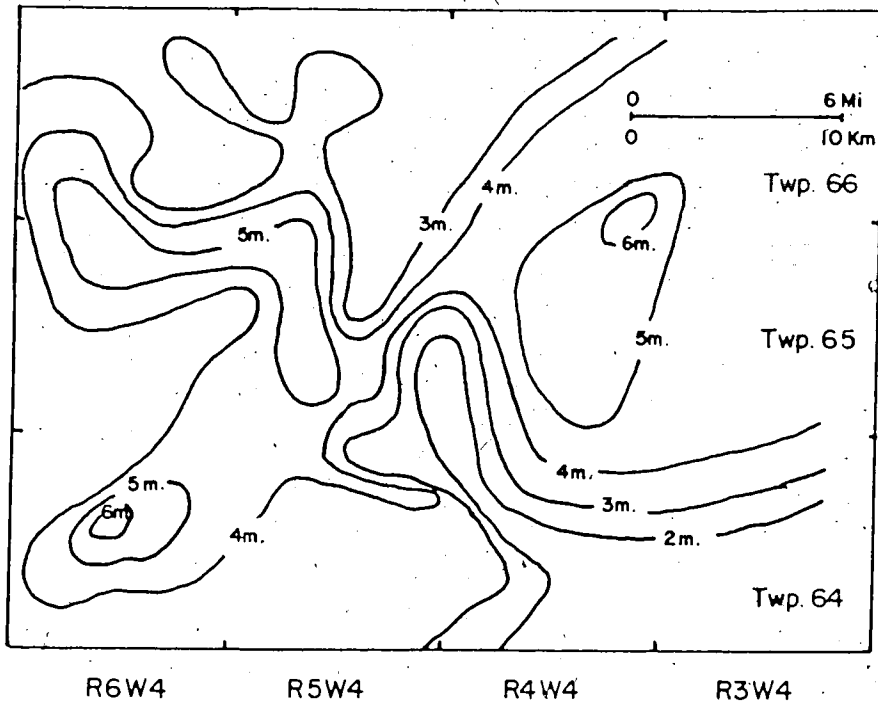


FIGURE 16. Stratigraphic unit I isopach map.

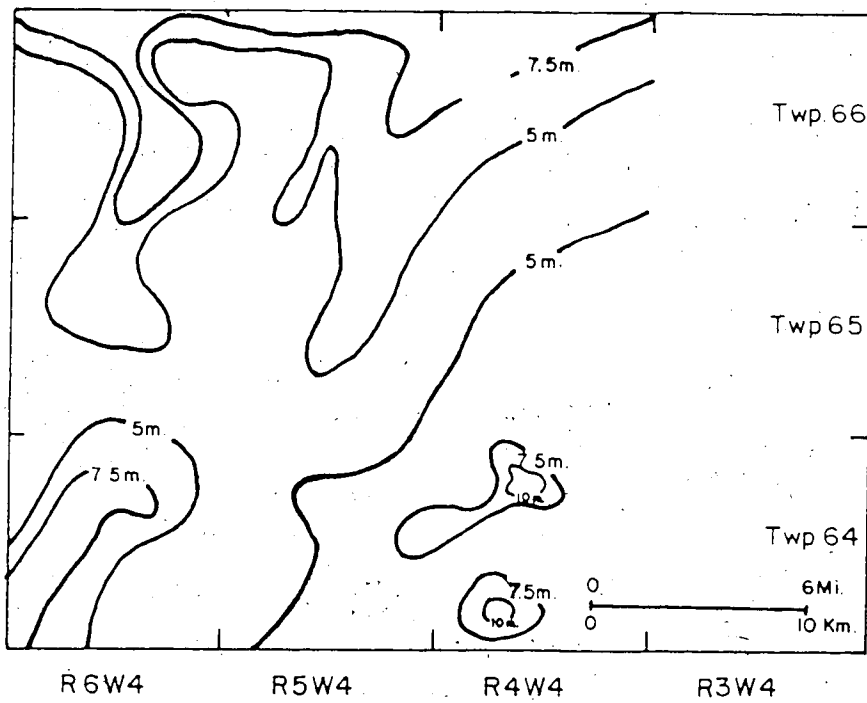


FIGURE 17. Stratigraphic unit H isopach map.

### Stratigraphic Unit G

Stratigraphic unit G (Figure 18) reaches a maximum thickness of 4.5 m (15 ft) over the pre-Cretaceous high in Township 64-6W4. It is thinnest in an east-west trending line through the central part of the area where it is 1.2 m (4 ft) to 2.1 m (7 ft) thick.

### Stratigraphic Unit F

The stratigraphic unit F isopach map (Figure 19) reveals a departure from previous sedimentation patterns. The thickest deposits are found in a line trending southeast-northwest through the centre of the region. Here accumulations of between 15.5 m (51 ft) in the northwest and 26.5 m (87 ft) in the southeast are found. The thick accumulation of sand in the northwest part of Township 64-5W4 and the southwest part of Township 65-5W4 represents the formation of large scale features.

The thinnest accumulations are 9.5 m (32 ft) and are located in the northeast and southwest parts of the region. The pre-Cretaceous unconformity has little effect on the sedimentation pattern for stratigraphic unit F as a whole.

The sand unit enclosed by silty shale (stratigraphic subunit F<sub>2</sub>) was also studied for regional patterns (Figure 20). The silty shale was identified on the basis of an increase in the gamma ray response as compared with the rest of the stratigraphic unit. The actual gamma ray API cutoff varied between wells. Only one silty shale unit could be identified in some wells indicating that this stratigraphic subunit is not regionally correlative. The total thickness of silty shale increases from 0.6 m (2 ft) in the south-central region to a high of 9 m (30 ft) in the north and west.

Thinnest accumulations of shale in stratigraphic subunit F<sub>2</sub> occur towards the southeast, while thicker accumulations occur towards the north and west, suggesting more open marine conditions prevailed in these areas.

The sand/shale ratio map (Figure 21) for this portion of stratigraphic unit F shows that the areas with thicker shales also have a thicker sand unit. Sand/shale ratios range from 0 in areas where there was only one shale bed to 0.75 in the British Petroleum Pilot Plant area (Township 66-5W4). There are definite loci of greater sand content. Some of these areas correspond to highs on the

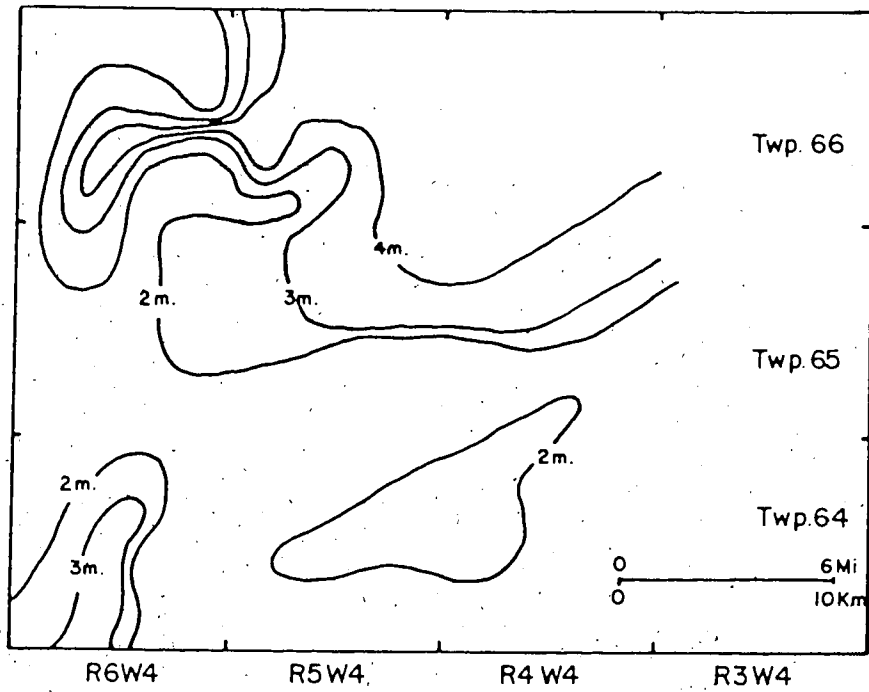


FIGURE 18. Stratigraphic unit G isopach map.

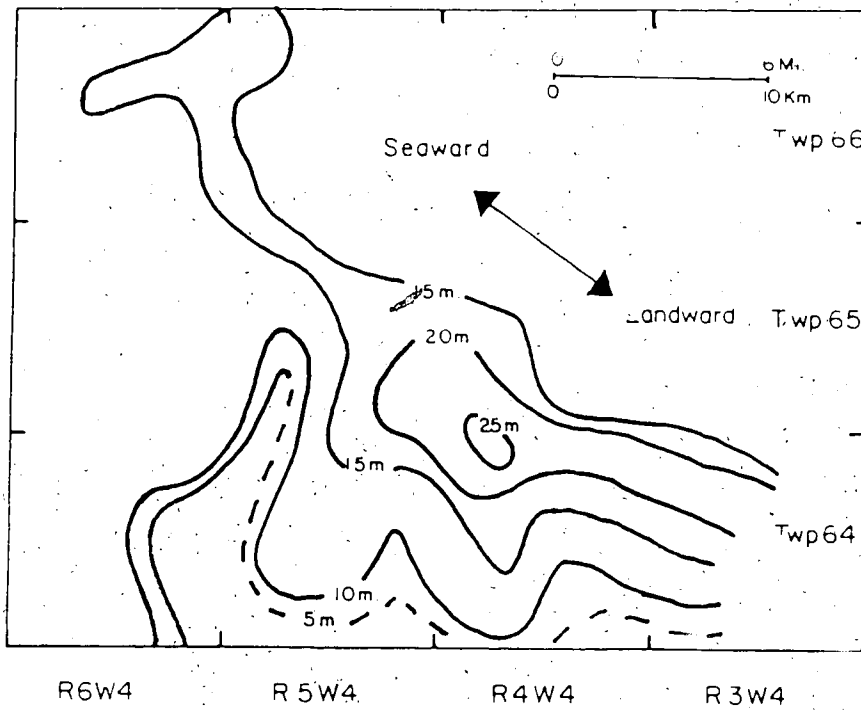


FIGURE 19. Stratigraphic unit F isopach map.

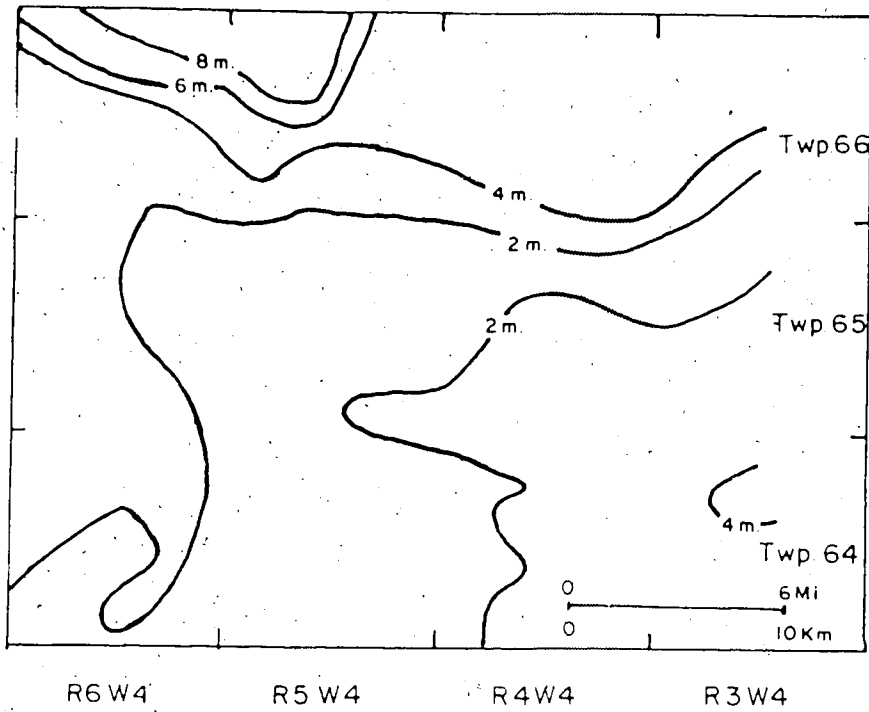


FIGURE 20. Stratigraphic subunit F<sub>2</sub> isopach map.

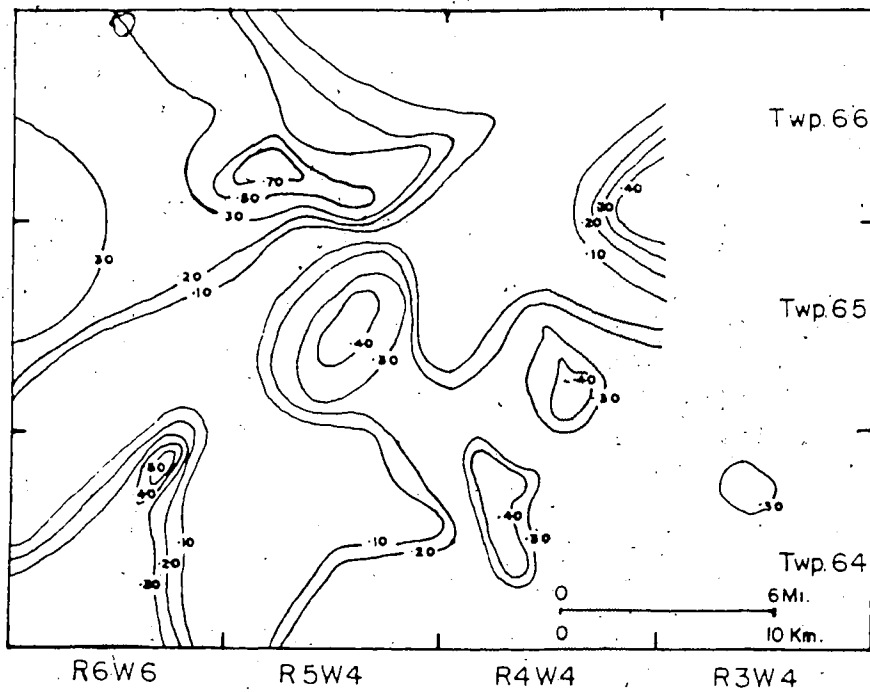


FIGURE 21. Stratigraphic subunit F<sub>2</sub> sand/shale ratio map.

pre-Cretaceous unconformities, whereas others do not. The patches of higher sand/shale ratio values in the southeast part of the region reflect major sites of sand deposition.

#### Stratigraphic Unit E

Stratigraphic unit E is very thin and was recognizable in only a few of the more recently logged wells. It has a very erratic distribution in the northwest part of the region and was not mapped. Its limited extent may be a result of the limitation of the geophysical well log or may reflect an actual limited distribution of this stratigraphic unit, suggesting localized processes for the deposition of this sediment.

#### Stratigraphic Unit D

The distribution of stratigraphic unit D is also erratic (Figure 22). It is thickest in a line trending northeast-southwest in the southwestern part of the region. Here it attains a maximum thickness of 7.2 m (24 ft). This stratigraphic unit is locally thick in the northwestern part of the region (Township 66-6W4) where it is 6.6 m (22 ft) thick. The highs on the pre-Cretaceous unconformity have some influence on the development of thicker accumulations of stratigraphic unit D in this region. This stratigraphic unit has a greater thickness over a high in the southeastern part of the region where accumulations reach 6.4 m (21 ft).

#### Stratigraphic Unit C

Stratigraphic unit C (Figure 23) continues the trends of stratigraphic unit D and attains thicknesses of 5.4 m (18 ft) in the southwest and 6.4 m (21 ft) in the northwest. The effect of the pre-Cretaceous unconformity in influencing thicker accumulations is more pronounced in the southwest. The thinnest accumulation is 1.8 m (6 ft) found in the western part of the region trending northeast-southwest. Stratigraphic unit C is also thick in the south-central part of the region where it attains a thickness of 4.8 m (16 ft).

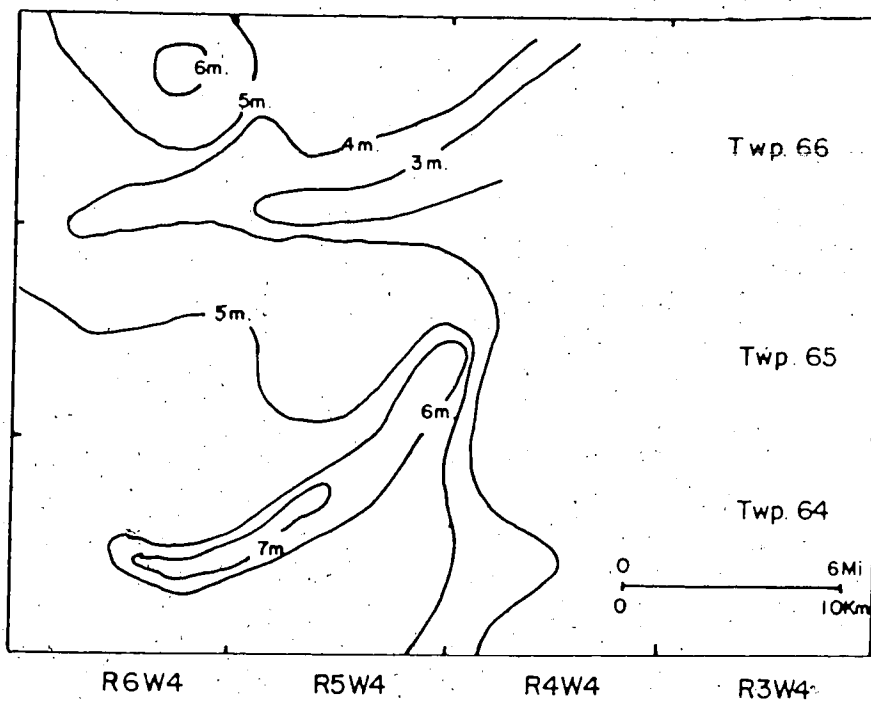


FIGURE 22. Stratigraphic unit D isopach map.

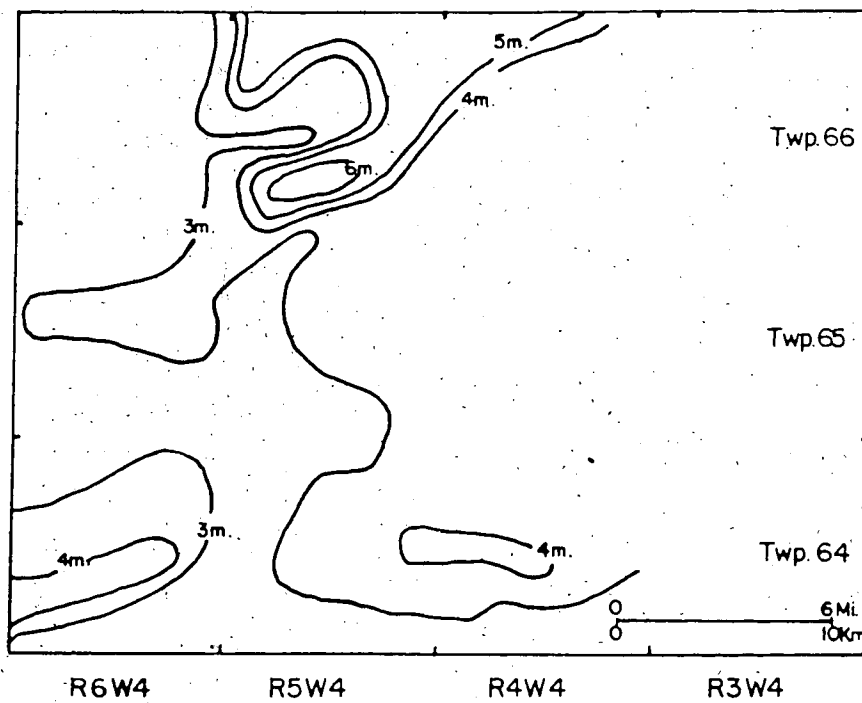


FIGURE 23. Stratigraphic unit C isopach map.



### Stratigraphic Unit B

The distribution of stratigraphic unit B (Figure 24) is similar to that of stratigraphic units C and D. Accumulations in the northwest and southwest are up to 2.1 m (7 ft) over the highs of the pre-Cretaceous unconformity and up to 2.4 m (8 ft) in the east-central area. Thinnest accumulations are again found in a northeast-southwest trend where only 0.6 m (2 ft) of stratigraphic unit B is present.

### Stratigraphic Unit A

Stratigraphic unit A (Figure 25) continues the distribution trend, although it is less variable in thickness. The thickness of this stratigraphic unit ranges from 7.7 m (26 ft) in the northwest and southwest to 6.6 m (22 ft) in the south-central portion of the region to 4.5 m (15 ft) in a northeast-southwest trend in the central part of the region.

## H. Facies Association Interpretation

### Introduction

The mineralogy throughout the Clearwater Formation in this area is a feldspathic litharenite to litharenite (Folk, 1968) with considerable glauconite. Texturally, the sediments are immature to submature (Folk, 1968). The abundance of glauconite and absence of any subaerial features (i.e., dessication cracks, rooted zones, caliches, etc.) suggest that the environment of deposition was marine.

The facies associations and the succession of stratigraphic units in the British Petroleum Pilot Plant area are the result of outer and inner shelf deposition in a shallow marine environment which received very fine-grained detritus from the southeast.

The facies association interpretation and summary of stratigraphic units (Figure 26) is applicable only to the Clearwater Formation in the Cold Lake oil sands deposit and is a local summary rather than a model (Walker, 1979a).

The study of shallow epeiric seas is complicated by limitations in terminology that can be applied to the environments of deposition. The gradient of the epeiric sea floor is low. No discernable slope break is evident in shallow epeiric seas and there is a gradual transition to deeper water sedimentation.

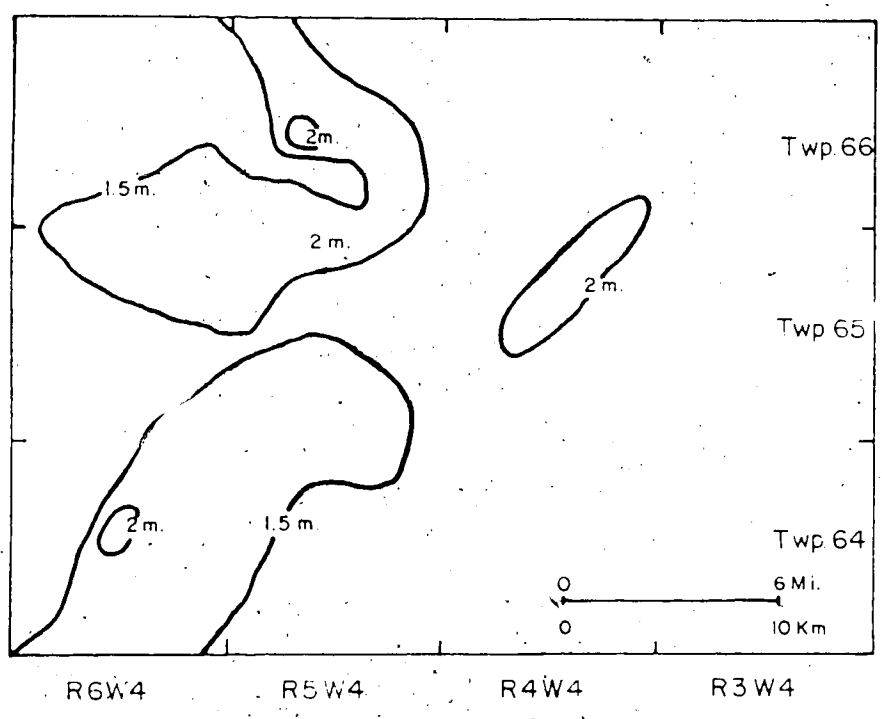


FIGURE 24. Stratigraphic unit B isopach map.

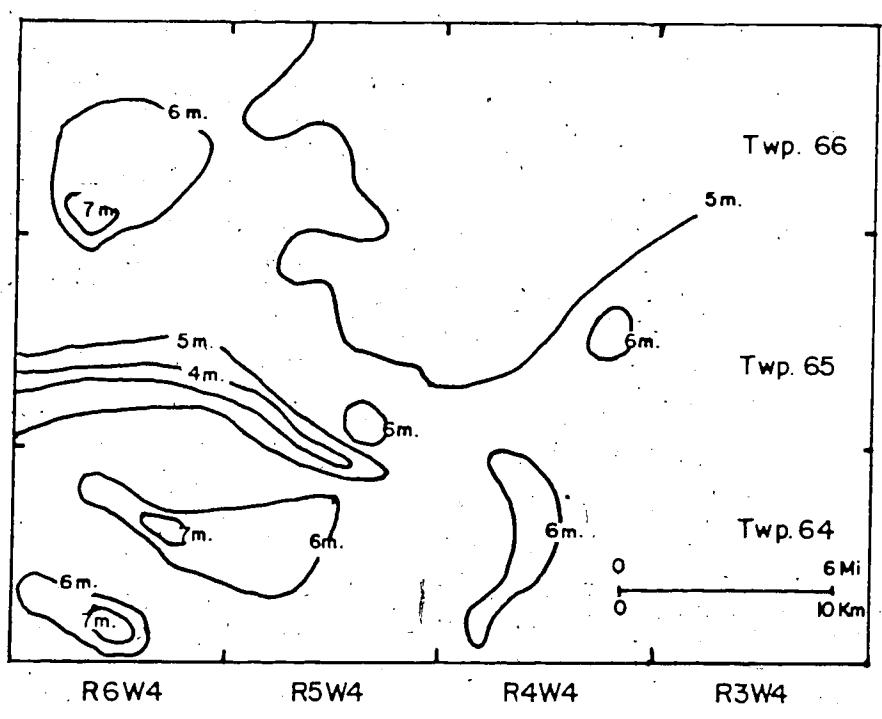


FIGURE 25. Stratigraphic unit A isopach map.

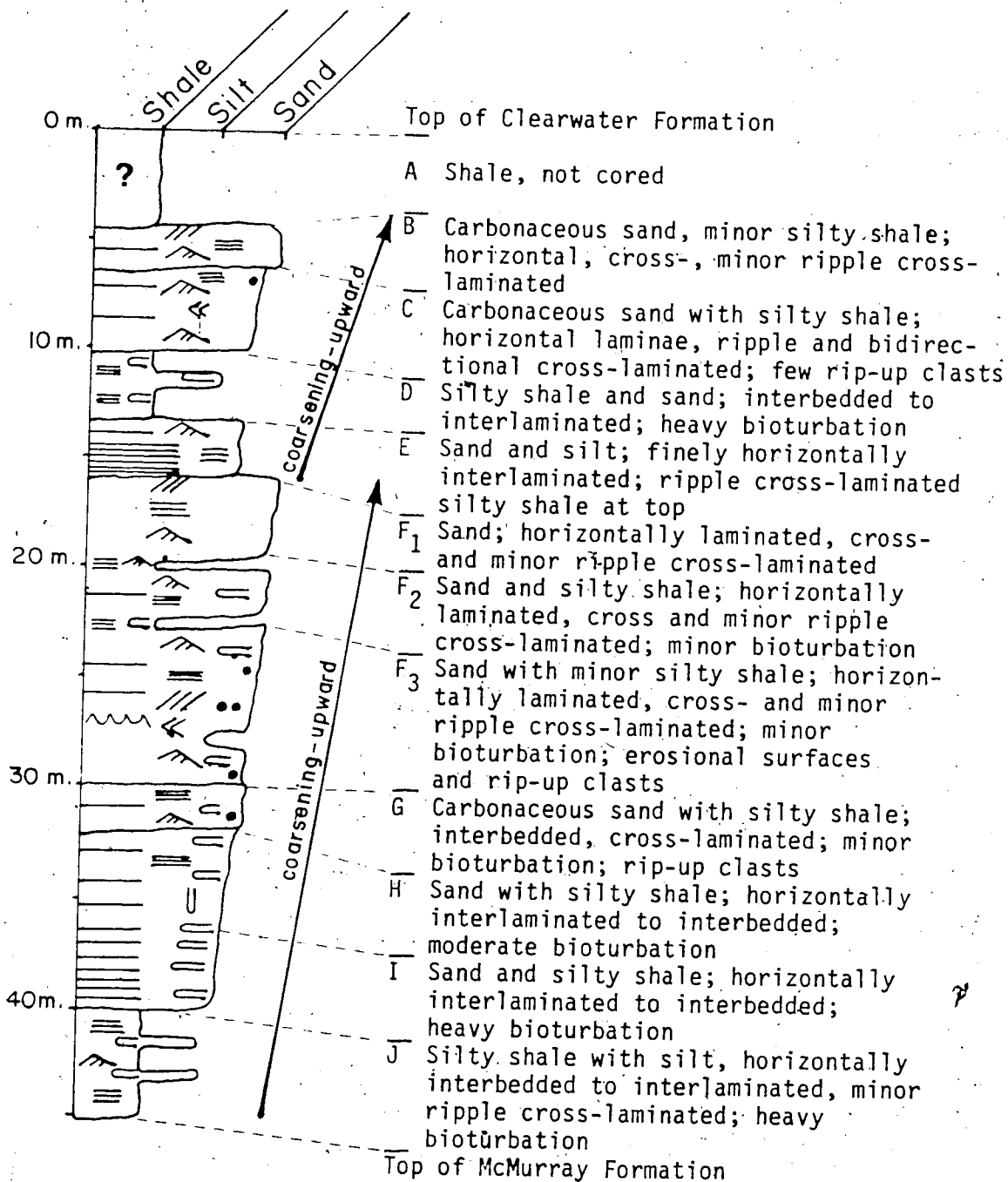


FIGURE 26. Local summary sequence of sedimentary facies associations, showing two coarsening-upward sequences.

The term "shelf" cannot be strictly applied to the siliciclastic sediments in a shallow epeiric sea because it implies the existence of a distinct shelf edge. However, little work has been done to develop a terminology for shallow siliciclastic environments in epeiric seas and the development of this terminology is beyond the scope of this study. The terminology of shelf sedimentation is used informally to describe relative water depth and is not intended to equate epeiric with pericontinental seas.

Depositional features of the shallow marine environment are highly variable and poorly understood. There is no one general theory of shelf sedimentation since many processes and resulting structures are involved (Anderton, 1976; Harms *et al.*, 1975). There are no modern analogues for the sedimentology of the Lower Cretaceous Period in western North America because there are no large modern epeiric seas. Some comparisons can be made between the deposits of modern continental and ancient epeiric seas because similar sand bodies are created (Walker, 1979b). However, caution must be used in the application of modern to ancient sedimentation since hydraulic conditions and basin geometry in continental and epeiric seas are not identical. Furthermore, much of the sediment in modern continental seas is relict glaciofluvial sediment rather than first-cycle sediment. Consequently, the relict paleotopographic structures inherited from previous sedimentation may affect subsequent sedimentation in modern sediments (Swift, 1969; Selley, 1978).

Several modern and ancient partial analogues (Table 2) have been used in the interpretation of the Clearwater Formation in the present study. Partial analogues are indirect comparisons of processes that produce similar deposits.

The shallow marine environment of the Clearwater Sea generated a complex of sedimentary types and grain size distributions, rather than a simple seaward-fining sequence. The shelf zone can be considered as transitional between coastal sands and deep shelf muds, and the sediments are usually clayey silt to silty sand.

A number of partially independent factors influence the sedimentary facies associations in shelf deposits. These include basin geometry and topography (Mooers, 1976), rate and type of sediment supply, type and intensity of hydraulic regime, sea level fluctuations, climate, chemical factors and animal-sediment interactions (Johnson, 1978).

Table 2.

Partial Analogues used in Facies Association Interpretation

## Modern Partial Analogues:

<u>Location</u>	<u>Source</u>
North Sea	Stride, 1963.
Florida and Bahamas	Ball, 1967.
North Sea	Reineck, 1967.
North Sea	Caston, 1972.
Various - review	Ginsberg, 1975.
Atlantic and North Sea	Brenner, 1980.
Bering Sea	Field <i>et al</i> , 1981.
Washington Continental Sea	Nittrouer and Sternberg, 1981.
New York Bight	Vincent <i>et al</i> , 1981.
North Sea	Harms <i>et al</i> , 1982.

## Ancient Partial Analogues:

<u>Location</u>	<u>Geologic Period</u>	<u>Source</u>
Carolina, U.S.A.	Upper Cretaceous	Swift, 1969.
Wyoming and Montana	Upper Jurassic	Brenner and Davies, 1973.
Various - review	Various - review	Ginsberg, 1975.
Wyoming	Upper Cretaceous	Harms <i>et al</i> , 1975.
Scotland	PreCambrian	Anderton, 1976.
Wyoming	Upper Cretaceous	Brenner, 1978.
Wyoming and Montana	Jurassic - Cretaceous	Brenner, 1980.
Norway	PreCambrian	Levell, 1980.
Western Interior, N.A.	Lower Cretaceous	Bridges, 1982.
Western Interior, U.S.A.	Upper Cretaceous	Harms <i>et al</i> , 1982.
Texas	Lower Cretaceous	Hobday and Morton, 1984.
Montana	Upper Cretaceous	Rice, 1984.
Montana	Upper Cretaceous	Shurr, 1984.
Western Interior, U.S.A.	Upper Cretaceous	Swift and Rice, 1984.
Wyoming	Upper Cretaceous	Tillman and Martinsen, 1984.

The hydraulic regime in the shallow marine setting is very complex, consisting of a number of interactive currents. Several depositional processes, such as tidal currents, meteorologic currents (both storm and rip currents), storm density currents, regional ocean currents, and various combinations of the above transport and rework the sediments (Howard, 1972; Johnson, 1978; Walker, 1979b; Harms et al., 1982).

There is discussion as to the relative significance of storm activity and tidal activity in the deposition of sediment in epeiric seas. Storms cause much of the mass movement of sediment in shallow marine environments (Brenner and Davies, 1973). Tides strongly influence the reworking of these sediments (Off, 1963; Johnson and Belderson, 1969; Swift, 1969; Klein, 1977). The tidal range during the Cretaceous Period has been estimated at 0.86 m with current velocities up to 10 cm/sec (Slater, 1984). When the bottom gradients are very low, tides can affect a large area. The sediments in the Clearwater Formation exhibit both storm and tidal depositional features as will be discussed in the following section.

Tectonic rather than eustatic sea level changes also affected sedimentation. The epeiric sea was located in a foreland basin adjacent to the developing Western Cordillera. This basin subsided in response to the loading of successive thrust plates in the Western Cordillera and in response to the weight of sediment being shed from these plates. Each thrust created a pulse of subsidence and sedimentation in the foreland basin (Jordan, 1981; Beaumont, 1981). A net sea level rise of 70 metres during Mannville time is predicted due to tectonic activity (Beaumont, 1981). Both orogenic activity and the pre-Cretaceous topography control sedimentation in the Clearwater Formation in Cold Lake.

The exact nature of the input mechanism for the Clearwater deposits is not known because no paleoshore features were preserved in the area of study. The distribution of the sands and the presence of higher amounts of silt and clay-sized material to the northwest suggest that the source of sediment was from the southeast.

Input of sediment may have been from a deltaic complex or from storm surge-ebb erosion of a generally prograding shoreline, similar to that described by Banks (1973) in the late Pre-Cambrian Innerelv Member of Norway. There is no concrete evidence for a well-developed deltaic complex in the Clearwater Formation. There is no evidence of

deposition of relatively thick units representing prodelta, delta front and delta top sequences. The alternation of sand, silt and shale found in most facies associations suggests that fluctuating currents played an important role in deposition and modification of the sediments. The presence of silty shale intraclasts in many of the facies associations also suggests periods in which high energy conditions existed. Consequently, it is proposed that the sediment supplied to the area was distributed by storm and other currents which were strong enough to preclude the development of a delta. The coarsening upward sequences are the result of general progradation of the shoreline.

#### **Coarsening-upward Sequence: Stratigraphic Units J to F**

This coarsening-upward sequence is similar to that described by Harms, *et al* (1982) as a series of broad sandy shoals (stratigraphic unit F) built upward from a floor of muddy shelf deposits (stratigraphic unit J). The coarsening-upward trend is seen in the geophysical well logs and in the core analysis. This represents an increase in the intensity of the currents which were able to carry a progressively coarser bedload. The sediment bypassed the nearshore environment largely due to density stratification currents generated by storms. Once deposited on the shelf, the sediment was reworked by currents. There was some influence by tidal currents indicated by widely scattered tidal current-generated structures, such as bi-directional low-angle cross-lamination. The textural and compositional immaturity of the sands suggests that tidal reworking and winnowing was minimal.

#### **Stratigraphic Unit J: Facies Association 2**

Stratigraphic unit J consists of a bioturbated silty shale with rare moderately oil stained argillaceous silt and very fine-grained sand interlaminae.

Stratigraphic unit J was deposited on the muddy outer shelf. The muds were deposited from the suspended load of an river which bypassed the coastal region by storms. The predominately horizontally laminated nature of the sediment is suggestive of deposition below effective wave base. Minor tidal and oceanic current influences are present in the southeast of the study area and are represented by bi-directional low angle cross-lamination and ripple cross-lamination. Sedimentary structures, the presence of greater amounts of carbonaceous debris,

the coarser-grained silty nature of well 6-3-66-5W4 and the overall thickening of the unit to the northwest indicate proximity to a shoreline towards the southeast. The occurrence of traces of Planolites nicholson (1873) is not in itself diagnostic of shelf sedimentation, but its presence in all cores suggests a low energy environment with a good food supply which supports the interpretation.

#### Stratigraphic Unit I: Facies Association 2

Stratigraphic unit I consists of a bioturbated silty shale with interbeds of silt and very fine-grained sand.

Sedimentation in this shelf facies was dominated by storm-generated density stratified currents. The intermittent storms divided the sediment into bedload and suspended load and moved it across the shelf. Similar sequences have been interpreted by Walker (1979b) for the Cardium Formation of Alberta and Swift and Rice (1984) for the Upper Cretaceous of Montana and Wyoming. The coarse sediments represent a periodic short-lived event when the silt and very fine-grained sand was introduced into an otherwise quiescent environment. Successive storms built up a silt and mud sequence. Between storms the silty shales were consolidated and bioturbated. This accounts for the relative paucity of storm rip-up clasts in the storm deposited sands. The high degree of bioturbation suggests that storm events were sufficiently far apart to allow for the establishment of large communities of organisms which fed on these deposits. After each storm event the communities re-established themselves. The more seaward portion of the stratigraphic unit is situated to the northwest where it is more shaly.

#### Stratigraphic Unit H: Facies Association 3

Stratigraphic unit H consists of a very fine-grained sand with interlaminae to interbeds of silty shale and silt. The silty shale is heavily bioturbated at the base of stratigraphic unit H and decreases upward.

The increased strength of storm currents in a shallow water environment is indicated by the sedimentation pattern of stratigraphic unit H. The density stratified storm currents were capable of transporting larger amounts of very fine-grained sand as bedload. The greater number of silty shale intraclasts in the sands suggests



that the silty shale did not develop enough cohesion to withstand the next storm pulse as effectively as in stratigraphic unit I. The fewer number of traces of Planolites nicholson (1873) suggest that higher energy conditions did not allow the establishment of large communities of organisms. This interpretation is reinforced by the presence of load casts indicating differential loading of the sands on water-saturated muds during deposition.

The presence of the trace of Skolithos linearis haldeman (1840) is not paleoenvironmentally diagnostic. Although many researchers (Seilacher, 1967; Crimes, 1970; Frey, 1975) claim that the presence of the trace of this suspension feeder indicates a nearshore environment, others (Alpert, 1974; Basañ and Frey, 1977) point out that this trace can be found in environments ranging from the outer shelf to the shoreface. These traces were made by organisms particularly adapted to unstable environments which are characterized by rapid sedimentation. The association of Skolithos linearis haldeman (1840) and Planolites nicholson (1873) is suggestive of an oxygen-depleted stressed environment (Ekdale et al., 1984).

#### Stratigraphic unit G: Facies Association 3

Stratigraphic unit G consists of very fine-grained sand with interlaminae to interbeds of silty shale and silt. Sand units are thicker than those in stratigraphic unit H. Bioturbation is less extensive than in stratigraphic unit H and decreases upward.

The structures and lithology of this stratigraphic unit suggest that it was deposited closer to the paleoshore in a shelf setting. The silty shale and sand interbeds are suggestive of storm surge-ebb deposition. Sand was deposited during the waning period of a storm and the silty shale was deposited and partially bioturbated during quiescent periods. The isopach map pattern (Figure 18) suggests that the pre-Cretaceous highs served as loci for stratigraphic unit G deposition. The abundance of organic material, especially in well 6-3-66-5W4, is suggestive of proximity to the paleoshore to the southeast. Some tidal current influence is indicated by the presence of bi-directional low angle cross-laminae. Inclined low-angle cross-laminae (which may be trough cross-laminated) suggest current reworking of the sediment. An exclusively tidal interpretation for this facies is difficult because the tidal-generated structures are found in association with

structures which may have been created by oceanic currents or waves.

Biogenic activity is sparse, indicating a slightly higher energy level and/or a more rapidly prograding substrate.

#### Stratigraphic Unit F: Facies Associations 4 and 6

Stratigraphic subunit F<sub>3</sub> (Facies Association 6) consists of finely laminated poorly sorted sand with rare carbonaceous silty shale laminae. Stratigraphic subunit F<sub>2</sub> (Facies Association 4) consists of a very fine-grained, moderately poorly sorted, laminated to inclined low-angle cross-laminated sand unit with silty shale and siltstone interbeds. Stratigraphic subunit F<sub>1</sub> (Facies Association 6) consists of horizontally laminated very fine-grained, poorly sorted sand with rare silty shale interlaminae.

Stratigraphic unit F represents large amounts of storm-transported very fine-grained sand, silt and clay modified by tidal, oceanic and subsequent storm currents. Similar sequences have been reported by Ball (1967) in recent sediment in Florida and the Bahamas, Amajor (1980) in the Lower Cretaceous Viking Sandstone of central Alberta, Brenner (1980) in the Jurassic and Cretaceous of Wyoming and Montana, Field *et al* (1981) in the Bering Sea, Vincent *et al* (1981) in the New York Bight, and Swift and Rice (1984) in the Upper Cretaceous of the western interior of the United States. Some of the sediment may have been transported during peak tides as well.

The coarsening-upward nature of the deposit and the thicker accumulation of sand may be due in part to shallowing as the inferred shoreline located towards the southeast prograded. The current-generated structures, the interlaminae of silty shales and the lack of bioturbation suggest that higher energy conditions existed at the time of deposition of stratigraphic unit F. Thick (up to 12 m) units of inclined low-angle cross-laminated sands suggest the formation and maintenance of large scale structures. The isopach map (Figure 19) shows a northwest to southeast trend to sediment distribution. This suggests that after initial deposition, the sediment was reworked and local topographically higher structures were created and maintained. It is proposed that stratigraphic unit F was deposited in the form of poorly developed bars and ridges.

The classification of sand deposits in the shallow marine environment is confused (Levell, 1980; Belderson *et al.*, 1982) and still in debate. The classification proposed by Shurr (1984) is based primarily on sand body geometry. According to this classification, the deposits in the Clearwater Formation are sand bars to sand ridges in well 6-5-66-5W4 where there is an accumulation of 12 m (40 ft) of cross-laminated to trough cross-laminated sand. Additional evidence is supplied by the spontaneous potential and gamma ray responses (Serra and Sulpice, 1975; Pirson, 1981b) both of which are subdued. This suggests the presence of bar-type deposits.

The deposits of stratigraphic unit F are similar to those described by Rice (1984) and Tillman and Martinsen (1984) in the Upper Cretaceous Shannon Sandstone of the northwestern plains area in the United States. The deposits were described as elongate discontinuous sand bodies on a shallow flat shelf with associated bar margin and interbar deposits. The deposits in stratigraphic unit F are also similar to those described by Brenner (1978) in the Sussex Sandstone of Wyoming as a shelf ridge complex. These deposits are comparable to the storm and tide built sand ridges on the modern Atlantic Continental Shelf or the Bight of the North Sea. However, the deposits found in Cretaceous sediments are on a smaller scale than the modern ridge because the epeiric sea was much more shallow which limited the vertical growth of the ridges. The presence of the coarsening-upward ridges reflects a shallowing of the Lower Cretaceous epeiric sea and an increase in the supply of siliclastic material to the area. The occurrence of these bars and ridges was controlled by topographic highs on the sea bottom. Their orientation was controlled by southeast-northwest trending currents (Figure 19). Slight topographic variations can result in spatial velocity gradients that induce deposition. Once deposition was initiated, the bars enhanced the topography and became self-perpetuating closed systems.

Thinner accumulations of very fine-grained sand and silty shale represent smaller scale sand waves and ripples superimposed on the bars and ridges. The structures exhibited include ripple cross-lamination, clay drapes on ripples and bi-directional low-angle cross-lamination. These sedimentary structures reflect

some tidal reworking of the sediment, although it is difficult to distinguish tidal current from other current deposits. Flaser structures found in this facies can be interpreted as either storm-generated or tidal-generated.

The interbedded finely laminated and ripple cross-laminated silty shale, argillaceous silt and very fine-grained sand found in stratigraphic unit F represent interbar and bar margin deposition.

Erosional surfaces represent uncorrelative channels. The presence of such channels is suggestive of proximity to the paleoshore. These channels are infilled by ripple cross-laminated and dune cross-laminated sands which migrated on the channel floor.

There is no evidence of emergence in these deposits, although wells 6-3-66-5W4 and 6-5-66-5W4 contain larger amounts of carbonaceous debris, indicating their proximity to the paleoshore.

#### **Coarsening-upward Sequence: Stratigraphic Units E to B**

This coarsening-upward sequence represents deposition in an inner shelf environment. The inner shelf environment is characterized by a progression towards a coarser sand-size fraction, a decrease in bioturbation and an increase in sorting of the sediment due to an increase in energy shoreward.

The inner shelf is dominated by wind (storm) effects unless there is a high tidal influence (Mooers, 1976; Harms *et al.*, 1982).

No foreshore or upper shoreface sedimentation was recognized in the cores and a paleoshore trend cannot be reconstructed. There are several explanations for this omission in the rock record. In this shallow marine environment with its low-sloping sea bottom any fluctuation in sea level will rapidly shift the shoreline over a great distance. This would preclude the development of distinct beach sequences. The effects of storms and tides would cause erosion of any beach deposits. This creates a paucity of shoreline deposits and a trend towards sand storage in submarine sand bodies rather than beach deposits. The zone of waves and tides in an epeiric sea may have been miles from the shore, preventing the the formation of beach deposits.

#### Stratigraphic Unit E: Facies Association 6

The basal portion of stratigraphic unit E consists of horizontal, finely interlaminated sand and silt. The upper portion consists of horizontally laminated and ripple cross-laminated silty shale and very fine-grained sand.

The deposit in stratigraphic unit E is the best indicator of tidal influence in the Clearwater Formation. The rhythmic finely interlaminated sediments are tidal bundles reflecting small scale repeated alteration in sediment transport conditions. The sand laminae were deposited as bedload during the higher velocity phase of the tidal cycle and are the remnants of very flat-crested ripples. The silt laminae were deposited during the slack phase of the tidal cycle when fines came out of suspension.

The presence of tidal bundles is not paleoenvironmentally diagnostic within tidal settings as they can be found in both intertidal and subtidal environments. The lack of emergent structures, such as mud cracks, suggests that the tidal bundles were deposited in a subtidal environment.

The presence of less well-developed tidal bundles and bi-directional low-angle cross-laminae in well 2-19-66-5W4 suggest that the effects of tidal currents were widely distributed. However, the lack of deposition of tidal bundles in wells 10-7-66-5W4 and 10-17-66-5W4 and the inability to trace this stratigraphic unit regionally suggest that tidal currents of sufficient regularity to produce tidal bundles were a locally restricted phenomena.

#### Stratigraphic Unit D: Facies Associations 1 and 3

Stratigraphic subunit D<sub>3</sub> (Facies Association 1) consists of a heavily bioturbated silty shale. Stratigraphic subunit D<sub>2</sub> (Facies Association 3) consists of a bioturbated poorly sorted sand with interbeds of bioturbated silty shale.

Stratigraphic subunit D<sub>1</sub> (Facies Association 1) consists of a heavily bioturbated silty shale.

A change in sediment supply is indicated by the deposition of stratigraphic unit D. The thick accumulations of bioturbated silty shale suggest that the supply of very fine-grained sand was interrupted. Mud zones can have a number of interpretations, such as a muddy coast, a nearshore mud belt, an mid-shelf mud belt, an outer-shelf mud belt or a mud blanket off a delta (McCave, 1972; Anderton,

1976; Johnson, 1978). With the exception of the outer-shelf mud belt, all of these features are of limited aerial extent. In the case of stratigraphic unit D, the shales have a broad distribution beyond the area of the regional study (Wightman, personal communication). The isopach map (Figure 22) suggests that thicker accumulations occur seaward to the north and west. This would suggest that broader forces, such as regional subsidence and/or a temporary decrease in coarser sediment supply due to a temporary cessation of tectonic activity in the Western Cordillera, which was the main source of detritus, were in effect at this time. This caused the development of an extensive shallow marine shelf mud.

The presence of intraclasts suggests that the interbed of very fine-grained sand represents storm-transported sediment. However, the highly bioturbated nature of the sand and the presence of the silty shale above it suggest that after sand deposition, relatively quiescent conditions continued. This allowed the extensive biogenic reworking of these sediments.

#### Stratigraphic Unit C: Facies Association 5

Stratigraphic unit C consists of graded sand, silt and shale interbeds.

The deposit in stratigraphic unit C represents a return to the previous very fine-grained sand, silt and clay sediments derived from a source situated to the southeast.

Stratigraphic unit C is interpreted as being located in an inner shelf, environment between the shoreface and deep water. Proximity to the paleoshore is suggested by the high organic content in the deposit, although there is no evidence of emergence. Storm and tidal influences were dominant in this environment. Storm-generated turbidity current deposits were common and were separated from each other by finer-grained deposits and wave ripple cross-laminated sands. Periodic storm turbidity currents transported the very fine-grained sand, silty shale intraclasts, silts and clays as suspended load creating a graded sand, silt and shale sequence of up to 0.37 m (1.25 ft) in thickness displaying Bouma sequences. The sediment load of the Western Interior Cretaceous seaway was very fine-grained and created sequences skewed towards the fine-grained end.

The deposits in stratigraphic unit C also reflect deposition from tidal currents, exhibited by bi-directional low-angle cross-lamination which is found in all cores studied. The inclined low-angle interlaminated silty shale, silt and sand represent accretion surfaces of a small scale bedform.

Weak bioturbation is indicative of fast migration of sediments in an inner shelf environment.

#### Stratigraphic Unit B: Facies Association 6

Stratigraphic unit B consists of poorly sorted laminated sand interlaminated to interbedded with laminated silty shale.

The accumulation of up to 2.1 m (7 ft) of horizontally laminated to inclined cross-laminated sands in stratigraphic unit B represents the development of small scale shoaling sand bars above the effective wave base in an inner shelf environment. The isopach map (Figure 24) outlines these bars and suggests that they were oriented parallel to the inferred shoreline to the southeast. This feature is best developed in well 10-17-66-5W4. The interlaminated silty shale represents bar margin and interbar sedimentation in the lee of these bars. Shallow marine tidal or storm-generated dunes are represented by the thinner accumulations of cross-laminated sands associated with laminated sand and silty shale.

There is no evidence of emergence in these deposits, although large concentrations of carbonaceous debris indicate proximity to the paleoshore. Weak bioturbation is indicative of the shallow water conditions and fast migration of sediments.

#### Stratigraphic Unit A

This stratigraphic unit was not cored so definite paleoenvironmental interpretation cannot be made. Equivalent shales in the Cold Lake, Wabasca and Athabasca oil sands deposits have been interpreted as open marine outer shelf muds (Mossop *et al.*, 1981 and others). This stratigraphic unit represents a transgression of the epeiric sea over the inner shelf sediments.

### Summary

The Clearwater Formation in the study area consists of two coarsening-upward sequences (Figure 26). The first sequence (stratigraphic unit J to stratigraphic unit F) was deposited in an outer shelf environment and the second sequence (stratigraphic unit E to stratigraphic unit B) was deposited in an inner shelf environment.

The first coarsening-upward sequence is approximately three times thicker than the second coarsening-upward sequence. This apparent discrepancy in thickness can be attributed to the presence of stacked offshore bars in stratigraphic unit F. The silty shale and siltstone in stratigraphic subunit F<sub>2</sub> represent interbar or bar margin deposits which delineate the sand bars. The inner shelf sediments (stratigraphic units B and C) were deposited after a period of subsidence. This subsidence resulted in a change in the basin geometry and the sediment source area. Consequently, the two coarsening-upward sequences represent different sets of processes and products and do not reflect a single prograding shoreline.



## IV. Mineralogy

### A. Bulk Mineralogy

Forty-one thin sections in well 10-17-66-5W4 were examined to establish the mineralogy of the Clearwater Formation at this location. Relative percentages of point counts are given in Appendix II. Mineralogic composition is summarized and compared with Putnam and Pedskalny (1982) and Harrison *et al* (1981) in Table 3.

Grain mineralogy consists of quartz with lesser amounts of chert and feldspar. Igneous, volcanic, metamorphic and sedimentary rock fragments were present in most samples. The complex mineralogy suggests a combination of source rocks. The rock is composed of feldspathic litharenites to litharenites, according to Folk's (1968) classification (Figure 27). Points plotting low on the feldspar / igneous rock fragments end of the ternary diagram contain a calcareous matrix which has replaced many feldspar grains as well as other primary mineralogy.

Composition compares well with Harrison *et al*'s (1981) study in Townships 64 and 65, Range 3W4 and Putnam and Pedskalny's (1983) study in Township 64, Range 4W4, both of which are situated southeast of the present study. However, the B.P. pilot plant site exhibits a more equitable distribution of feldspathic litharenites and litharenites and contains slightly more quartz grains. This is due to farther transport of the sediments to the B.P. pilot plant site. While there are no obvious trends in the distribution of the two compositions, the upper stratigraphic units (B, C and D<sub>2</sub>) and the lower stratigraphic units (G, H, and I) are composed predominantly of feldspathic litharenites. In stratigraphic units E and F, litharenites predominate, although feldspathic litharenites are a component of stratigraphic subunits F<sub>2</sub> and F<sub>3</sub>.

The dominant lithic grains are metamorphic rock fragments (29.5 percent). This finding is at variance with Harrison *et al* (1981) and Putnam and Pedskalny (1983) who found that volcanic rock fragments and chert were the dominant lithic grains. The main reason for this discrepancy is that the large proportion of polycrystalline quartz rock fragments were classified as volcanic rock fragments by Putnam and Pedskalny (1983) and presumably by Harrison *et al* (1981), while the present study classifies them as metamorphic rock fragments. This discrepancy will be discussed in detail under

Table 3.

COMPARATIVE MINERALOGY

	<u>THIS STUDY</u>		Putnam	Harrison
	Overall Composition (%)	Recalculated to 100%	and Pedskalny (1982) (%)	et al (1981) (%)
Quartz	15.7	33.3	22.8	21.0
Chert	4.0	8.5	11.4	20.0
Feldspar	4.7	10.0	27.9	28.0
Igneous Rock Fragments	3.4	7.2	—	—
Metamorphic Rock Fragments	13.9	29.5	10.0	5.0
Sedimentary Rock Fragments	2.1	4.5	11.4	3.0
Volcanic Rock Fragments	3.3	7.0	16.5	23.0
Clastic Carbonates	4.0	<u>100.0</u>	<u>100.0</u>	<u>100.0</u>
Glaucanite	2.3			
Mica	0.5			
Chlorite	2.3			
Sericite	0.5			
Zircon	0.8			
Opaques	0.5			
Organics	7.4			
Clay	4.0			
Oil	7.2			
Pore Space	4.4			
Matrix	6.3			
Calcareous Cement	9.7			
Quartz Overgrowths	0.7			
Unidentified Rock Fragments	<u>0.2</u>			
	100.0			

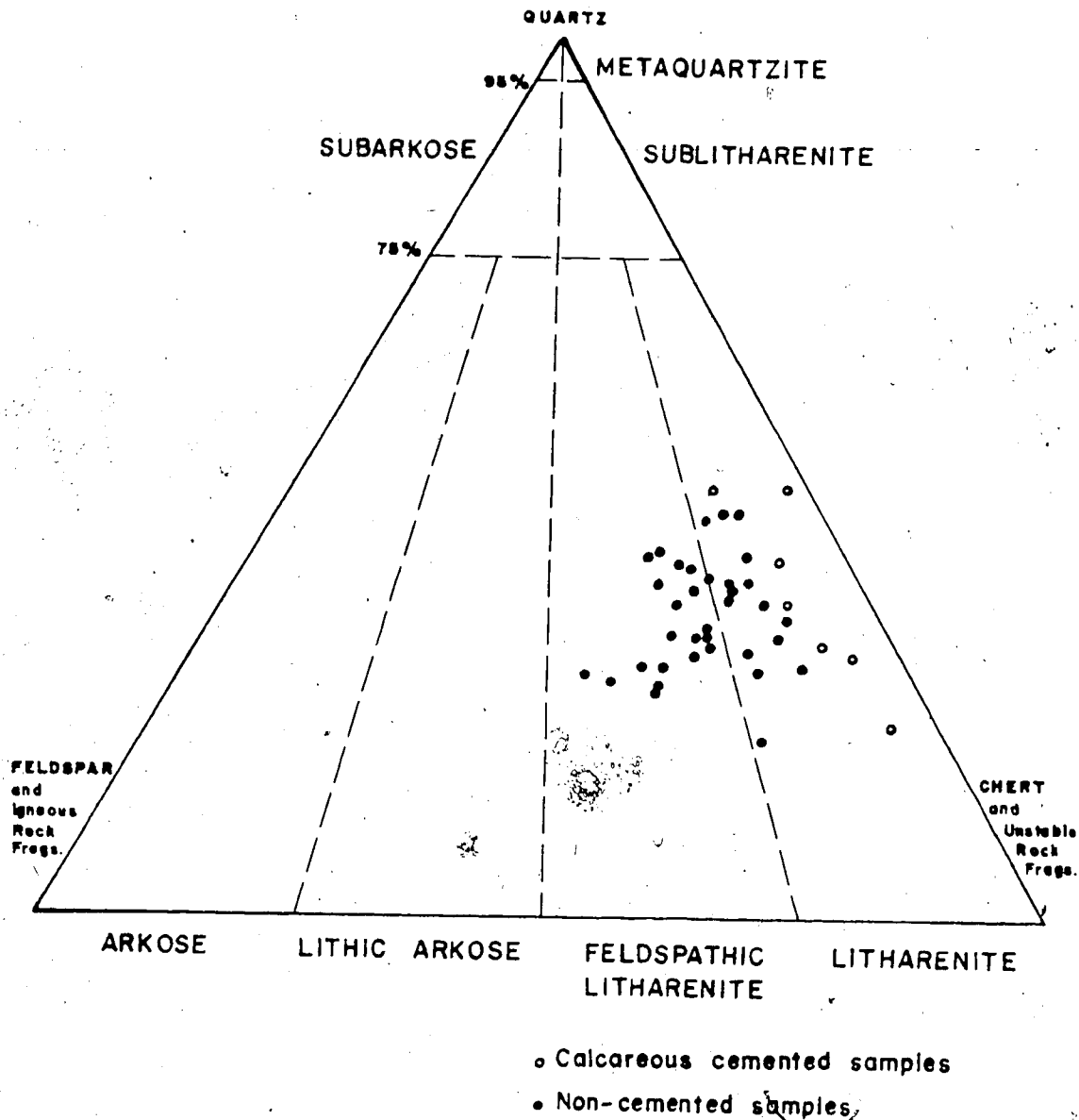


FIGURE 27. Ternary plot of point-counted thin sections from well 10-17-66-5W4, showing classification of sands as feldspathic litharenites and litharenites.

(after Folk, 1968)

metamorphic rock fragments. Note that the classification of polycrystalline quartz rock fragments does not affect the ternary diagram, since both metamorphic and volcanic rock fragments plot as labile rock fragments.

### Quartz

Unicrystalline quartz grains make up between 1 percent and 24 percent of the total mineralogy. They are generally subangular to subrounded and uniformly very fine-grained. Some very well-rounded grains were observed in the massive sands of stratigraphic unit F, suggesting reworking of this sediment. Straight and undulous or strained extinction was observed in the quartz grains.

Authigenic quartz overgrowths (Plate 6-2) are a minor constituent, but were found in most thin sections examined. Most of these overgrowths exhibit weathering and are derived from a previous depositional cycle.

Authigenic feldspar overgrowths (Plate 4-1) are rare and show abrasion, indicating formation in a previous depositional cycle.

### Chert

Chert grains make up between 1 percent and 7 percent of total rock volume. This can only be considered an estimate, since it is difficult to differentiate between some polycrystalline quartz grains and chert. An arbitrary distinction was made which assigned grains with randomly oriented microcrystals, less than 10 microns in diameter to chert (Folk, 1968, p. 70). The colour of chert ranges from white to black. Most grains are subangular, although rare rounded grains and lathe-shaped fragments were noted in stratigraphic unit B.

### Feldspar

Feldspars, both plagioclase and potassium, are found throughout the core. They make up between 1 percent and 9 percent of total rock volume. Many of the plagioclase feldspars exhibit a euhedral crystal outline, well-defined crystal faces and albite twinning (Plate 4-2), all indicative of a volcanic origin (Scholle, 1979). Potassium feldspars are dominantly orthoclase. Most feldspar grains are subangular with some platy fragments

noted. This suggests moderate transport distances. Overburden pressure is sufficient to fracture some feldspar grains (Plate 4-3). Alteration of the feldspars to kaolinite clay and calcite is seen, but many feldspar fragments are quite fresh, a reflection of little reworking and good preservation of the sediment.

### Rock Fragments

Plutonic (igneous and volcanic), metamorphic and sedimentary rock fragments are found throughout the core and can contribute up to 38 percent of the total rock volume.

Igneous rock fragments were distinguished from metamorphic rock fragments on the bases of the presence of igneous trachytic texture, coarse equant crystals and unequal crystal sizes in the grain (Scholle, 1979). Many grains are highly corroded. The proportion of igneous rock fragments increases from none at the base of the core to 13 percent in stratigraphic unit B which is situated near the top of the formation. This suggests a shift in source area during Clearwater Formation time.

While it is agreed that the immature nature of the rock composition indicates that the major source of detritus is from the newly-forming Cordillera to the west (Williams, 1963; Maycock, 1964; Rudkin, 1964; Cameron, 1965; Rapson, 1965; Putnam and Pedskalny, 1983), the presence of the degraded igneous fragments may suggest a minor component of detritus from the Shield area to the northeast (Mellon, 1967; Keeler, 1980; Harrison *et al.*, 1981). Further petrographic work is needed to confirm this proposition.

Volcanic rock fragments, derived from the Cordilleran region to the west (Putnam and Pedskalny, 1983) are found throughout the core in relative percentages ranging from 1 percent to 8 percent. Searlesite fragments were observed in stratigraphic unit B. The identification of volcanic rock fragments was based primarily on the presence of predominately feldspathic micropheocrysts. These micropheocrysts are commonly untwinned and strongly zoned (Plate 4-4).

Metamorphic rock fragments contribute between 3 percent and 26 percent to the mineralogy. Grains exhibit strongly oriented, sutured and rare schistose textures and are subangular to subrounded, indicative of moderate transport. Polycrystalline quartz was identified as a metamorphic rock fragment (Plate 5-1) rather than a volcanic rock fragment (c.f., Putnam and Pedskalny, 1983). Quartz from a volcanic source is usually

monocrystalline and fractured (Blatt *et al.*, 1980, p. 289). Rapson (1965) could not recognize volcanic quartz in age equivalent sediments deposited in the southern Rocky Mountains of Alberta. It is proposed, therefore, that polycrystalline or composite quartz is indicative of a metamorphic source (Mellon, 1967; Scholle, 1979; Blatt, 1982).

Metamorphic quartz exhibiting inclusions was also noted (Plate 7-3).

Fine-grained sedimentary rock fragments of silt, silty shale, and shale contribute between 1 percent and 5 percent to total rock volume. Most grains exhibit microscopic orientation, reflecting original lamination. Another distinguishing characteristic is plastic deformation due to compaction (Plate 7-1).

Clastic carbonates are found throughout the core. These grains contribute between 1 percent and 5 percent to total rock volume and are subangular to angular, indicating short transport distances. In a 4 m (12 ft) long portion of core in stratigraphic unit E and the upper portion of stratigraphic unit F, clastic carbonate concentrations of up to 24 percent are found. Increased concentrations have been reported from other wells in the area (Wightman, personal communication). The clastic carbonates are derived from erosion of pre-Cretaceous highs in the area. The high concentrations are probably reflective of increased tectonic activity resulting in uplift of the pre-Cretaceous islands which then shed more carbonate detritus into the basin at the time of deposition of stratigraphic unit E and the upper portion of stratigraphic unit F.

### **Glaucanite**

Glaucanite is common throughout the core and can attain concentrations of up to 10 percent of total rock volume, although concentrations average 4 percent. Most pellets are well rounded, slightly larger than surrounding grains and occasionally deformed due to compaction. Pellet morphology is that of singular spheroid or ovoid grains (Plate 5-3). The pellets have the structure of an illite-smectite clay and can be derived from these clays or micas, mud fillings of organisms, or fecal pellets (Burst, 1956; Triplehorn, 1966). Glaucanite occurs in both detrital (Johnson, 1978) and early authigenic forms, replacing sedimentary rock fragments and biogenic pellets. It is formed during and shortly after deposition (Mellon, 1967) at the sediment-water interface (Wilson and Pitman, 1977). An example of glaucanite replacing original oolites can be seen in Plate 5-3. Most glaucanite

found in the Clearwater Formation appears to have been formed in situ. Its presence reinforces a marine origin for these sediments.

### Calcareous Cement

Calcareous cement is a diagenetic product found in discrete beds and lenses. It has several habits. The cement is found replacing original matrix and most mineral grains (Plate 5-4) or as calcareous veins displacing the original rock framework (Plate 6-1). Although this cannot be seen in core, it is assumed that the calcareous cement is nodular. At best, it can be correlated over short distances as elongate lenses.

Cone-in-cone structure is found in stratigraphic subunit F<sub>2</sub>, in both wells 2-19-66-5W4 and 10-17-66-5W4. This structure is described as an early diagenetic product resulting from differential pressure during crystal growth (Fairbridge and Bourgeois, 1978). It is characterized by an abundance of tight circular cones which stand with the cone axis perpendicular to the cone-in-cone layer (Pettijohn, 1975).

The structures and occurrence of cone-in-cone in the Clearwater Formation are similar to those described by Gilman and Metzger (1967) from the Upper Devonian Canadaway Formation. In both cases there are two sets of cones, one pointing upward and the other downward, separated by a layer of calcareous cemented siltstone. Fractures infilled with calcareous cement are associated with the cone-in-cone structures. Gilman and Metzger (1967) postulate that these structures originate from a syngenetic concretion of fibrous aragonite caused by pressure during dewatering of the surrounding sediments.

Siderite cemented nodules with diameters of up to 4 cm occur rarely in stratigraphic units I and J. This is indicative of reducing conditions during formation of these nodules (Scholle, 1979).

### Organic Debris

Organic fragments are ubiquitous, but exhibit a highly variable distribution, ranging up to 33 percent at the 442.9 m (1452 ft) depth of stratigraphic unit C and as low as 2 percent in the basal portion of the same stratigraphic unit. Several small coal laminae were observed in core in basal stratigraphic unit B and upper stratigraphic unit C. A similar variable distribution can be seen in most other stratigraphic units. Organic fragments and

laminae show a preferred orientation in thin section (Plate 6-1) and are commonly distorted due to compaction. The organic fragments are usually much larger than surrounding mineral grains (Plate 6-2) due to their lower specific gravity.

Presence of organics usually reflects proximity to a shoreline, but due to their low specific gravity, organics can be transported far out onto the shelf as well. In stratigraphic units B and C, the high organic content may be indicative of proximity to a shoreline or relatively higher organic input at this time. In other stratigraphic units, the organic component is explained as normal shelf input in an area of high organic activity on land.

### Accessories

Small amounts of both biotite and muscovite mica (Plate 7-1), hematite and chlorite grains (Plate 5-2) were observed in thin section. Relative percentages never exceed 2 percent. Chlorite grains exhibit both ultra-blue birefringence and normal low birefringence (Scholle, 1979). Very fine-grained zircon is the most abundant non-opaque heavy mineral in this area, ranging up to 6 percent in stratigraphic unit F. Dead oil is also quite common as a pore lining and as a stain on clay (Plate 7-3). Differentiation of oil and clay is difficult in thin section (Scholle, 1979). The authigenic clay was formed subsequent to burial of the sediments by precipitation from fluids or the alteration of unstable detrital grains. Examples of feldspar partially altered to kaolinite and biotite mica partially altered to chlorite were seen in thin section.

Authigenic pyrite is commonly seen as discrete cubes lining pore spaces along with clays. It is also found as irregular and framboidal masses, replacing grains and organic matter (Plate 7-2).

### B. Clay Mineralogy

The Clearwater Formation in well 10-17-66-5W4 is composed of a complex suite of detrital and authigenic clays.

Clay mineralogy was determined by X-ray diffraction for thirty-one oil sands and five shale samples (Table 4). Crushed samples were centrifuged to obtain a less than 2 micrometer fraction and smear slides were made. Humidity conditions were controlled by treating the samples with ethylene glycol. The samples were then analyzed using a



Table 4. Relative Percentages of Clay Minerals by X-ray Diffraction  
( $<2\mu\text{m}$  size fraction)

Sample #	Log Depth (ft.)	Strat. Unit	Sieve % Clay	Relative Percentage Clay			
				Kaolinite	Illite	Smectite	Chlorite
Sands							
80-9-1	1442.0	B	0.68	90.0	10.0	0.0	0.0
80-9-2	1444.3	B	2.30	100.0	0.0	0.0	0.0
80-9-3	1447.5	B	1.65	90.0	5.0	5.0	0.0
80-9-6	1452.0	C	1.87	94.0	5.0	1.0	0.0
80-9-7	1454.2	C	2.74	79.0	10.0	10.0	1.0
80-9-11	1467.9	D2	3.92	25.0	50.0	20.0	5.0
80-9-16	1478.0	E	0.98	25.0	55.0	5.0	15.0
80-9-17	1481.0	F1	0.84	50.0	40.0	0.0	10.0
80-9-18	1484.0	F1	0.50	45.0	50.0	0.0	5.0
80-9-25	1501.2	F3	1.63	55.0	20.0	15.0	10.0
80-9-26	1505.0	F3	1.02	80.0	15.0	0.0	5.0
80-9-27	1511.8	F3	2.20	60.0	15.0	15.0	10.0
80-9-28	1515.0	F3	1.77	60.0	15.0	10.0	15.0
80-9-29	1518.4	F3	1.66	60.0	15.0	10.0	15.0
80-9-30	1522.0	G	2.75	50.0	25.0	20.0	5.0
80-9-33	1532.5	G	1.18	80.0	10.0	0.0	10.0
Argillaceous Sands							
80-9-5	1451.7	C	2.02	40.0	20.0	20.0	20.0
80-9-14	1475.3	E	5.88	65.0	25.0	5.0	5.0
80-9-22	1489.0	F2	1.84	25.0	40.0	20.0	15.0
80-9-34	1534.0	H	4.16	50.0	15.0	30.0	15.0
80-9-35	1542.5	H	4.45	50.0	20.0	25.0	5.0
80-9-37	1550.1	I	4.12	40.0	25.0	25.0	10.0
Interlaminated Sand and Shale							
80-9-4	1449.5	B	11.00	15.0	30.0	50.0	5.0
80-9-13	1471.2	D3	33.52	20.0	45.0	25.0	10.0
80-9-21	1487.8	F2	16.17	15.0	55.0	20.0	10.0
80-9-23	1490.4	F2	16.24	1.0	54.0	30.0	15.0
80-9-24	1495.8	F2	12.82	10.0	25.0	65.0	0.0
80-9-31	1526.0	G	10.66	10.0	35.0	50.0	5.0
80-9-32	1527.5	G	8.42	25.0	35.0	15.0	25.0
80-9-36	1549.1	I	5.88	15.0	25.0	40.0	20.0
80-4-27	1552.3	I	38.92	5.0	35.0	55.0	5.0
Shale							
80-9-8	1457.8	C	n/a	15.0	30.0	40.0	15.0
80-9-9	1459.5	D1	n/a	1.0	35.0	44.0	20.0
80-9-10	1466.0	D1	n/a	1.0	44.0	35.0	20.0
80-9-12	1469.8	D3	n/a	20.0	35.0	30.0	15.0
80-9-15	1476.7	E	n/a	15.0	45.0	20.0	20.0

diffractometer. When the presence of chlorite in the clay mineral assemblage was suspected, the sample was heated and analyzed by the diffractometer again. The heating treatment separates the kaolinite and chlorite peaks.

Relative percentages of kaolinite, illite, smectite and chlorite were determined by the peak intensity method. This method gives relative percentages comparable with those generated by the weighted peak-area method also in use (Scafe, personal communication).

Detailed Scanning Electron Microscopy to determine authigenesis of the clays was beyond the scope of this study.

Relative percentage clay types are highly variable, but the distribution of clay types relates well to the lithology of the samples. Sand, argillaceous sand, mixed sand and clay, and shale samples can be differentiated on the basis of their clay content.

### **Sand Samples**

Oil sands samples are characterized by a very fine, grain-supported texture with good oil saturation. Samples never exceed four percent clay by sieve analysis. The clays are primarily authigenic (Wilson and Pitmann, 1977). With the exception of samples 80-9-11 and 80-9-16, all samples contain a high proportion of kaolinite. Illite is found in low amounts except in stratigraphic units D and E and stratigraphic subunit F<sub>1</sub>, where it is found in amounts equivalent to those of kaolinite. Smectite and chlorite are found in lesser amounts, but are slightly more significant in the sands of stratigraphic units D and E, stratigraphic subunit F<sub>1</sub> and uppermost stratigraphic subunit F<sub>2</sub>.

Some clay was observed in thin section as discrete particles, oil stained booklets of kaolinite lining pore spaces and bridges (usually illite) between grains (Neasham, 1977). Care was taken to distinguish between genuine bridging and apparent bridging due to plucking of grains during thin sectioning.

### **Argillaceous Sand Samples**

These samples, containing 1 to 6 percent clay by sieve analysis, occur in close proximity with shales or shale intraclasts. The clays exhibit a tendency towards equal amounts of kaolinite, illite and smectite, although kaolinite still predominates. Chlorite is an accessory clay mineral here.

### **Mixed Sand and Clay Samples**

Matrix clay samples contain comparatively large amounts of silt-sized detrital clays (six to thirty-nine percent by sieve analysis). These clays are derived from the crushing and disintegration of argillaceous rock fragments (Rapson, 1965). Samples which contained large lenses of silt-sized material or were entirely composed of matrix-supported grains were placed in this category.

Due to their silt size and compaction of the sediment, these clays were not identifiable in thin section. X-ray diffraction results show that illite and smectite are the major constituents, while kaolinite and chlorite are accessory clay minerals. There is an association between illite and chlorite in that both seem to increase and decrease at the same rate.

### **Shale Samples**

The clay in shale interbeds is predominately illite and smectite with chlorite as a minor constituent. Kaolinite is an accessory clay mineral in these samples.

## V. Geophysical Well Log Response in Shaly Sands

### A. Previous Work

The composition of the bitumen in the Cold Lake oil sands area is considered transitional between that of the Athabasca and Lloydminster areas. It has an API gravity of between 10° and 14° (Mellon, 1967). Reserve estimates for the 3,500 square mile reserve were originally thought to be 75 billion barrels (Mellon, 1967), but have been raised to 164 billion barrels (Energy Resources Conservation Board, 1973).

The Clearwater Formation contains the most continuous reservoirs in Cold Lake (Vigrass, 1968; Buckles, 1979). The reservoirs here are between 10 m and 15 m thick (Matheny, 1979; Mossop et al., 1981) with local thicknesses of up to 35 m (Mossop et al., 1981). Porosity of the reservoir sands is between 28 and 43 percent, averaging 37 percent (Jardine, 1974; Matheny, 1979), while permeability is between 300 and 1300 millidarcies (Jardine, 1974). Oil saturation is 14 to 16 weight percent (Mossop et al., 1981). Control on the oil saturation has been considered to be primary porosity and permeability since post-depositional changes were considered minimal (Mossop et al., 1981). Several mechanisms and combinations of mechanisms have been proposed to account for the accumulations of oil in the Clearwater Formation at Cold Lake.

Structure, specifically the influence of Paleozoic highs, is one of the major factors controlling oil accumulation (Wickenden, 1948; Mellon, 1967; Energy Resources Conservation Board, 1973; Carrigy and Kramers, 1974; Jardine, 1974; Mossop et al., 1981). Salt collapse during and after Mannville time (Jardine, 1974) has also been invoked as a structural control on bitumen accumulation.

In the Clearwater Formation at Cold Lake, major oil occurrences have been located on large, structurally high features which coincide with Paleozoic highs, while small 30 foot oil accumulations were found scattered on structural highs downdip to the southwest of the major accumulations (Vigrass, 1968). Water is located on the flanks of these features (Kendall, 1977). On the eastern edge of the oil sands deposit, synclinal features create a gentle eastward dip which marks the termination of oil accumulation (Energy Resources Conservation Board, 1973).

Stratigraphy has been identified as another major control on oil accumulation in the Cold Lake oil sands area (Wickenden, 1948; Vigrass, 1968; Carrigy and Kramers, 1974; Jardine, 1974; Mossop *et al.*, 1981). The Clearwater Formation, which contains 40 percent of Cold Lake hydrocarbons (Buckles, 1979), has the thickest, most laterally continuous sands (Kendall, 1977; Buckles, 1979; Mossop *et al.*, 1981). However, the vertical continuity of the Clearwater Formation is disrupted by shale interbeds and cemented siltstones (Kendall, 1977). The clay and shale interbeds and differential compaction of sediments (Jardine, 1974) reduce the effectiveness of these reservoirs.

Petrography also influences oil accumulation (Buckles, 1979; Harrison *et al.*, 1981). The complex mineralogy of the deposit influences quantitative log interpretation (Buckles, 1979). Mean grain size, the amount of fines, and the presence of diagenetic clay all affect the emplacement and recovery of the oil (Harrison *et al.*, 1981). The diagenetic clays have detrimental effects on the recovery of oil from the oil sands (Gallup, 1974).

## **B. Introduction to Geophysical Well Log Study**

The geophysical well log study of the Clearwater Formation highlights the problems associated with the interpretation of reservoir characteristics in a shaly sand deposit.

A shaly sand is defined as a sand which contains greater than five percent clay (Fertl, 1972). The ultimate aim is to deal with the various clay types, the distribution of the clay in the sediment and the effect of the clays on the geophysical parameters measured (Helander, 1980).

Core-derived parameters, such as porosity, weight percent bitumen and weight percent water are inaccurate for several reasons which will be discussed in detail below. It is difficult if not impossible to obtain accurate values for these parameters from unconsolidated sands under conditions truly representative of *in situ* conditions (Collins, 1977). Parameters derived from individual well logs are also inaccurate due to the various influences of the clays and other minerals on the log response. Consequently, multiple porosity log analysis techniques have been developed to reconcile log-derived parameters with one another and with those derived through routine core analysis (Tixier *et al.*, 1968; Poupon and Gaymard, 1970; Heslop, 1975).

This study will focus on a number of areas of shaly sand analysis. Parameters from geophysical well logs can be used to discern lithology through the construction of an M-N plot. Various porosity logs and the corrected bulk density log are used to develop the parameters: volume of shale, volume of dispersed shale, effective porosity and bulk volume clay fraction. These parameters are then compared through the use of cross-plots with the core-derived parameters to establish relationships between them.

The resultant relationships between core analysis and the geophysical well logs are limited in their application to the Clearwater Formation within a limited geographic area (Wyllie and Rose, 1950). Reservoir conditions cannot be assumed to be uniform throughout the Cold Lake oil sands deposit. However, the conclusions of the present study can serve as a guide for further study of this deposit.

#### Function of Well Logging Tools

It is important to understand the functioning and limitations of the various geophysical well logging tools which were run on well 10-17-66-5W4 (Appendix I) before analyzing the shaly sand of the Clearwater Formation (Fertl, 1979).

The resolution of most geophysical well logging tools is in the order of 0.6 m (2 ft). Consequently, some of the more finely interbedded and the interlaminated lithologies will not be detected as discrete units by the geophysical well logs.

#### Caliper

The caliper records the diameter of the borehole and indicates areas of borehole collapse. The density and neutron readings depend upon a good contact between the tool and the borehole wall for accurate readings. The caliper readings for well 10-17-66-5W4 indicate that little borehole collapse has occurred and that readings can be considered reliable.

#### Spontaneous Potential/Dual Induction Laterolog

This is an electric log which imparts an electric current into the formation. Three simultaneous resistivity recordings were run in well 10-17-66-5W4. The laterolog 8 records a shallow reading of the resistivity of the zone invaded by drilling fluids. The medium induction log explores further into the formation and may

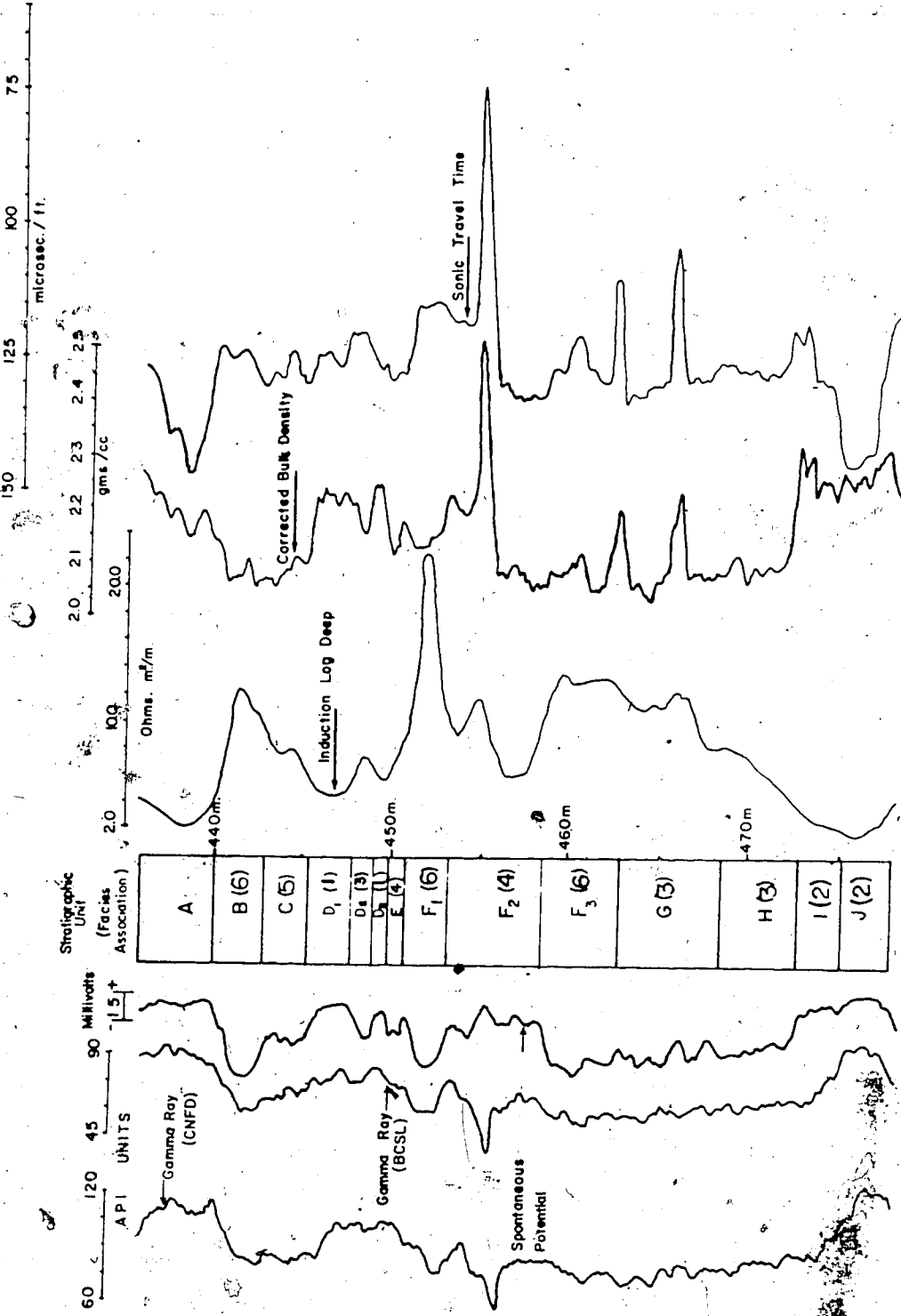


FIGURE 28. Selected geophysical well logs for well 10-17-66-5W4.

penetrate the undisturbed zone. The deep induction log penetrates furthest into the formation and usually records true resistivity. The conductivity is simply the inverse of the true resistivity.

The spontaneous potential log measures the natural potential differences between a surface electrode and a movable electrode in the mud column. The spontaneous potential detects the electrical potential created by the difference in the salinities of the formation water and the drilling mud filtrate. The presence of an effective shale is indicated by a deflection to the right on the Spontaneous Potential curve. The spontaneous potential is most useful as a shaliness indicator in water-bearing sands of low to moderate resistivity where the shale is laminated. When hydrocarbons and dispersed shales are present, the spontaneous potential response is subdued and the calculated volume of shale values are too high (Helander, 1980). Because the Clearwater Formation is saturated with heavy oil and consists of dispersed laminated and structural shales, shaly sand analysis using the spontaneous potential log was not performed.

#### Gamma Ray Log

The gamma ray log is considered to be a lithology log which can indicate the shaliness of a formation by measuring the intensity of naturally-occurring gamma rays. The gamma ray logging tool accompanying the borehole compensated sonic log is situated in the centre of the borehole and may be less sensitive due to gamma ray attenuation in drilling muds. Consequently, the readings from this log are lower, and possibly less reliable, than those from the compensated neutron-formation density log. Therefore, the gamma ray values obtained from the compensated neutron-formation density log will be considered more reliable and representative.

Shales are generally more radioactive than sandstones and carbonates. However, the gamma ray log can be misleading in shaly sands since not all clays are radioactive (e.g., kaolinite and chlorite) and consequently will not be detected by the gamma ray log. Furthermore, the gamma ray log will detect radioactive minerals other than those in shales. For these reasons it cannot be considered a completely reliable lithologic tool.



### Corrected Bulk Density Log

This tool uses gamma rays to measure the electron density of the formation. Its measurements are a function of the density of the rock matrix and the density of the fluids and/or gases filling the pore space. It detects both pore water and clay-bound water (Juhasz, 1979). The density porosity log converts the bulk density into apparent sandstone porosity units, assuming a clean sand density of 2.65 gms/cc.

### Sonic or Acoustic Log

The sonic log measures the travel time of sound through the formation. The values generated are inversely proportional to the speed of sound and a function of lithology, porosity, and the types of fluids present. The sonic porosity is usually a good approximation of the total porosity, that is, the effective plus the non-effective porosity (Tixier et al., 1959).

The sands of the Clearwater Formation are not compacted and the sonic log signal is decelerated because the grains are not always in direct contact with one another. A compaction correction calculated from the sonic log must be applied to the sonic porosity. The compaction correction reduces overly optimistic sonic porosity values in uncompactedsands.

### Neutron Log

The neutron log is based on the concept that the mass of a neutron is approximately equal to the mass of a hydrogen atom. This log measures the amount of hydrogen in the formation by bombarding the formation with neutrons, which then collide with the hydrogen nuclei (Fertl, 1972). Because it detects the hydrogen atoms in both water and in the lattice of the clay minerals (Hill et al., 1979; Juhasz, 1979), it can be used in the determination of both the volume of shale and the porosity of the formation (Truman et al., 1972). It is used extensively in shaly sand analysis because it gives good volume of shale values in hydrocarbon-saturated sediments (Poupon and Gaymard, 1970).

### The Effects of Clays on Geophysical Well Log Response

Shaly sand analysis attempts to deal with the distribution of various types of clays and their effects on the geophysical well log response.

The manner in which clay is distributed in the sediment affects the geophysical well log response. Three forms of clay distribution are recognized (Fertl, 1972; Heslop, 1975; Ransom, 1977; Helander, 1980). They are dispersed clay, structural clay and laminar clay. The core and thin section studies show that all three forms are present in the Clearwater Formation.

Dispersed clay can be detrital or authigenic and is found on grain surfaces or occupies the void space between grains. This habit of shale affects both porosity and permeability. The shale acts as a permeability barrier for the transmission of fluids. The framework porosity is decreased by the combined effects of the volume of dispersed clay and the bound or adsorbed water associated with the clay.

Structural clay supports overburden pressure. It is composed of fragments or crystals which are part of the rock framework. While this type of clay does not affect the total pore volume, it does reduce the effective porosity by the amount of adsorbed water associated with the clay.

Laminar clay consists of both dispersed and structural clays. It occupies space in both the rock framework and in the void space between grains. Since it contains both dispersed and structural clays, it reduces both porosity and permeability.

#### Clay Composition

Each clay type affects the geophysical well log response differently. The water contained in the pores of a shaly sand is closely associated with the clay as adsorbed water. The chemical composition of the clay and the amount of adsorbed water associated with it causes deviations from the geophysical response as compared to that of a quartz sand.

#### Kaolinite

Kaolinite is non-radioactive and is detected as a sand by the gamma ray, resistivity and spontaneous potential logs (Hilchie, 1982). It is therefore termed a non-effective clay. The gamma ray and spontaneous potential

responses for this clay are low and the resistivity response is high. The density of kaolinite is 2.43 gms/cc which is lower than that of quartz sand.

#### Illite

Illite is a radioactive effective clay and is detected as a shale. Both the spontaneous potential and gamma ray logs record illite as a shale. The density of illite is very close to that of quartz sand and is 2.61 gms/cc.

The presence of this clay is indicated when the neutron porosity is much higher than the density porosity. The density porosity is lower than the true porosity when illite is the major constituent in the sediment. Illite cannot be differentiated from smectite on the sonic porosity log.

#### Smectite

Smectite is usually non-radioactive, but can be a radioactive effective clay when uranium in solution is attracted to the charged smectite clay particles. When uranium is present in large amounts, smectite is detected by a rapid increase in the gamma ray log. The presence of smectite is also indicated by low resistivity values. The density of this clay is 2.30 gms/cc which is lower than the density of quartz sand. Consequently, sediments that contain large amounts of smectite will register low bulk density values.

All three porosity logs will record much higher porosities than the true porosity when smectite is present. While all clays exhibit interparticle swelling, smectite exhibits both interparticle and interlayer swelling and provides the largest total surface area for adsorption of water (Jenkins and Bush, 1971). Smectite can have up to four layers of adsorbed water in uncompacted sands, such as those of the Clearwater Formation. The neutron porosity log will be affected by the number of layers of adsorbed water since it detects hydrogen atoms (Hill *et al.*, 1979). While all porosity log values will be much higher than the true porosity, the neutron log will exhibit much higher porosity values than the others when smectite is present.

### Chlorite

Like kaolinite, chlorite is a non-radioactive non-effective clay which is detected as a sand by the gamma ray and spontaneous potential logs. It has a low gamma ray and high resistivity response and a density of from 2.78 gms/cc to 3 gms/cc which makes it slightly more dense than a quartz sand. This high density is reflected by the density porosity log which is usually very low as compared to the sonic and neutron porosity logs. The sonic and neutron porosity logs exhibit higher porosities similar to those for kaolinite. Consequently it is difficult to differentiate between kaolinite and chlorite on geophysical well logs:

### Summary

X-ray diffraction analyses of samples from well 10-17-66-5W4 indicate that kaolinite, illite, smectite and chlorite are present in varying amounts with the sediments of the Clearwater Formation. These clays are found in dispersed, structural and laminar forms. The mixture of effective and non-effective clays (Hilchie, 1982) and the wide variety of forms these clays take (Ransom, 1977), complicates the shaly sand analysis to the extent that clear linear relationships between geophysical parameters and core-derived parameters cannot be expected.

### C. Shaly Sand Plots

The data for the various plots are derived from the hand-digitization of the geophysical well logs, the mathematical transformations of these data and the core analysis values. In the case of the M-N plot, all 301 points digitized were used.

In cross-plots using the data derived from the geophysical well logs, the points representing the calcareous cemented zones were omitted because they obscure the shaly sand analysis. The number of points plotted is reduced to 264.

The cross-plots that incorporate data derived from the core analysis do not include thick sections of shale (all of stratigraphic units A and J and the upper and basal shales of stratigraphic unit D). In these cases, core was not sampled and the number of points plotted is 165.

### Sources of Error in the Determination of Core-derived Parameters

Sampling procedures and the method of obtaining weight percentages of oil and water contribute greatly to the sources of error in the core analysis of shaly sands.

A considerable amount of water can be added to the samples during coring so that weight percent water becomes higher than that found in situ. Core porosities as high as 40 percent are probably the result of water gain through core expansion and imbibition during coring (Eade, 1975). Some of the core porosities determined for the Clearwater Formation are as high as 43 percent. Conversely, water loss due to evaporation after coring can range up to 60 percent (Eade, 1975). This affects the values for the weight percent water and the core porosity, although the weight percent oil is not affected.

Higher core porosities can also be caused by core expansion due to the release of overburden pressure (Woodhouse, 1976; Collins, 1977). The amount of expansion has been estimated to be 6 percent in the Athabasca oil sands area (Woodhouse, 1976). While no figures are available for the Clearwater Formation in Cold Lake, the amount of expansion is probably higher due to the greater thickness of overburden in this area. Core expansion further complicates the relationship between core- and log-derived parameters. The Dean-Stark method (Kidston, personal communication) was used to analyze the oil sands samples. In this method, toluene is used to separate the oil from the sample. Because toluene boils at 111°C., both adsorbed water and moveable water are removed from the sample. This contributes to overly-optimistic values for core porosity (Bush and Jenkins, 1969; Jenkins and Bush, 1971; Woodhouse, 1976). The Dean-Stark method assumes that fluids occupy the total pore space and that there is no air present in the sample. This contributes to inaccurate values for weight percent bitumen and water.

These sources of error make it difficult to quantitatively resolve core-derived with log-derived parameters, although general trends can be observed. It is imperative that better methods of core extraction and more precise methods of core analysis be developed to minimize these problems.

### **M-N Plot**

The M-N plot (Figure 29) is used to determine general lithology using the neutron, density and sonic logs (Pirson, 1981b). The values of M and N (Appendix III) are dependant on fluid and matrix characteristics, but are independant of porosity (Schlumberger, 1979). The plot is based on the concept that the various well logging tools respond in different ways to the various material components of a complex lithology (Helander, 1980). The logging devices have a characteristic response to the major components of reservoir rocks: quartz, calcite, dolomite, anhydrite and gypsum.

When the resultant plot is compared with the M-N plot for points of single mineral formations, the shaliness of the Clearwater Formation is apparent. All points plot well below the clean sand point and are shifted in the direction of the shales.

The sample points were characterized as calcareous-cemented sands, relatively clean sands, shaly sands or shales by the dominant lithology found at equivalent depths in the core. When these categories are plotted on the M-N plot the shaliness of the formation can be observed influencing all lithologies by pulling them down and to the left. There is some separation of shaly sands and shales into two end members, but there is also a large area of overlap. The shale category represents the shales in stratigraphic units A and J.

### **Corrected Sonic Porosity versus Neutron Porosity**

The sonic porosity was derived mathematically (Appendix III). A compaction correction was applied to the sonic porosity because the overburden pressure is considerably less than the formation pressure (Tixier *et al.*, 1968). The lack of compaction of the sands causes considerable attenuation of the sonic signal. The need for a compaction correction is indicated when the sonic travel time in shales closely associated with the sands exceeds 100 microsec./foot (Tixier *et al.*, 1959). In the case of the Clearwater Formation in well 10-17-66-5W4, the closely associated shales of stratigraphic unit D exhibit a travel time of approximately 130 microsec./foot. Consequently, compaction correction of 1.3 was applied to the sonic porosity.

All of the log-derived porosities plot in a narrow band between 30 percent and 60 percent. Porosities are high due to the effects of the clays. The corrected sonic

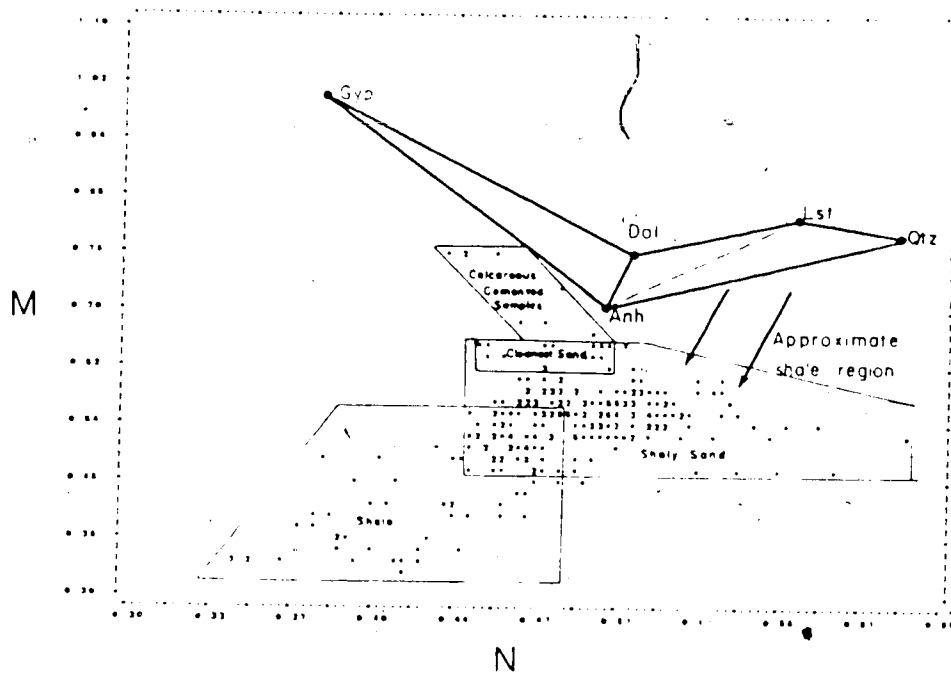


FIGURE 29. M versus N lithoplot, showing the effect of clays on the lithology of Clearwater sediments.

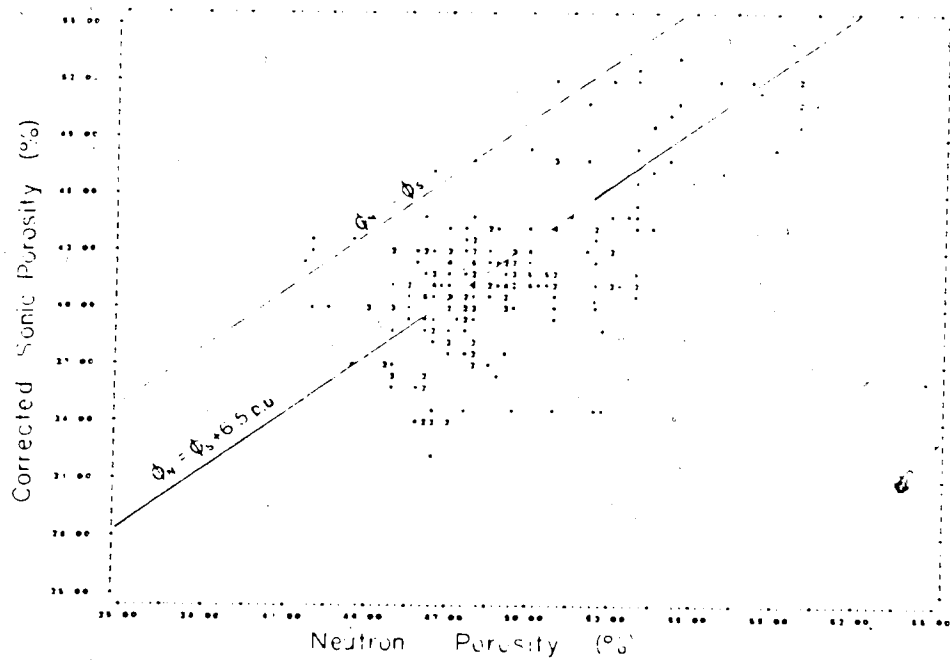


FIGURE 30. Corrected sonic porosity versus neutron porosity, showing the difference in the response of the acoustic and neutron tools. ( $r = 0.63$ )

porosity-neutron porosity plot (Figure 30) exhibits the best direct relationship ( $r=0.63$ ) since both logs reflect total porosity. However, the neutron log also detects hydrogen in the clay crystal lattice. This would account for the average 6.5 porosity unit increase in the neutron porosity as compared to the sonic porosity. The discrepancy between the neutron and sonic logs is particularly evident in the lower porosities where the sample points are more shaly. In these areas the neutron porosity can be up to 19 porosity units higher than the sonic porosity.

### Shaliness Indicators

Several plots were generated to obtain more realistic values for volume of shale and effective porosity throughout the Clearwater Formation. Shaliness indicators in the porosity logs, the corrected bulk density log and the gamma ray log give good values or the upper limit for the volume of shale in a shaly sand formation where there are no clean 100 percent water-saturated sands which can serve as a reference. Usually the lowest of the upper limits for volume of shale values are taken as the most realistic values (Poupon and Gaymard, 1970; Helander, 1980).

Effective porosity calculated from multiple log analyses provides the most meaningful values for true porosity of shaly sands (Heslop, 1975).

### Corrected Density versus Neutron Porosity

This cross-plot was generated to obtain values for the volume of shale and effective porosity. This method was first described by Poupon and Gaymard (1970) and is discussed by others (Krug and Cox, 1976; Ransom, 1977; Helander, 1980). A mathematical approach to the determination of volume of shale and effective porosity was described by Krug and Cox (1976).

In the corrected bulk density-neutron porosity treatment (Figure 31) the wet clay point is defined in an associated shale with the highest neutron porosity. This assumes that the wet clay represents a shale which is 100 percent effective. If it is not 100 percent effective, volume of shale figures will be high for the more shaly points but close in the cleaner sands (Hilchie, 1982). The clean quartz sand point is placed at a neutron sandstone porosity of 0 percent and a density of 2.65 gms/cc which is the density of a pure quartz sand. The water point is placed at 100 percent



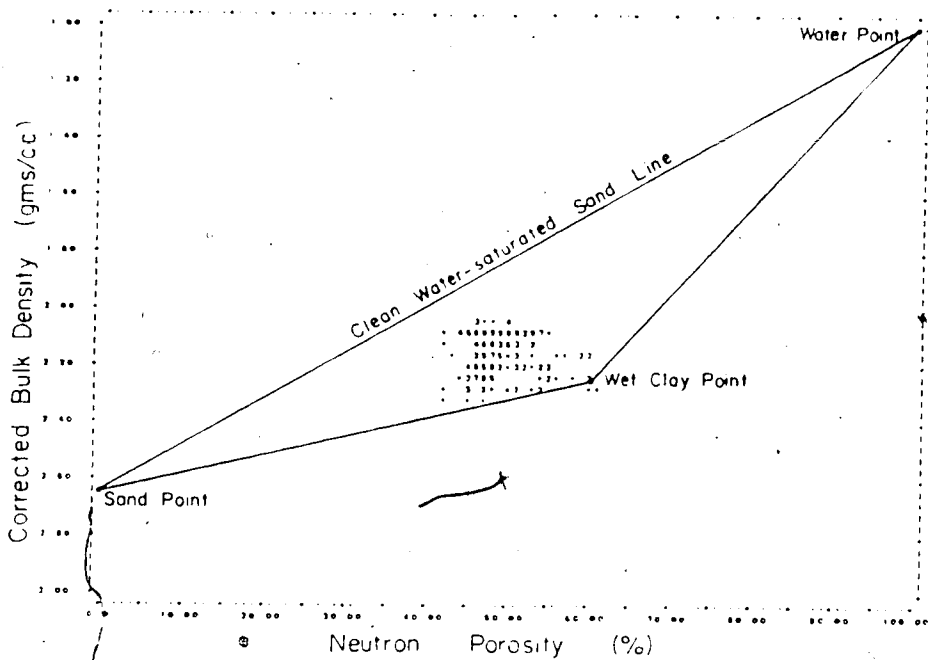


FIGURE 31. Corrected bulk density versus neutron porosity, illustrating the construction of the shaly sand plot.

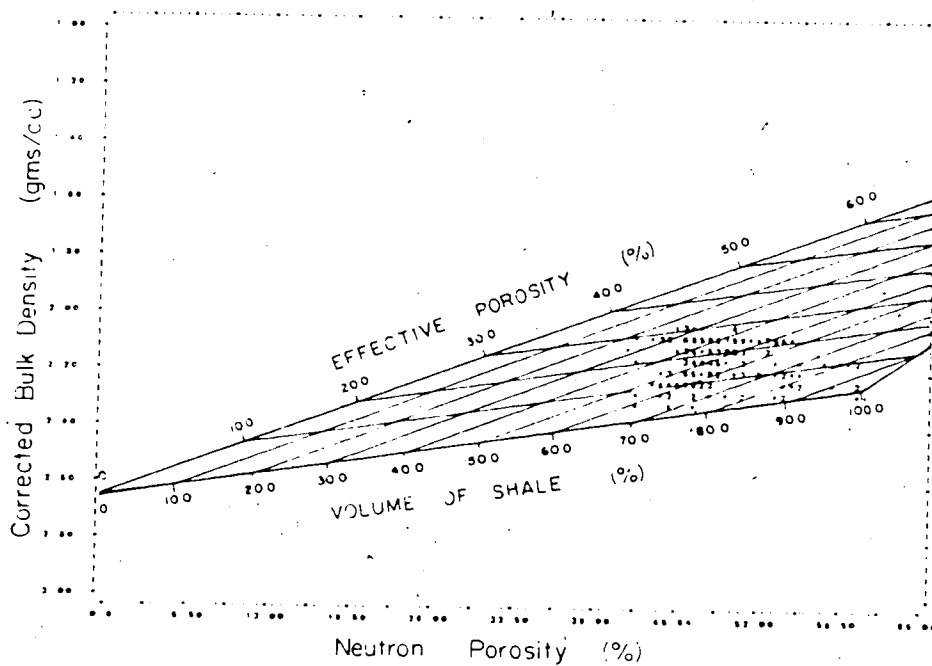


FIGURE 32. Detail of shaly sand plot, showing relationship of points to volume of shale and effective porosity.

porosity and a water density of 10 gm/cc. This triangular plot defines end points for a pure quartz sand, a pure shale and 100 percent porosity. The points on the corrected bulk density-neutron porosity cross-plot are projected onto these lines and values for volume of shale and effective porosity are obtained (Figure 32). Points which plot outside the triangle of the shaly sand plot represent anomalous shales which have values for bulk density and neutron porosity outside the range of accepted values.

Several factors influence the shaly sand plot generated by the corrected bulk density-neutron porosity cross-plot. The influence of the density of large amounts of heterogeneous solid matter can shift the plot (Figure 33). Several components of the sediment in the Clearwater Formation have an effect on the density log. As can be seen, values for the corrected bulk density of the digitized points range between 2.0 gms/cc and 2.40 gms/cc which is much lower than that of sand which is 2.65 gms/cc. Biotite, zircon, siderite, hematite, magnetite and pyrite are all much more dense than a pure quartz sand and tend to pull the points down (Edmundson and Raymer, 1979). Given the low densities of the digitized points, it seems that the more dense minerals are not present in sufficient amounts to significantly affect the bulk density. With the exception of chlorite which is slightly more dense than quartz, the clays identified and the carbonaceous debris lower the density values. These components appear to have the most effect on the density log in the formation under study since the bulk density values are low when compared with the density of a clean quartz sand.

The second factor to take into account is the effect of light hydrocarbons. Corrections must be made for the presence of light hydrocarbons in the formation since they affect the readings of the sonic, density and neutron logs (Poupon and Gaymard, 1970). The degree of influence of the hydrocarbons is a function of the degree of hydrocarbon saturation and the density of the hydrocarbons (Juhasz, 1979) and is determined by the calculation of the hydrocarbon index. The neutron porosity of the hydrocarbon can then be calculated and if it is significantly different from 100 percent a hydrocarbon correction is indicated. The density of the hydrocarbons present in the Clearwater Formation was determined by several

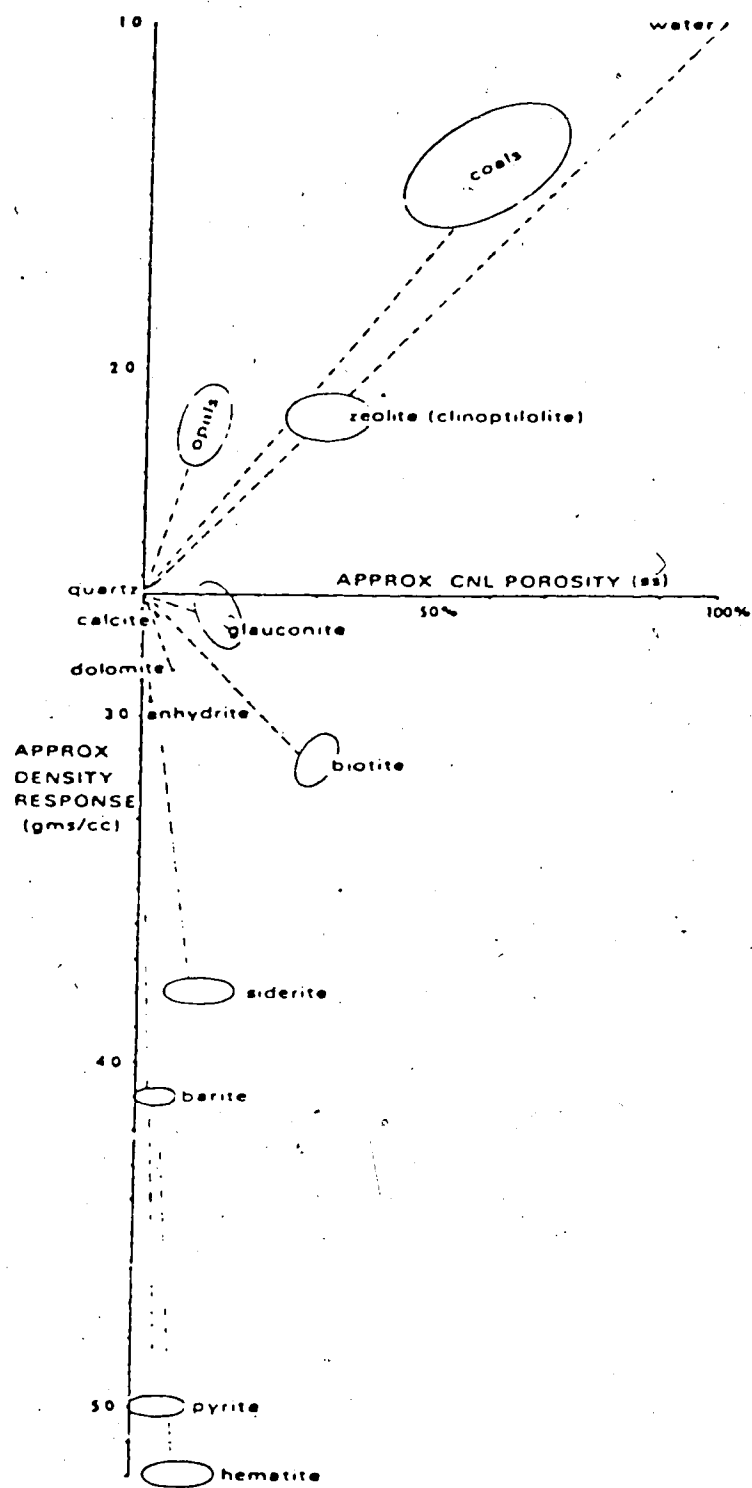


FIGURE 33. Effect of various minerals on the corrected bulk density versus neutron (CNL) porosity plot.  
(after Ransom, 1977)

independent studies to be 0.999 gms/cc at 15°C, which is very close to the density of water. The neutron porosity was determined to be 100 percent for the hydrocarbon. This means that the hydrocarbons have no effect on the neutron, sonic and density logs.

The presence of light hydrocarbons was also checked for by the neutron-density overlay method (Tixier *et al.*, 1968) which showed that no gas was present in the formation.

Consequently, no correction was needed for the values of volume of shale and effective porosity.

The corrected bulk density-neutron porosity cross-plot shows that no clean water saturated sands are present in the formation. The concentration of points at the clay point indicates that the shales in the formation have a high clay component and a low silt component (Bosworth, personal communication). The volume of shale ranges from 25 percent in the cleanest sands to 100 percent in the pure shales. Effective porosity ranges from 0 percent in the shales to 31 percent in the cleanest sands. This cross-plot gave the lowest upper limit for the volume of shale and was used in further computations.

A cross-plot was generated to compare the effective porosity and the volume of shale (Figure 34). It exhibits a good inverse relationship ( $r=-0.91$ ), showing that as the volume of shale increases the effective porosity decreases. This relationship was also noted by Heslop (1975).

The effective porosity also exhibits a good direct relationship ( $r=0.91$ ) with the density porosity (Figure 35). Although there is some scatter, in general the porosity is much higher than the effective porosity at lower porosity values (representing shales) and converges at approximately 50 porosity units in the cleaner sands.

#### Apparent Sandstone Density Porosity versus Neutron Porosity

This cross-plot was generated to compare and confirm the values for volume of shale and effective porosity obtained by the cross-plot of corrected bulk density and neutron porosity.

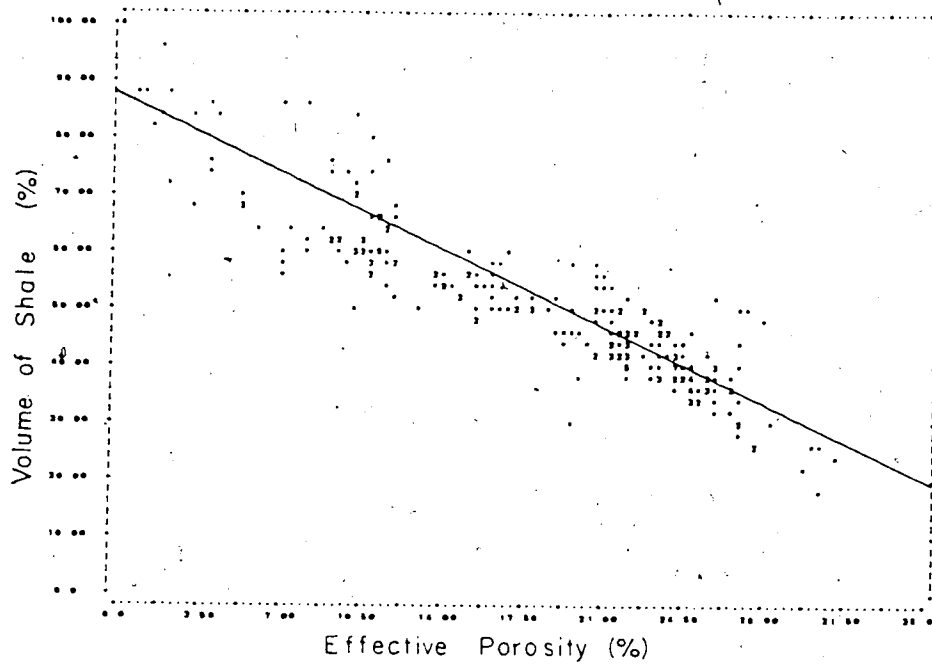


FIGURE 34. Volume of shale versus effective porosity, showing good inverse relationship. ( $r = -0.91$ )

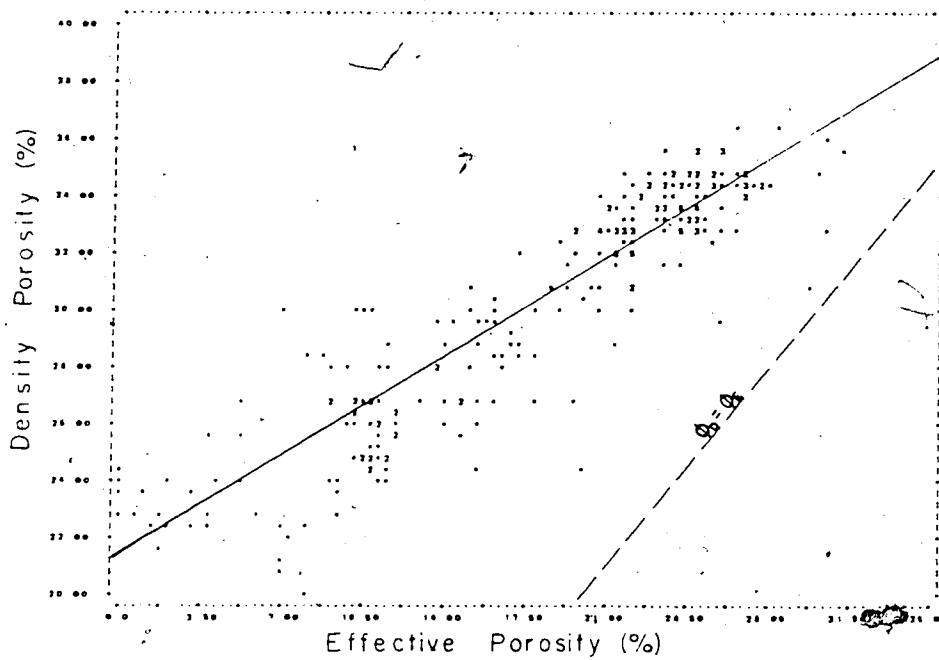


FIGURE 35. Sandstone density porosity versus effective porosity, showing good direct relationship. ( $r = 0.91$ )

Because the density and neutron tools detect both effective and non-effective porosity, a method was developed to calculate effective porosity only. This shaly sand plot (Figure 36) was first described by Poupon *et al* (1970) and is discussed in other papers (e.g., Ransom, 1977; Helander, 1980; Hilchie, 1982).

In the density-neutron porosity treatment, a wet clay point is defined in an associated shale as 100 percent volume of shale and 0 percent effective porosity. The position of the wet clay point is dependant upon the type of clay, the amount of water associated with the clay and the mineralogic response of the neutron tool (Ransom, 1977). In this case, the clay point is defined by a smectite-dominated shale because it has high density and neutron porosity values. This is confirmed by x-ray diffraction. Points which plot outside the triangle of the shaly sand plot represent anomolous shales which have values for density porosity and neutron porosity outside the range of accepted values. A clean water sand line is constructed from the 0 percent neutron and density porosities to the fluid point at 100 percent neutron and density porosities. These two lines are then divided from 0 to 100 percent and represent volume of shale and effective porosity values. Plotted points are projected onto these lines and values for volume of shale and effective porosity are obtained (Figure 37).

The density-neutron porosity cross-plot confirms that there are no clean water-saturated sands in the formation. Volumes of shale range from 20 percent in the cleaner sands to 100 percent in the shales. Effective porosity ranges from 0 percent in the shale to 30 percent in the cleaner sands. The values for volume of shale and effective porosity compare well with those generated by the corrected bulk density-neutron porosity cross-plot but are slightly less optimistic. Consequently, these values were not used for further computations.

#### Gamma Ray Index versus Volume of Shale

The gamma ray log from the compensated neutron-formation density was used to obtain gamma ray index values (Appendix III). The gamma ray index values are an indication of the volume of shale (Woodhouse, 1976) and can be compared to the volume of shale generated by the corrected bulk density-neutron porosity cross-plot (Figure 38).

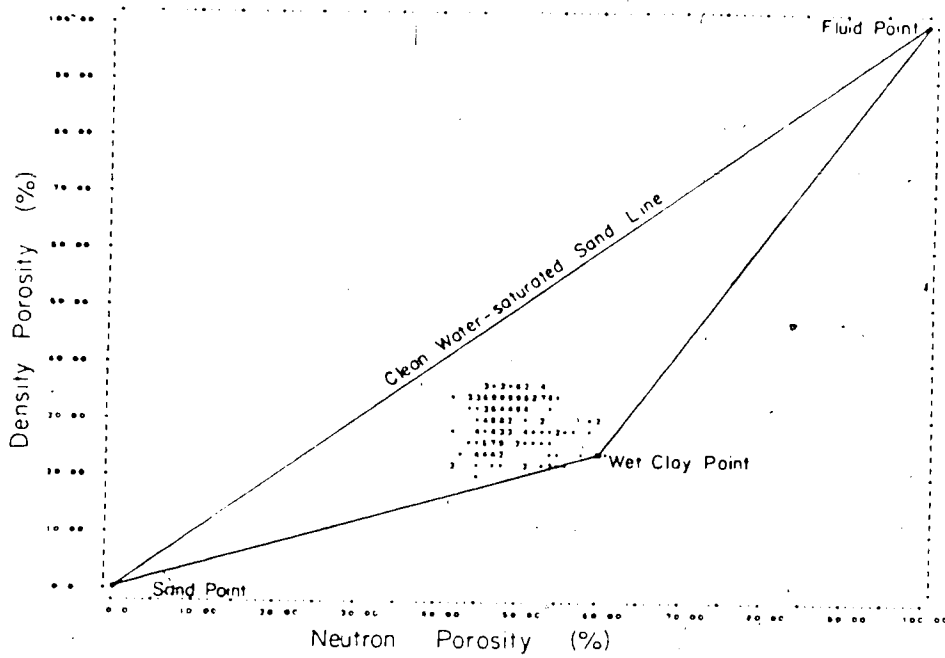


FIGURE 36. Density porosity versus neutron porosity, illustrating the construction of the shaly sand plot.

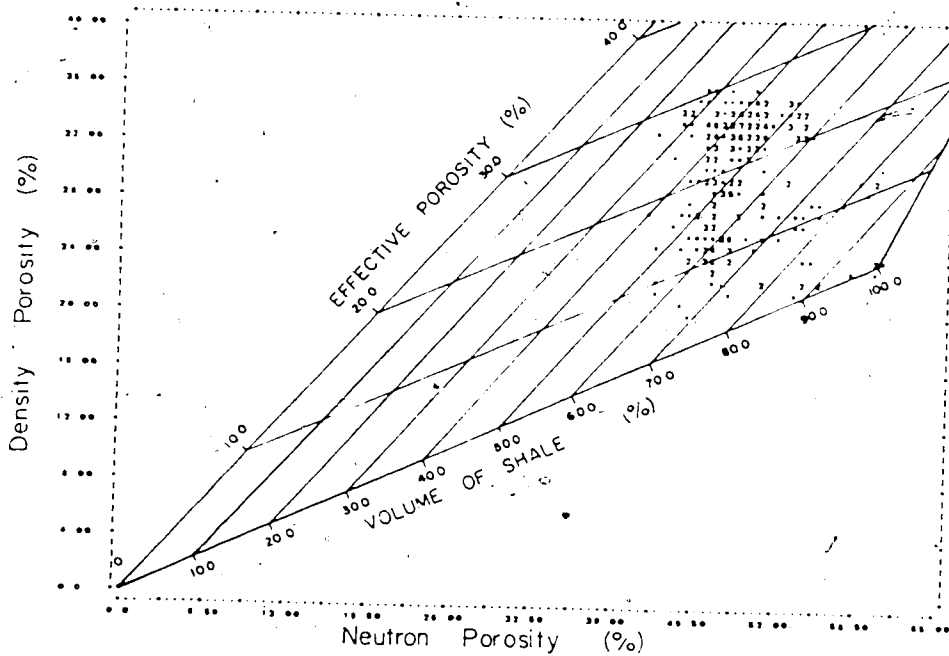


FIGURE 37. Detail of shaly sand plot, showing relationship of points to volume of shale and effective porosity.

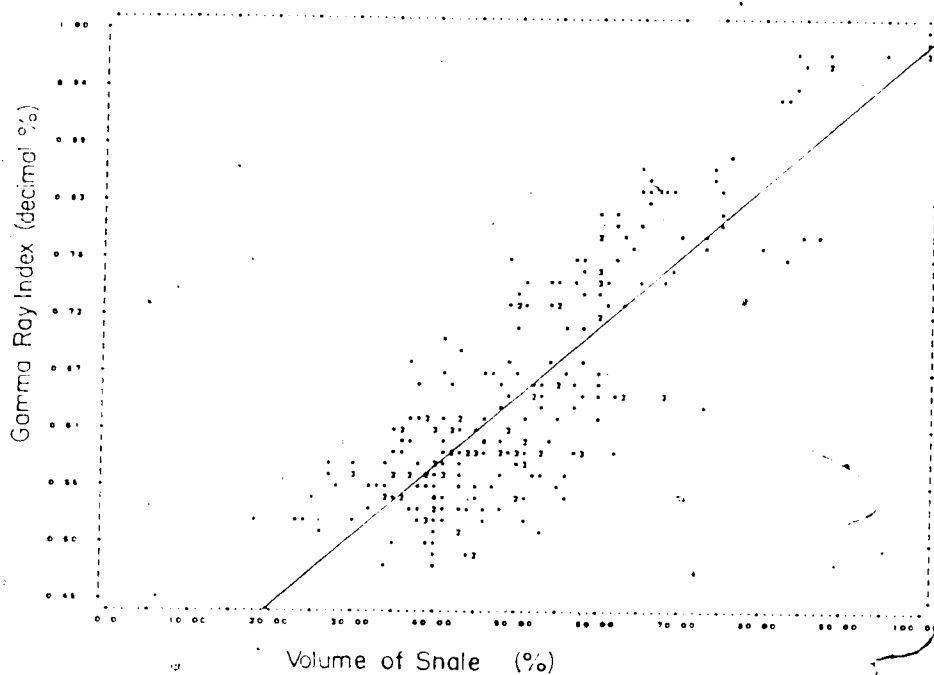


FIGURE 38. Gamma ray index versus volume of shale, showing consistently larger percentage of shale indicated by gamma ray index. ( $r = 0.85$ )

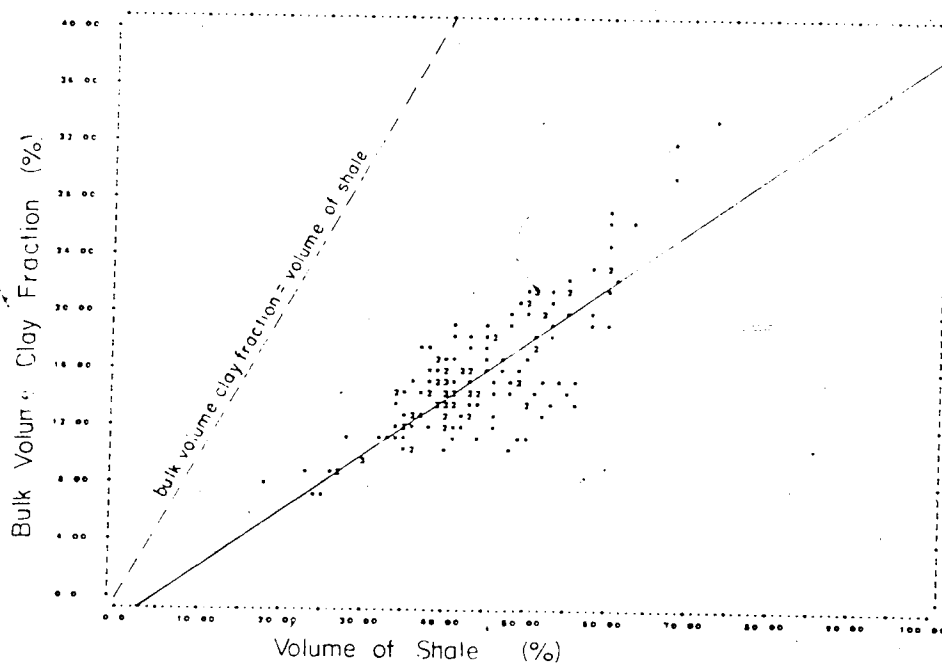


FIGURE 39. Bulk volume clay fraction versus volume of shale, illustrating that the bulk volume of clay and the adsorbed water on the clays are directly related to the volume of shale. ( $r = 0.82$ )



This cross-plot exhibits a good indirect relationship ( $r=0.85$ ) between these two values for the volume of shale. The gamma ray index values are consistently higher than those from the corrected bulk density-neutron porosity cross-plot. This suggests that the gamma ray log is not simply detecting the shale radioactivity, but also radioactive minerals in the sands. The presence of glauconite and feldspars in the sediments can greatly increase the gamma ray readings (Edmundson and Raymer, 1979). This will create higher apparent volume of shale values. Consequently, the gamma ray index-generated values for volume of shale were not used in further computations.

### **Relationships between Log- and Core-derived Parameters**

Both the geophysical log and core data were used to generate a number of parameters. These values were then compared.

The high variability of clay composition and form and the previously-discussed problems associated with core analysis meant that few relationships between these parameters could be discerned. The following is a presentation of the clearest relationships found for the Clearwater Formation in well 10-17-66-5W4.

#### **Bulk Volume Clay Fraction versus Volume of Shale**

This cross-plot (Figure 39) attempts to resolve core-derived and log-derived parameters. The bulk volume clay fraction represents the fraction of the bulk volume occupied by adsorbed water on the clays and is calculated by subtracting effective porosity values from the core porosities (Appendix III). The plot indicates that the bulk volume of clay and consequently the percentage of adsorbed water is directly related ( $r=0.82$ ) to the volume of shale, especially in the cleaner sands. This confirms that the volume of shale is a good total shaliness indicator.

#### **Volume of Dispersed Shale versus Volume of Shale**

The volume of dispersed shale in the pore space is calculated by sonic and neutron porosity measurements (Appendix III). The cross-plot (Figure 40) shows that as the volume of shale increases the total volume of

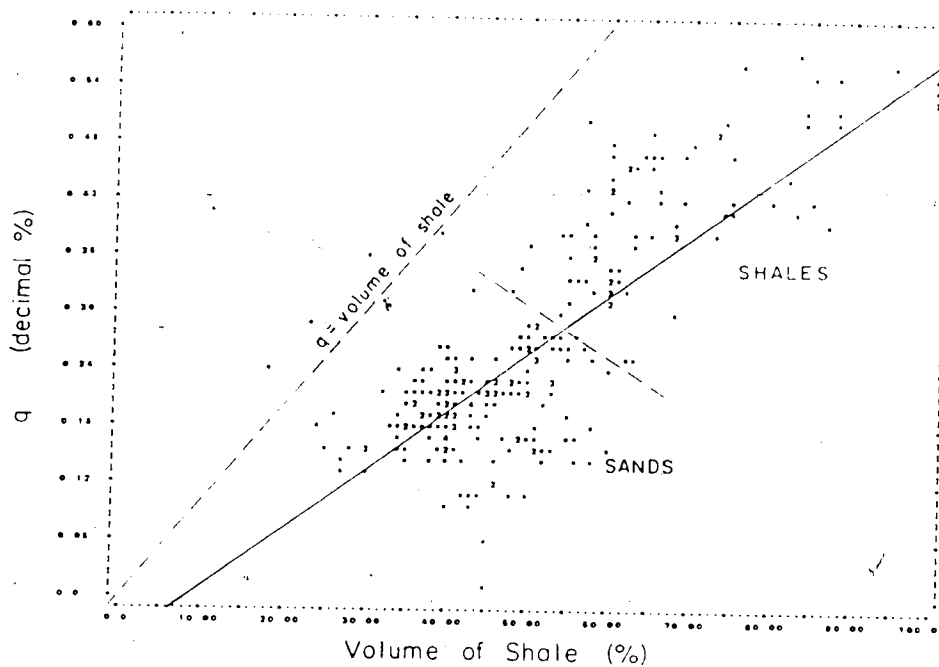


FIGURE 40. Volume of dispersed shale versus volume of shale, illustrating a direct relationship and the presence of laminae and structural shale. ( $r = 0.79$ )

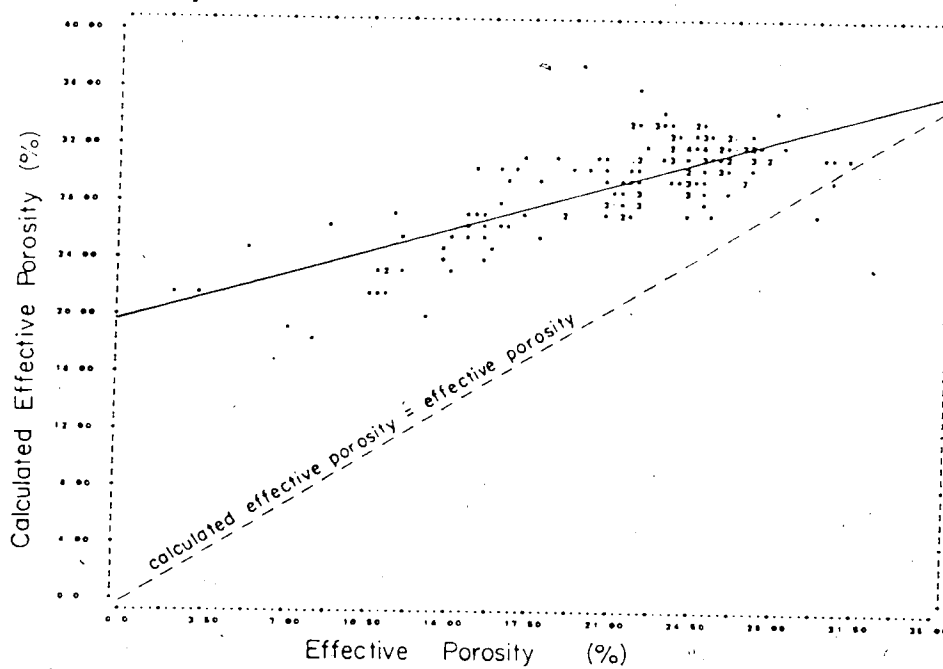


FIGURE 41. Calculated effective porosity versus effective porosity, illustrating the relationship between log-derived and core-derived porosities. ( $r = 0.75$ )

dispersed shale also increases ( $r=0.79$ ). However, the volume of shale is up to twice the amount of dispersed shale. This confirms that considerable amounts of structural and laminar shales are present in the sands.

#### Calculated Effective Porosity versus Effective Porosity

This cross-plot attempts to resolve all log-derived porosity measurements and the core-derived porosity measurement. The calculated effective porosity is a function of the corrected sonic porosity, the density porosity and the core porosity (Appendix III). The effective porosity is a function of the corrected bulk density and the neutron porosity.

The calculated effective porosity is consistently higher than the effective porosity (Figure 41), especially in the lower porosity values ( $r=0.75$ ). The two independently calculated porosities tend to converge at higher porosity levels. The major reason for the discrepancy is that the core porosities are overly inflated because the clay porosity measurement reflects adsorbed water as well as free pore water. The core porosity measurements may also be inflated due to core expansion and other previously-discussed sources of error.

#### Volume of Dispersed Shale versus Effective Porosity

This plot (Figure 42) shows that two independent computations of the three log-derived porosity measurements give correlatable results. This reflects the internal consistency of the log-derived parameters. The cross-plot exhibits a good inverse relationship ( $r=-0.84$ ), showing that as the volume of dispersed shale increases, the effective porosity decreases.

The plot can be divided on the basis of lithology. There is a good concentration of points in the shaly sands which contain between 12 percent and 25 percent dispersed shale and between 20 percent and 30 percent effective porosity.

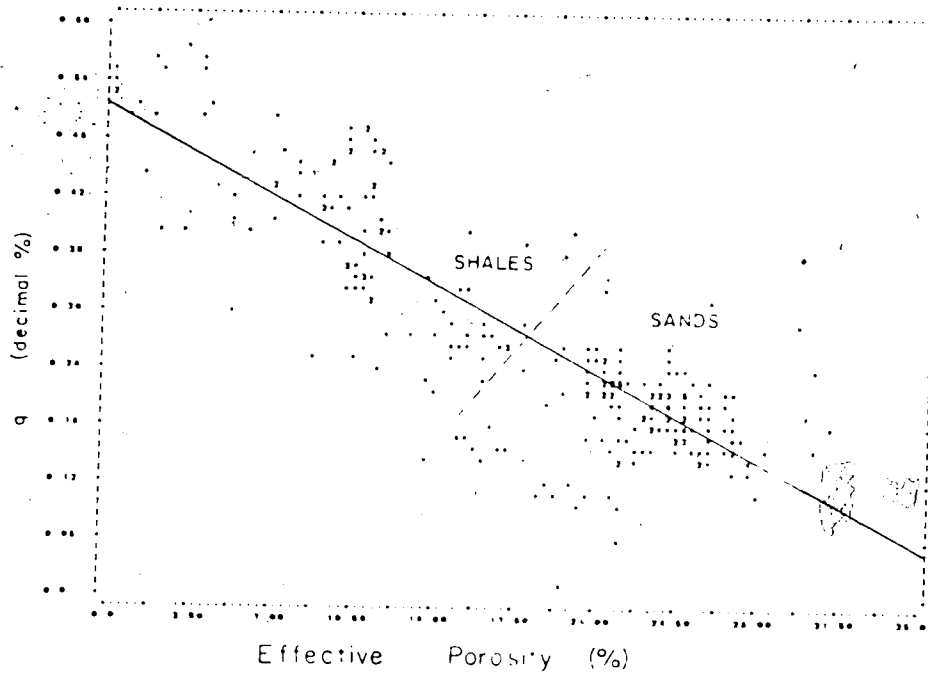


FIGURE 42. Volume of dispersed shale versus effective porosity, showing decrease in porosity with increase in dispersed shale. ( $r = -0.84$ )

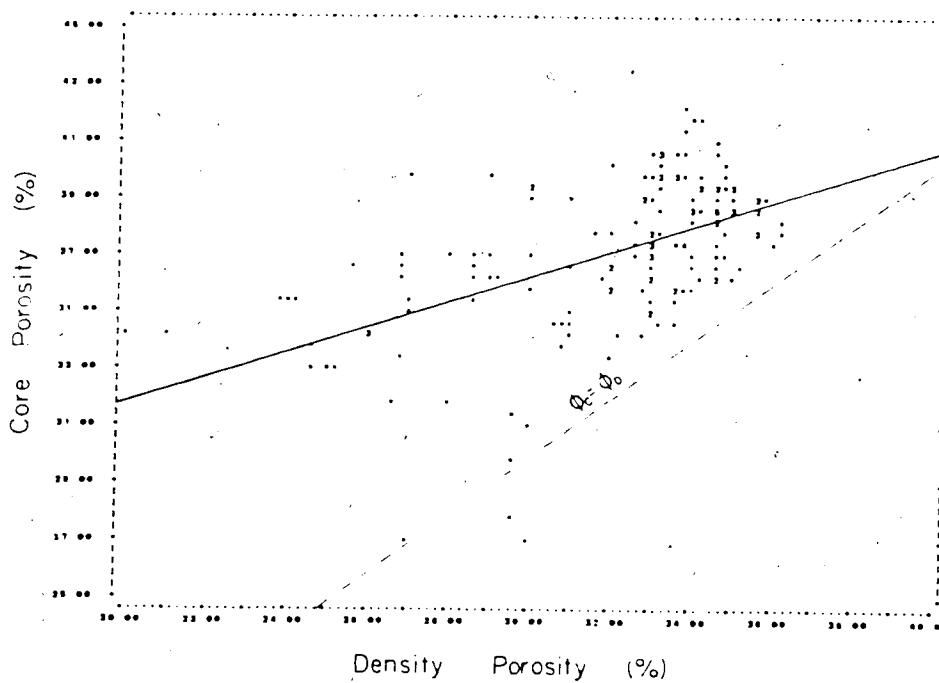


FIGURE 43. Core porosity versus density porosity, illustrating the poor relationship between log-derived and core-derived porosities. ( $r = 0.55$ )

#### Core Porosity versus Apparent Sandstone Density Porosity

All log-derived porosities were cross-plotted with the core porosity.

The relationship between the core porosity and the apparent sandstone density porosity (Figure 43) does not show a very consistent relationship ( $r=0.55$ ) and much scatter is evident. The difference between the core and density porosities is greatest at lower porosity levels, but values tend to converge at higher levels. The discrepancies between these two porosity measurements are caused by a combination of highly variable mineralogic control on the density porosity and the inflated core porosity measurements:

#### Core Porosity versus Corrected Sonic Porosity

The sonic porosity is considered to be the best approximation of total porosity (Juhasz, 1979). Total porosity is also represented by core porosity. The cross-plot (Figure 44) indicates a fair direct relationship ( $r=0.66$ ) between corrected sonic porosity and core porosity. On average, the corrected sonic porosity is 3.2 porosity units higher than the core porosity, although it ranges between 5 porosity units lower than the core porosity at one point to 7 porosity units higher at several points. These discrepancies are primarily due to the fact that corrected sonic porosity was measured every 0.15 m (6 in), whereas core porosities were generalized from one plug sample to represent core up to 1 m long. The plot suggest that a compaction correction of between 1.3 and 1.4 will reconcile the core and sonic porosities in Clearwater Formation shaly sands.

#### Core Porosity versus Effective Porosity

One major aim of shaly sand analysis is to link effective porosity and core porosity in a quantitative fashion. Since total core porosity includes adsorbed water on the clays and effective porosity does not, the difference between the two values should indicate the amount of bound water (Heslop, 1975; Ransom, 1977; Juhasz, 1979).

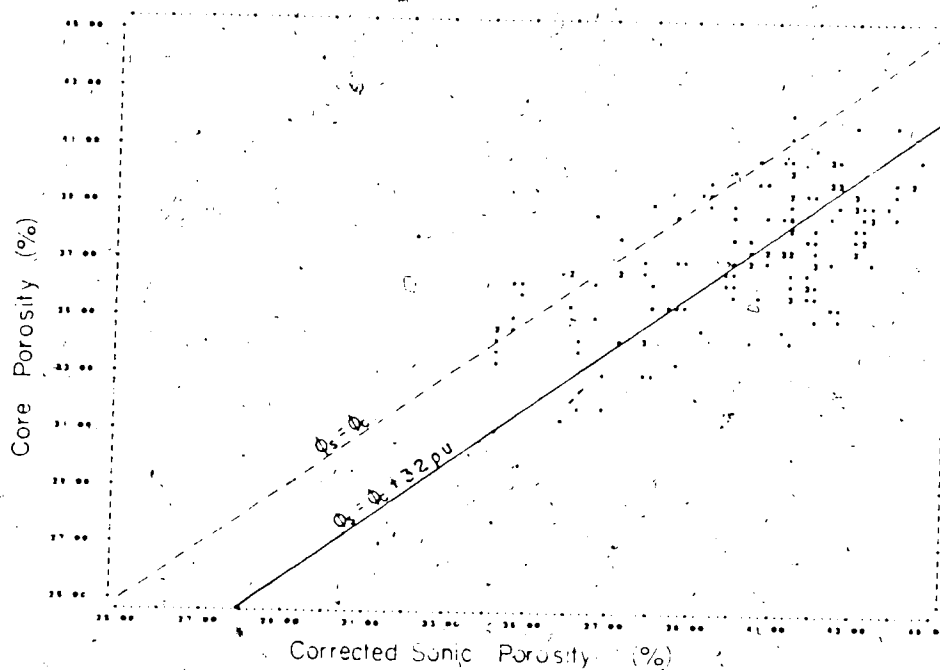


FIGURE 44. Core porosity versus corrected sonic porosity, illustrating a good relationship between log-derived and core-derived porosities. ( $r = 0.66$ )

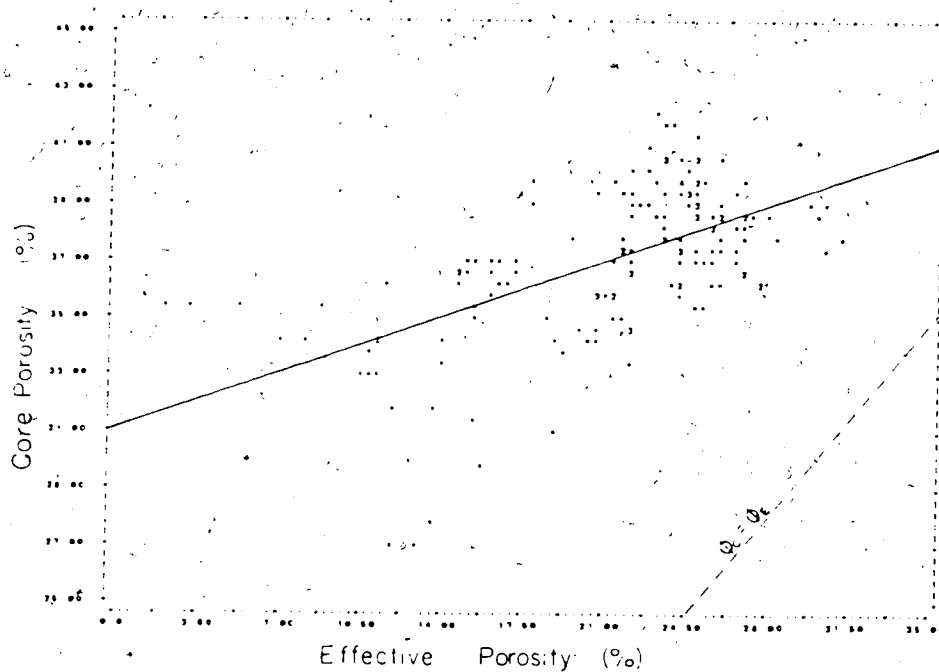


FIGURE 45. Core porosity versus effective porosity, illustrating the large discrepancy between these parameters. ( $r = 0.59$ )

The plot of core porosity versus effective porosity (Figure 45) indicates that all samples contain adsorbed water ( $r=0.59$ ). The core porosities are consistently much higher than the effective porosities. The proportion of adsorbed water is greater in the region of lower effective porosity values which represent the more shaly sands. The effective and core porosities are less divergent in the cleaner sands which contain less clay. This is indicated by the convergence of the line of equal porosity values with the line defining the relationship between the core and effective porosities.

The cleaner sands plot in the upper right-hand part of the cross-plot. Here the effective porosity ranges between 7 porosity units and 17 porosity units lower than the total or core porosity. This discrepancy is caused by a combination of greater amounts of adsorbed water in the clays of the more shaly sands and the previously-discussed inaccuracies in obtaining core porosities. On the average, the effective porosity in the cleaner shaly sands is 12 porosity units lower than the core-derived porosity.

#### Effective Porosity versus Bulk Volume Water

The plot of the effective porosity versus the bulk volume water (Figure 46) illustrates the problems with the core analysis techniques discussed previously. The wide degree of scatter ( $r=-0.24$ ) is a function of the generalized values obtained by the core analysis.

The general trend is to increased bulk volume water in the shaly sands with lower effective porosity values. This is due to the greater amounts of adsorbed water in the more shaly samples.

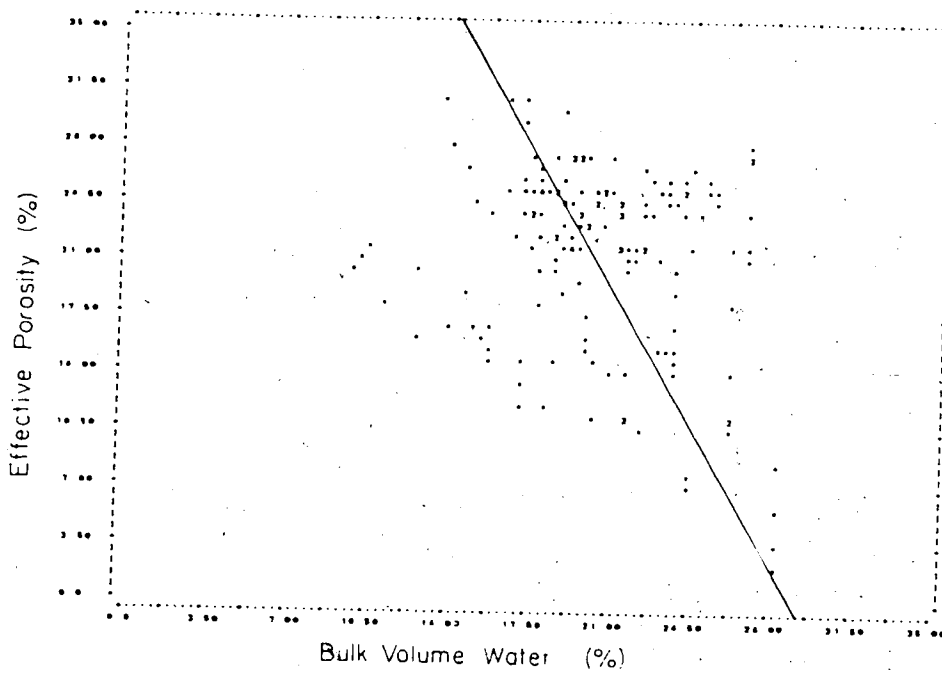


FIGURE 46. Effective porosity versus bulk volume water, showing a poor relationship and reflecting an increased amount of bound water in shalier sands. ( $r = -0.24$ )



## VI. Conclusions

### A. Sedimentologic Implications

1. The facies association analysis and grain size analysis indicate that the Clearwater Formation consists of two coarsening-upward sequences. The first represents the deposition of poorly developed offshore marine bars and ridges on a muddy shelf base. The second represents the deposition of nearshore sediments, including tidal, bundles, storm graded deposits small-scale bars and associated interbar muds and silts. This second sequence also contains a shale deposit which represents a period of non-deposition of coarser-grained sediments.

This environment of deposition is highly complex and better well control is needed in order to trace the position of the sand bars and ridges. The site holds promise for the discovery of more potentially hydrocarbon-bearing fine-grained sand bars and ridges. These bars will be of limited vertical and horizontal extent. The silty shale and shale interlaminae and interbeds may at times act as permeability barriers and serve to trap hydrocarbons. However, they also may complicate the recovery process. Many of these laminae and beds are discontinuous, rather than continuous, which will be advantageous to recovery.

Calcareous cemented zones may also act as permeability barriers, depending upon their aerial extent.

2. The Clearwater Formation in the study region consists of very fine-grained feldspathic litharenites and litharenites. The mineralogy of this formation is complex and highly variable.

In situ hydrocarbon recovery methods will have to be developed that can deal with the large amounts of complex authigenic clay mineral assemblages in order to ensure that the reservoir will not be destroyed by clay alteration and migration into the pore spaces.

## B. Geophysical Well Logging Implications

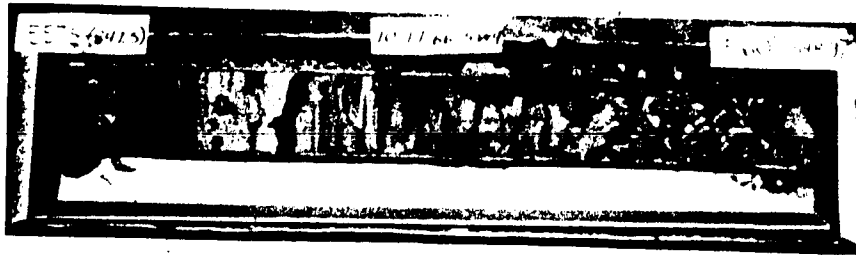
1. The corrected sonic porosity is the best indicator of total porosity (effective and non-effective) and correlates best with the core porosity. On the average, the corrected sonic porosity is 3.2 porosity units higher than the core porosity. A compaction correction of the sonic porosity of between 1.3 and 1.4 is indicated in order to reconcile sonic and core porosities.
2. The cross-plot of corrected bulk density and neutron porosity gives the most realistic effective porosity values and is a good shaliness indicator. The cleanest sand in the Clearwater Formation is found in Facies F and has a volume of shale in the order of 25 percent. The highest effective porosity is 31 percent. The high percentage of shale indicates that the formation is at the borderline of producibility.
3. The actual effective porosity of the cleaner shaly sands is approximately 12 porosity units lower than that indicated by core analysis of well 10-17-66-5W4.
4. The proportion of dispersed shale increases in the more shaly sands. The dispersed shale generally accounts for one-half of the total shale present. The remainder is in the form of structural and laminar shale.
5. The gamma ray is not a good indicator of shaliness in shaly sands which contain large amounts of non-effective clay, such as kaolinite. It is also not a good shaliness indicator in sediments which contain radioactive minerals, such as glauconite and certain feldspars which cause high gamma ray values, not reflective of shale.
6. Better shaly sand analysis techniques are needed to deal with formations, such as the Clearwater Formation, which contain both effective and non-effective clays and a mixture of dispersed, structural and laminar clays. A natural gamma ray spectroscopy log would help differentiate between clay/shale types as would a density lithology log. These logs may also be able to identify other radioactive minerals such as glauconite. Other computer programs developed by the well logging industry may be able to establish approximate sand, silt, shale and matrix percentages.
7. Core analysis techniques should be refined to deal more effectively with core in unconsolidated shaly sands. In particular, a core analysis technique is required that more clearly distinguishes between adsorbed water on clays and grain surfaces and

moveable fluids:

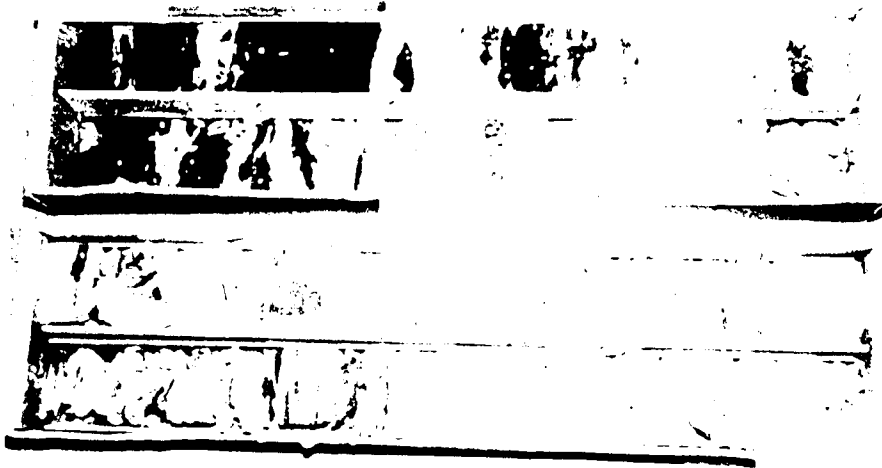
**Plates**

**Plate 1: Core Photographs for Stratigraphic Units J to H**

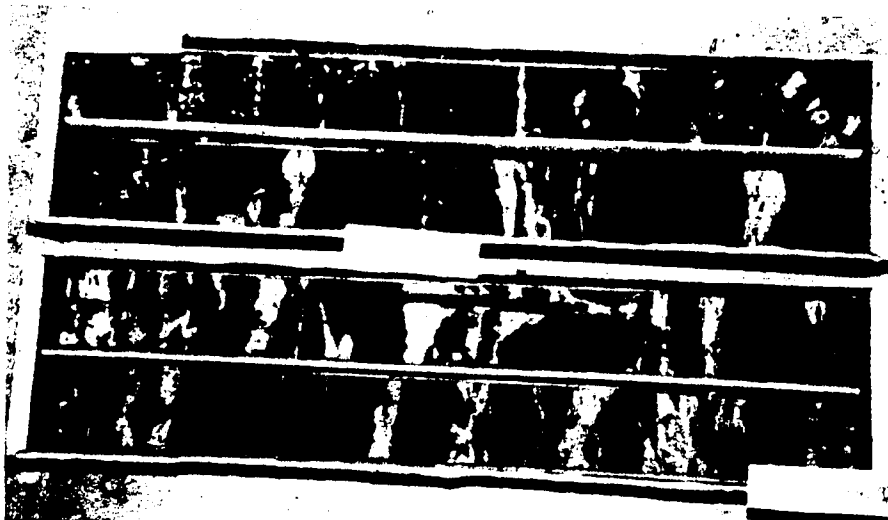
1. Stratigraphic unit J.  
Facies Association 2. Heavily Bioturbated Silty Shale to Silt and Sand.  
Horizontally laminated; interlaminae and interbeds of lightly oil stained argillaceous silt; bioturbated by traces of Planolites nicholson (1873).  
Syndepositional fault at 475 m (1558.25 ft) marks contact with stratigraphic unit I.  
Well 10-17-66-5W4: 475 m (1557.5 ft) at left to 475.8 m (1560 ft) at right.  
Scale: 1 cm = 7.6 cm
  
2. Stratigraphic unit I.  
Facies Association 2. Heavily Bioturbated Silty Shale to Silt and Sand.  
Horizontally interlaminated to interbedded; heavily bioturbated by traces of Planolites nicholson (1873).  
Thicker sandstone bed at 472 m (1548.5 ft) marks contact with stratigraphic unit H.  
Well 10-17-66-5W4: 471.7 m (1547.5 ft) at top left to 475 m (1557.5 ft) at bottom right.  
Scale: 1 cm = 7.3 cm
  
3. Stratigraphic unit H.  
Facies Association 3. Moderately to Heavily Bioturbated Sand with Silt and Silty Shale.  
Horizontally interbedded to interlaminated; moderately bioturbated by traces of Planolites nicholson (1873).  
Large trace of Skolithos linearis haldeman (1840) from 470.5 m (1543.5 ft) to 470.7 m (1544.4 ft).  
Well 10-17-66-5W4: 468.6 m (1537.5 ft) at top left to 471.7 m (1547.5 ft) at bottom right.  
Scale: 1 cm = 7.3 cm



1-1



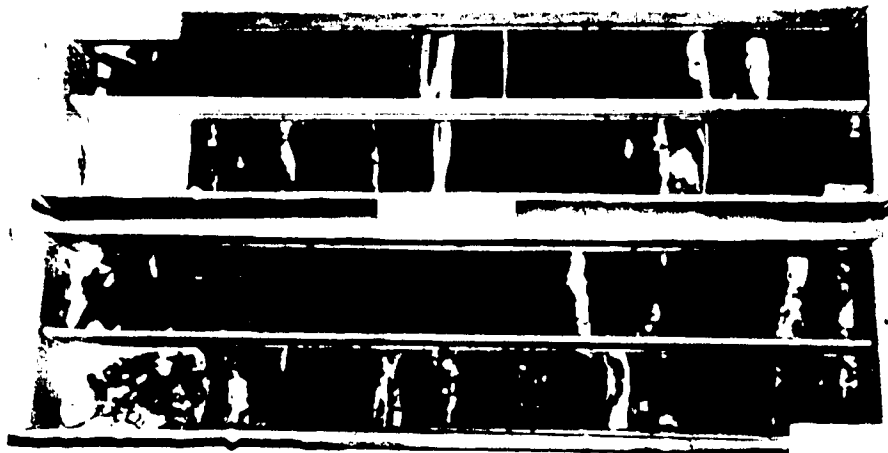
1-2



1-3

## Plate 2: Core Photographs for Stratigraphic Units G to E

1. Stratigraphic unit G.  
Facies Association 3. Moderately to Heavily Bioturbated Sand with Silt and Silty Shale.  
Horizontally bedded; silty shale ripple drapes common; lightly bioturbated by traces of Planolites nicholson (1873).  
Silty shale intraclasts at 464.4 m (1523.6 ft).  
Well 10-17-66-5W4: 463.3 m (1520 ft) at top left to 465.7 m (1528 ft) at bottom right.  
Scale: 1 cm = 6.8 cm
  
2. Stratigraphic unit F.  
Stratigraphic subunit F<sub>1</sub> from 451.1 m (1480 ft) to 452.3 m (1484 ft).  
Facies Association 6. Sand and Carbonaceous Sand.  
Horizontally laminated very fine-grained sand.  
Stratigraphic subunit F<sub>2</sub> from 452.3 m (1484 ft) to 453.5 m (1488 ft).  
Facies Association 4. Sand, Silt and Silty Shale.  
Horizontally laminated and ripple cross-laminated sands; horizontally and undulating silty shale; silty shale ripple drapes.  
Rare bioturbation by traces of Planolites nicholson (1873).  
Well 10-17-66-5W4: 451.1 m (1480 ft) at top left to 453.5 m (1488 ft) at bottom right.  
Scale: 1 cm = 8.5 cm
  
3. Stratigraphic unit E.  
Facies Association 4. Sand Silt and Silty Shale.  
Finely interlaminated to very finely interlaminated (note: curved edges caused by coring).  
Thick sand at 464.5 m (1524 ft) marks contact with stratigraphic unit F.  
Shale at 462.4 m (1517 ft) marks contact with stratigraphic unit D.  
Well 6-5-66-5W4: 462.2 m (1516 ft) at top left to 465.2 m (1526 ft) at bottom right.  
Scale: 1 cm = 8.5 cm



2-1



↳

2-2



2-3



**Plate 3: Core Photographs for Stratigraphic Units D to B**

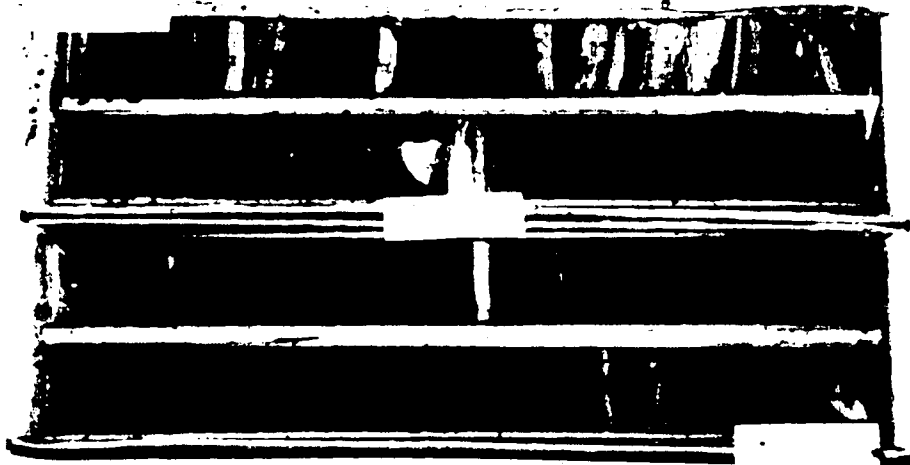
1. Stratigraphic unit D.  
 Stratigraphic subunits D<sub>2</sub> and D<sub>1</sub> from 446.2 m (1464 ft) to 446.8 m (1466 ft) and from 447.8 m (1469.2 ft) to 448.7 m (1472 ft).  
 Facies Association 1. Heavily Bioturbated Silty Shale.  
 Fissile silty shale; remnant horizontal lamination.  
 Stratigraphic subunit D<sub>2</sub> from 446.8 m (1466 ft) to 447.8 m (1469.2 ft).  
 Facies Association 3. Moderately to Heavily Bioturbated Sand with Silt and Silty Shale.  
 Very fine-grained sand and silty shale interlaminated to interbedded.  
 Entire subunit bioturbated by traces of *Planolites nicholson* (1873).  
 Well 10-17-66-5W4: 446.2 m (1464 ft) at top left to 448.7 m (1472 ft) at bottom right.  
 Scale: 1 cm = 6.8 cm
  
2. Stratigraphic unit C.  
 Facies Association 5. Graded Sand, Silt and Shale with Bouma Sequences.  
 Interbedded sand, silty shale and argillaceous silt; horizontal laminae, ripple cross-laminae; silty shale ripple drapes.  
 Complete graded-storm turbidity current deposit with Bouma sequence from 443.6 m (1455.2 ft) to 443.7 m (1455.7 ft).  
 Sand at 441.7 m (1449.2 ft) marks contact with stratigraphic unit B.  
 Well 10-17-66-5W4: 444.4 m (1448 ft) at top left to 443.8 m (1456 ft) at bottom right.  
 Scale: 1 cm = 6.8 cm
  
3. Stratigraphic unit B.  
 Facies Association 6. Sand and Carbonaceous Sand.  
 Horizontally laminated and inclined laminae; undulating silty shale laminae.  
 Shale at 456.7 m (1498.2 ft) marks contact with stratigraphic unit C.  
 Well 6-3-66-5W4: 454.8 m (1492 ft) at bottom right to 457.8 m (1502 ft) at top left.  
 Scale: 1 cm = 7.3 cm



3-1



3-2



3-3

**Plate 4: Mineralogy**

1. Authigenic feldspar overgrowth (appears as one grain under plain light). Dust at boundary. Entire grain is subangular and exhibits abrasion, indicating formation during a previous depositional cycle. Grain surrounded by matrix material.  
Sample 80-4-25; Facies D; 445.3 m (1461 ft)  
Magnification: 390.63 X
2. Detrital plagioclase feldspar exhibiting crystal zoning and albite twinning.  
Sample 80-9-5; Facies C; 442.5 m (1451.7 ft)  
Magnification: 390.63 X
3. Detrital microcline feldspar exhibiting typical grid twinning. Offset fracture caused by overburden pressure.  
Sample 80-9-2; Facies B; 440.2 m (1444.3 ft)  
Magnification: 390.63 X
4. Volcanic rock fragment; untwinned zoned feldspar microphenocryst within finely-crystalline volcanic groundmass.  
Sample 80-9-2; Facies B; 440.2 m (1444.3 ft)  
Magnification: 390.63 X



4-1



4-2



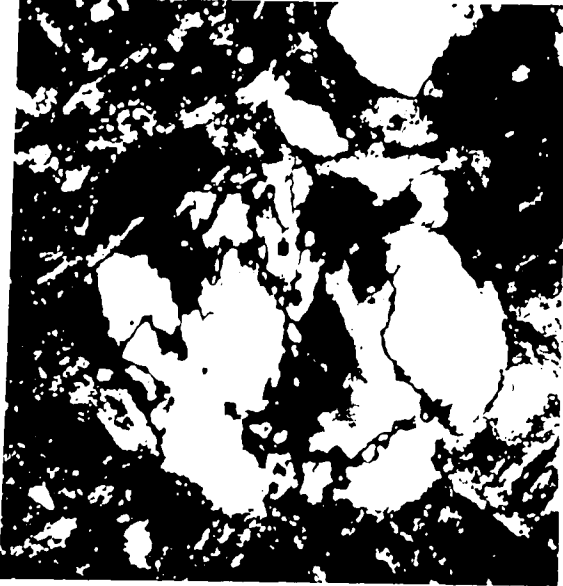
4-3



4-4

**Plate 5: Mineralogy**

1. Polycrystalline quartz of metamorphic origin. Note sutured texture of grain.  
Sample 80-9-4; Facies B; 441.8 m (1449.5 ft)  
Magnification: 390.63 X
2. Chlorite grain (identified by ultra blue birefringence). Grain is embedded in a larger glauconite grain exhibiting soft sediment deformation.  
Sample 80-9-5; Facies C; 442.5 m (1451.7 ft)  
Magnification: 390.63 X
3. Glauconite replacement of original oolite. Grain has been abraded.  
Sample 80-9-6; Facies C; 442.6 m (1452 ft)  
Magnification: 390.63 X
4. Calcareous cement: cone-in-cone structure (to the right) displaces the original fabric; calcareous cement (to the left) replaces original matrix, pore spaces and some detrital grains.  
Sample 75-1-2; Facies F; 454.5 m (1491 ft)  
Magnification: 156.25 X



5-1



5-2



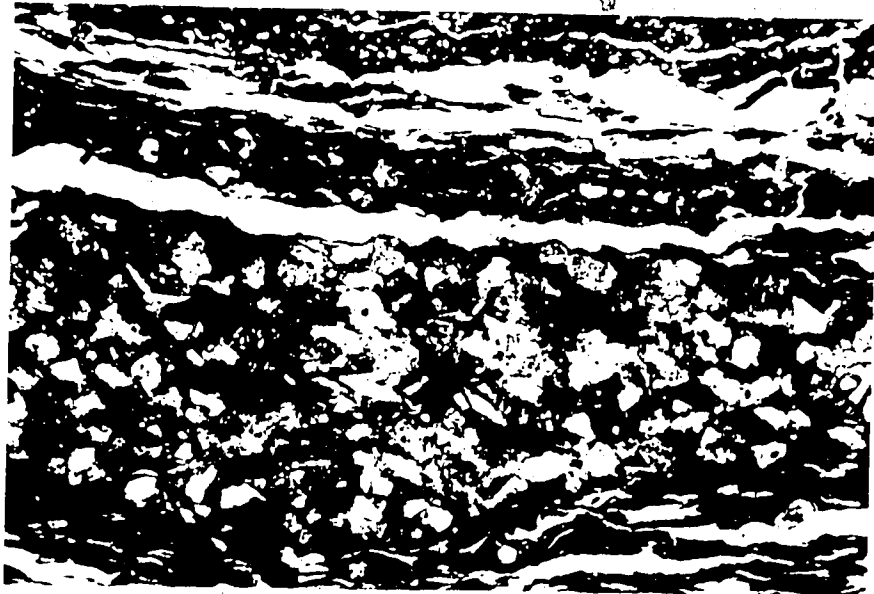
5-3



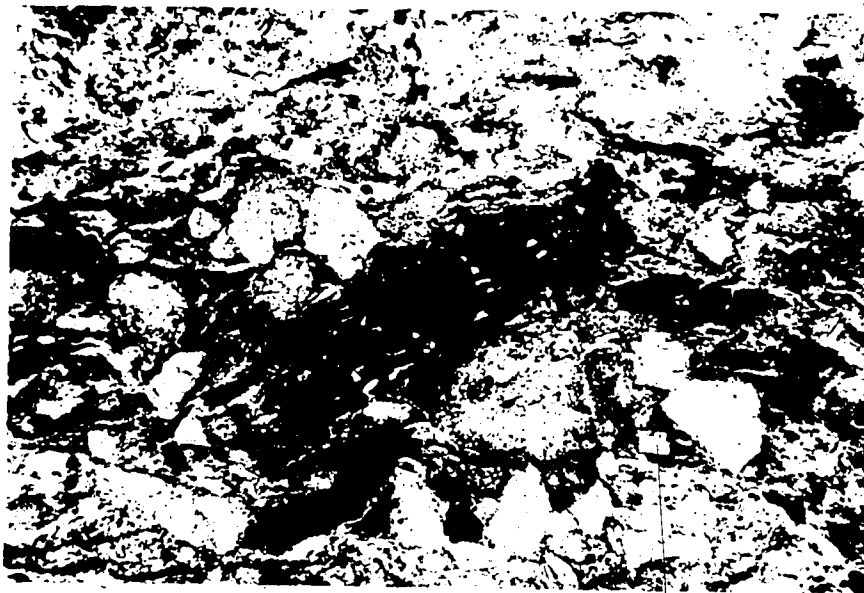
5-4

**Plate 6: Mineralogy and Textures**

1. Calcite veins (white) displacing poorly sorted very fine-grained sand with a slight offset.  
Organic debris (black) exhibiting preferred orientation aligned parallel to partings. Note that organic debris is also found within the calcite veins. Detrital grains include subangular quartz with some chert.  
Individual laminae poorly sorted.  
Sample 80-9-23; Facies F; 454.3 m (1490.4 ft)  
Magnification: 156.25 X
2. Organic fragment exhibiting original cell structure. Note larger size of fragment as compared to other detrital grains. This is due to the lower specific gravity of the organic fragment. Quartz grains at 4 o'clock with respect to the organic fragment cemented by quartz overgrowths. Poorly sorted nature of Clearwater Formation is also exhibited.  
Sample 80-9-4; Facies B; 441.8 m (1449.5 ft)  
Magnification: 156.25 X



6-1



6-2

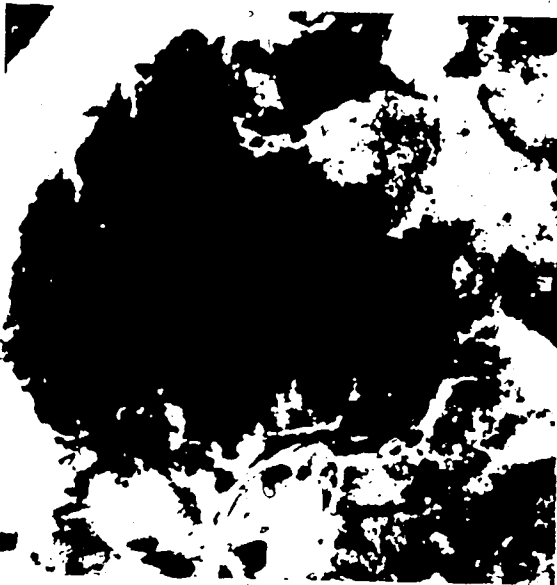


**Plate 7: Mineralogy**

1. Muscovite mica grain (just above centre of photograph) and sedimentary rock fragment (to left of mica) deformed by compaction between quartz grain on top and subangular chert grains on bottom. Note rims of oil-stained clays lining the pore spaces.  
Sample 80-9-2; Facies B; 440.2 m (1444.3 ft)  
Magnification: 156.25 X
2. Large mass of authigenic pyrite. Many cubic crystals can be seen in outline on the edge of the mass. Individual pyrite crystals infill pore spaces.  
Sample 80-9-5; Facies C; 442.5 m (1451.7 ft)  
Magnification: 156.25 X
3. Subangular metamorphic quartz grain with numerous sillimanite(?) needle-like inclusions. Oil stained clay lines the pore space and is found at grain-to-grain contacts. Small clay particles are seen within the pore space as well. Some may be in place, but most have been displaced during thin section preparation.  
Sample 80-9-1; Facies B; 439.5 m (1442 ft)  
Magnification: 390.63 X



7-1<sup>a</sup>



7-2



7-3

## Bibliography

- Alpert, S.P., 1974, Systematic review of the genus Skolithos; *Journal of Paleontology*, Vol. 48, No. 4, p. 661-669.
- Amajor, L.C., 1980, Chronostratigraphic, depositional patterns and environmental analysis of sub-surface Lower Cretaceous (Albian) Viking reservoir sandstones in central Alberta and part of southwestern Saskatchewan; unpublished PhD. Thesis, University of Alberta, 596 p.
- Anderton, R., 1976, Tidal-shelf sedimentation: an example from the Scottish Dalradian; *Sedimentology*, Vol. 23, p. 429-458.
- Badgley, P.C., 1952, Notes on the subsurface stratigraphy and oil and gas geology of the Lower Cretaceous series in central Alberta; *Geological Society of Canada, Paper* 52-11, 12 p.
- Ball, M.M., 1967, Carbonate sand bodies of Florida and the Bahamas; *Journal of Sedimentary Petrology*, Vol. 37, No. 2, p. 556-591.
- Banks, N.L., 1973, Innerelv Member: Late Pre-Cambrian marine shelf deposit, East Finnmark; *Norg. geol. Unders.*, Vol 288, p. 7-25.
- Basan, P.B. and Frey, R.W., 1977, Actual-palaeontology and neoichnology of salt marshes near Sapelo Islands, Georgia in *Ftrace Fossils 2* (Crimes, T.P. and Harper, J.C., Eds.); *Geological Journal Special Issue No. 9*, p. 41-70.
- Beaumont, C., 1981, Foreland basins; *Geophysical Journal of the Royal Astronomical Society*, Vol. 65, p. 291-329.
- Belderson, R.H., Johnson, M.A. and Kenyon, N.H., 1982, *Bedforms in Offshore Tidal Sands: processes and deposits* (Stride, A.H., Ed.); Chapman and Hall, New York, p. 27-57.
- Blatt, H., 1982, *Sedimentary Petrology*; W.H. Freeman and Company, p. 153-155.
- Blatt, H., Middleton, G. and Murray, R., 1980, *Origin of sedimentary rocks*; Prentice-Hall, Incorporated, New Jersey, 782 p.
- Brenner, R.L., 1978, Sussex Sandstone of Wyoming: example of Cretaceous offshore sedimentation; *Bulletin American Association of Petroleum Geologists*, Vol. 62, No. 2, p. 181-200.
- Brenner, R.L., 1980, Construction of process-response models for ancient epicontinental seaway depositional systems using partial analogues; *Bulletin American Association of Petroleum Geologists*, Vol. 64, No. 8, p. 1223-1244.

- Brenner, R.L. and Davies, D.K., 1973, Storm-generated coquinooidal sandstone: genesis of high energy marine sediments from the Upper Jurassic of Wyoming and Montana; Geological Society of America Bulletin, Vol. 84, p. 1685-1698.
- Bridges, P.H., 1982, Ancient offshore tidal deposits in Offshore Tidal Sands: processes and deposits (Stride, A.H., Ed.); Chapman and Hall, New York, p. 172-192.
- Buckles, R.S., 1979, Steam stimulation heavy oil recovery at Cold Lake, Alberta; American Institute of Mining, Metallurgical and Petroleum Engineers, Incorporated, SPE 7994, 7 p.
- Burst, J.F., 1956, Glauconite pellets: their mineralogic nature and applications to stratigraphic interpretations; Bulletin American Association of Petroleum Geologists, Vol. 42, No. 2, p. 310-327.
- Bush, D.C. and Jenkins, R.E., 1969, Proper hydration of clays for rock property determinations; Society of Petroleum Engineers of A.I.M.E., Paper SPE 2589, 8 p.
- Cameron, E.M., 1965, Application of geochemistry to stratigraphic problems in the Lower Cretaceous of western Canada; Bulletin American Association of Petroleum Geologists, Vol. 49, No. 1, p. 62-80.
- Campbell, F.A. and Williams, G.D., 1965, Chemical composition of shales of the Mannville Group (Lower Cretaceous) of central Alberta, Canada; Bulletin American Association of Petroleum Geologists, Vol. 49, No. 1, p. 81-87.
- A. Carrigy, M.A., 1963, Criteria for differentiating the McMurray and Clearwater Formations in the Athabasca oil sands; Research Council of Alberta, Bulletin 14, 32 p.
- Carrigy, M.A. and Kramers, J.W., 1974, Geology of Alberta oil sands in Athabasca Oil Sands; Conference Proceedings, Engineering Institute of Canada, Western Region, p. 13-24.
- Caston, V.N.D., 1972, Linear sand banks in the southern North Sea; Sedimentology, Vol. 18, p. 63-78.
- Clack, W.J.F., 1968, Sedimentology of the Mannville Group in the Cold Lake area, Alberta; unpublished M.Sc. thesis, University of Calgary, 95 p.
- Collins, H.N., 1977, An integrated approach to unconsolidated sand evaluation; Transactions, Canadian Well Logging Society, Sixth Formation Evaluation Symposium, 10 p.
- Conybeare, C.E.B. and Crook, K.A.W., 1968, Manual of sedimentary structures; Australia Department of National Development, Bureau of Mineral Resources, Geology and Geophysics, Bulletin No. 102, 327 p.

- Crimes, T.P., 1970, The significance of trace fossils in sedimentology, stratigraphy and paleoecology with examples from Late Paleozoic strata in *Trace Fossils* (Crimes, T.P. and Harper, J.C., Eds.); Seel House Press, Liverpool, p. 101-126.
- Eade, J.R., 1975, Round robin study of analytical procedures of various laboratories on assay analysis of Athabasca tar sands; Fifth Formation Evaluation Symposium of the Canadian Well Logging Society, No. 5, 15 p.
- Ekdale, A.A., Bromley, R.G. and Pemberton, S.G., 1984, Ichnology, trace fossils in sedimentology and stratigraphy; Short Course Notes No. 15, Society of Economic Paleontologists and Mineralogists, 317 p.
- Edmundson, H. and Raymer, L.L., 1979, Radioactive logging parameters for common minerals; Society of Professional Well Log Analysts Twentieth Annual Logging Symposium, 20 p.
- Energy Resources Conservation Board, 1973, Geology and proved in place reserves of the Cold Lake oil sands deposits; E.R.C.B. Report 73-L-GEOL, 20 p.
- Esso Resources, 1978, Report to the Energy Resources Conservation Board, Sec. 3, 11 p.
- Fairbridge, R.W. and Bourgeois, J., 1978, The encyclopedia of sedimentology; Academic Press, p. 587-588.
- Fertl, W.H. 1972, Status of shaly sand evaluation; Canadian Well Logging Society Fourth Formation Evaluation Symposium, 22 p.
- Fertl, W.H. 1981, Evaluation of heavy oil and tar sand deposits using geophysical well logging techniques in open and cased wellbore in *The Future of heavy Crude Oils and Tar Sands* (Meyer, R.F. and Steele, C.T., Eds.); UNITAR, McGraw-Hill, Incorporated, New York, p. 283-300.
- Field, M.E., Nelson, C.H., Cacchione, D.A. and Drake, D.E., 1981, Sand waves on an epicontinental shelf: northern Bering Sea in *Sedimentary Dynamics of Continental Shelves* (Nittrouer, C.A., Ed.); *Developments in Sedimentology* No. 32, Elsevier, p. 233-258.
- Folk, R.I. 1968, *Petrology of sedimentary rocks*; Hemphill's Book Store, Austin, Texas, 170 p.
- Frey, R.W., 1975, *The study of trace fossils*; Springer-Verlag, New York, 562 p.
- Gallup, W.B. 1974, The geological history of McMurray-Clearwater deposition in the Athabasca oil sands area in *Oil Sands, Fuel of the Future* (Hills, F.V., Ed.); Canadian Society of Petroleum Geologists, Memoir 3, p 100-114.

- Gilman, R.A. and Metzger, W.J., 1967, Cone-in-cone concretions from western New York; *Journal of Sedimentary Petrology*, Vol. 37, No. 1, p. 87-95.
- Ginsberg, R.N., 1975, Tidal deposits, a casebook of recent examples and fossil counterparts; Springer-Verlag, 428 p.
- Glaister, R.P., 1957, Lower Cretaceous of southern Alberta and adjoining areas; Doctoral dissertation, Evanston, Illinois, 118 p.
- Glaister, R.P., 1959, Lower Cretaceous of southern Alberta and adjoining areas; *Bulletin American Association of Petroleum Geologists*, Vol. 43, No. 3, p. 590-640.
- Harms, J.C., Southard, J.B. and Walker, R.J., 1975, Depositional environments as interpreted from primary sedimentary structures and stratification sequences; *Society of Economic Paleontologists and Mineralogists, Short Course No. 2*, 161 p.
- Harms, J.C., Southard, J.B. and Walker, R.J., 1982, Structures and sequences in clastic rocks; *Society of Economic Paleontologists and Mineralogists, Short Course No. 9*, 289 p.
- Harrison, D.B., Glaister, R.P. and Nelson, H.W., 1981, Reservoir description of the Clearwater oil sand, Cold Lake, Alberta, Canada in *The Future of Heavy Crude Oils and Tar Sands* (Meyer, R.F. and Steele, C.T., Eds.); UNITAR, McGraw-Hill, Incorporated, New York, p. 264-279.
- Heckel, P.H., 1972, Ancient shallow marine environments in *Recognition of Ancient Sedimentary Environments* (Rigby, J.K. and Hamblin, W.K., Eds.); *Society of Economic Paleontologists and Mineralogists Special Publication No. 16*, p. 226-286.
- Hedberg, H.D. (Ed.), 1976, *International stratigraphic guide*; International Subcommittee on Stratigraphic Classification of IUGS, Commission on Stratigraphy, Wiley-Interscience Publications, Toronto, 200 p.
- Helander, D.P., 1980, Shaly sand interpretation in *Formation Evaluation Unit II Notes* (Helander, D.P., Ed.); Oil and Gas Consultants International Incorporated, 106 p.
- Heslop, A., 1972, Gamma ray response of shaly sandstones; *Canadian Well Logging Society Journal*, Vol. 5, No. 1, p. 29-37.
- Heslop, A., 1975, Porosity in shaly-sands; *Canadian Well Logging Society Journal*, Vol. 8, No. 1, p. 7-19.
- Hilchie, D.W., 1982, Shaly sandstone interpretation in *Advanced Well Log Interpretation*; Douglas W. Hilchie Limited, p. VII-1-VII-42.

- Hill, H.J., Shirley, O.J. and Klein, G.E., 1979, Bound water in shaly sand, its relation to Qv and other formation properties; Log Analyst: Society of Professional Well Log Analysts Newsletter, Vol. 20, No. 3, p. 3-17.
- Hobday, D.K. and Morton, R.A., 1984, Lower Cretaceous shelf storm deposits, northeast Texas in *Siliciclastic Shelf Sediments* (Tillman, R.W. and Seimers, C.T., Eds.); Society of Economic Paleontologists and Mineralogists Special Publication No. 34, p. 205-213.
- Howard, J.D., 1972, Nearshore sedimentary processes as geologic studies in *Shelf Sediment Transport: process and pattern* (Swift, D.J.P., Duane, D.B. and Pilkey, O.H., Eds.); Dowden, Hutchinson and Ross, Stroudsburg, Pennsylvania, p. 645-648.
- Jardine, D., 1974, Cretaceous oil sands of western Canada in *Oil Sands, Fuel of the Future* (Hills, L.V., Ed.); Canadian Society of Petroleum Geologists, Memoir 3, p. 50-67.
- Jenkins, R.E. and Bush, D.C., 1971, Improved method for the analysis of reservoir rocks containing clays; Canadian Well Logging Society, Third Formation Evaluation Symposium, Paper No. 7053, p. 24-30.
- Johnson, H.D., 1978, Shallow siliciclastic seas in *Environments and Facies* (Reading, H.G., Ed.); Elsevier, New York, p. 207-258.
- Johnson, M.A. and Belderson, R.H., 1969, The tidal origin of some vertical sedimentary changes in epicontinental seas; *Journal of Geology*; Vol. 77, p. 353-357.
- Jordon, T.E., 1981, Thrust loads and foreland basin evolution, Cretaceous, western United States; *Bulletin American Association of Petroleum Geologists*, Vol. 65, No. 12, p. 2506-2520.
- Juhasz, I., 1979, The central role of Qv and formation-water salinity in the evaluation of shaly formations; Log Analyst: Society of Professional Well Log Analysts Newsletter, Vol. 20, No. 4, p. 3-13.
- Keeler, R.G., 1980, Lower Cretaceous (Mannville Group) Grand Rapids Formation, Wabasca A oil sand deposit area, northeast Alberta in *Lloydminster and Beyond: Geology of Mannville Hydrocarbon Reservoirs* (Beck, L.S., Christopher, J.E. and Kent, D.M., Eds.); Saskatchewan Geological Society, Special Publication No. 5, p. 96-1.
- Kendall, G.H., 1977, Importance of reservoir description in the evaluation of *in-situ* recovery methods for Cold Lake heavy oil: part I - reservoir description; *Journal of Canadian Petroleum Technology*, January-March, p. 41-47.
- Klein, G. de V., 1970, Depositional and dispersal dynamics of intertidal sand bars. *Journal of Sedimentary Petrology*, Vol. 40, No. 4, p. 1095-1127.

- Klein, G. de V., 1977, Clastic tidal facies. Continuing Education Publication Company, 149 p.
- Klein, G. de V. and Ryer, T.A., 1978, Tidal circulation patterns in Pre-Cambrian, Paleozoic and Cretaceous epeiric and mioclinal shelf seas, Geological Society of America Bulletin, Vol. 89, No. 7, p. 1050-1058.
- Kramers, J.W., 1974, Geology of the Wabasca A oil sand deposit (Grand Rapids Formation) in Oil Sands, Fuel of the Future (Hills, L.V., Ed.); Canadian Society of Petroleum Geologists Memoir 3, p. 50-67.
- Kramers, J.W., 1975, Primrose Lake air weapons range oil sand evaluation program, 1974-1975; Alberta Research Council Report, 75 p.
- Krug, J.A. and Cox, D.O., 1976, Shaly sand cross-plot: a mathematical treatment; The Log Analyst, Vol. 17, p. 11-15.
- Levell, B.K., 1980, A late PreCambrian tidal shelf deposit, the Lower Sandfjord Formation, Finnmark, North Norway; Sedimentology, Vol. 27, p. 539-557.
- MacCallum, G.T., 1981, Geology of Lloydminster play, Alberta in The Future of Heavy Crude and Tar Sands (Meyer, R.F. and Steele, C.T., Eds.); UNITAR, McGraw-Hill, Incorporated, New York, p. 223-236.
- Martin, R. and Jamin, F.G.S., 1963, Paleogeomorphology of the buried Devonian landscape in northeast Alberta in K.A. Clark Volume: a collection of paper on the Athabasca oil sands (Carrigy, M.A., Ed.); Research Council of Alberta, Information Series, No. 45, p. 31-42.
- Matheny, S.L., 1979, WECO expands Cold Lake heavy oil production; Oil and Gas Journal, Vol. 77, No. 44, p. 104-118.
- Maycock, I.D., 1964, Petrographic and sedimentological associations of Upper Mannville sandstones in western Saskatchewan in Proceedings, Billings Geological Society, North Dakota Geological Society, Saskatchewan Geological Society, Third International Williston Basin Symposium, p. 153-168.
- McCave, I.N., 1970, Deposition of fine-grained suspended sediment from tidal currents; Journal of Geophysical Research, Vol. 75, No. 21, p. 4151-4159.
- McCave, I.N., 1972, Patterns of fine sediment dispersal in Shelf Sediment Transport: process and pattern (Swift, D.J.P., Duane, D.B. and Pildey, O.H., Eds.); Dowden, Hutchinson and Ross, Stroudsburg, Pennsylvania, p. 225-248.
- McConnell, R.G., 1891, Report on a portion of the District of Athabaska, comprising the country between Peace River and Athabaska River, north of Lesser Slave Lake, Geological Survey of Canada, Vol. V, 1890-1891, Sec. D, p. 5-7.



- McLearn, F.H., 1917, Athabasca River section, Alberta; Geological Survey of Canada, Summary Report, 1916, p. 145-151.
- McLearn, F.H., 1918, Peace River section, Alberta; Geological Survey of Canada, Summary Report, 1917, Part C, p. 14-21.
- McLearn, F.H., 1931, The Gastroplites and other Lower Cretaceous faunas of the northern Great Plains; Transactions of the Royal Society of Canada, Series 3, Vol. 25, Sec. 4, p. 1-8.
- McLearn, F.H., 1932, Problems of the Lower Cretaceous of the Canadian interior; Transactions of the Royal Society of Canada, Series 3, Vol. 26, Sec. 4, p. 157-175.
- Mellon, G.B., 1967, Stratigraphy and petrology of the Lower Cretaceous Blairmore and Mannville Groups, Alberta foothills and plains; Research Council of Alberta, Bulletin 21, 270 p.
- Mellon, G.B. and Wall, J.H., 1956, Geology of the McMurray Formation; Research Council of Alberta, Report No. 72, 43 p.
- Mellon, G.B. and Wall, J.H., 1963, Correlation of the Blairmore Group and equivalent strata; Bulletin of Canadian Petroleum Geologists, Vol. 11, p. 396-409.
- Minken, D.F., 1974, The Cold Lake oil sands, geology and a reserves estimate in Oil Sands, Fuel of the Future (Hills, L.V., Ed.); Canadian Society of Petroleum Geologists, Memoir 3, p. 84-99.
- Mooers, C.N., 1976, Introduction to the physical oceanography and fluid dynamics of continental margins in Marine Sediment Transport and Environmental Management (Stanley, D.J. and Swift, D.J.P., Eds.); American Geological Institute, Wiley-Interscience, Toronto, p. 7-21.
- Mossop, G.D., 1984, Alberta Geological Survey research; Geoscience Canada, Vol. 11, No. 7, p. 3-15.
- Mossop, G.D., Kramers, J.W., Flach, P.D. and Rottenfusser, B.A., 1981, Geology of Alberta's oil sands and heavy oil deposits in The Future of Heavy Crude and Tar Sands (Meyer, R.F. and Steele, C.T., Eds.); UNITAR, McGraw-Hill, New York, page 197-207.
- Nauss, A.W., 1945, Cretaceous stratigraphy of Vermilion area, Alberta, Canada; Bulletin American Association of Petroleum Geologists, Vol. 29, No. 11, p. 1605-1629.
- Neasham, J.W., 1977, The morphology of dispersed clay in sandstone reservoirs and its effect on sandstone shaliness, pore space and fluid flow properties; Society of Petroleum Engineers of A.I.M.E., Paper SPE 6858, 8 p.

- Nie, N.H., Hull, C.H., Jenkins, J.G., Steinbrenner, K. and Bent, D.H., 1975, Statistical package for the social sciences; McGraw-Hill Company; Toronto, 675 p.
- Nittrouer, C.A. and Sternberg, R.W., 1981, The formation of sedimentary strata in an allothonous shelf environment: the Washington continental shelf; *Marine Geology*, Vol. 42, p. 201-232.
- Off, T., 1963, Rhythmic linear sand bodies caused by tidal currents; *Bulletin American Association of Petroleum Geologists*, Vol. 47, No. 2, p. 324-341.
- Outtrim, C.P. and Evans, R.G., 1977, Alberta's oil sands reserves and their evaluation in *The Oil Sands of Canada-Venezuela* (Redford, D.A. et al, Eds.); Canadian Institute of Mining and Metallurgy, Special Volume No. 17, p. 36-66.
- Pettijohn, F.J., 1975, *Sedimentary Rocks*; Harper and Row, New York, p. 470-471.
- Pirson, S.J., 1981a, Sedimentological studies by log curve shapes in *Geological Well Log Analysis*; Gulf Publication Company, p. 44-71.
- Pirson, S.J., 1981b, Paleo-facies logging and mapping in *Geological Well Log Analysis*; Gulf Publication Company, p. 163-190.
- Poupon, A., Clavier, C., Dumanoir, J., Gaymard, R. and Misk, A., 1970, Log analysis of sand-shale sequences: a systematic approach; *Journal of Petroleum Geology, Transactions*, Vol. 249, p. 867-881.
- Poupon, A. and Gaymard, R., 1970, The evaluation of clay content from logs; *Society of Professional Well Log Analysts Eleventh Annual Logging Symposium, Transactions*, 21 p.
- Putnam, P.E., 1979, *The sedimentology of the Colony Formation, east-central Alberta*; unpublished M.Sc. thesis, 126 p.
- Putnam, P.E. and Pedskalny, A., 1982, Lithic sandstones with a large volcanic component: the Mannville Group (Lower Cretaceous) of the Tucker Lake area, east-central Alberta, Canada (Abstr.); *International Association of Sedimentologists Eleventh International Congress*, p. 88.
- Putnam, P.E. and Pedskalny, A., 1983, Provenance of Clearwater Formation reservoir sandstones, Cold Lake, Alberta: with comments on feldspar composition; *Bulletin of Canadian Petroleum Geology*, Vol. 31, No. 3, p. 148-160.
- Raaf, J.F.M. de and Boersma, J.R., 1971, Tidal deposits and their sedimentary structures; *Geologie en Mijnbouw*, Vol. 50, No. 3, p. 479-504.

- Ransom, R.C., 1977, Methods based on density and neutron well-logging responses to distinguish characteristics of shaly sandstone reservoir rocks; *The Log Analyst*, Vol. 17, p. 47-62.
- Rapson, J.E., 1965, Petrography and derivation of Jurassic-Cretaceous clastic rocks, southern Rocky Mountains, Canada; *Bulletin American Association of Petroleum Geologists*, Vol. 49, No. 9, p. 1426-1452.
- Reading H.G., 1978, *Facies in Sedimentary Environments and Facies* (Reading, H.G., Ed.); Elsevier, New York, p. 4-14.
- Reineck, H.E., 1967, Layered sediments of tidal flats, beaches and shelf bottoms of the North Sea in *Estuaries* (Lauff, G.H., Ed.); American Association of Advanced Science, Special Publication No. 83, p. 191-206.
- Rice, D.D., 1984, Widespread, shallow marine, storm generated sandstone units in the Upper Cretaceous Mosby Sandstone, central Montana in *Siliciclastic Shelf Sediments* (Tillman, R.W. and Siemers, C.T., Eds.); Society of Economic Paleontologists and Mineralogists Special Publication No. 34, p. 143-161.
- Rudkin, R.A., 1964, Lower Cretaceous in *Geological History of Western Canada* (McCrossan, R.G. and Glaister, R.P., Eds.); Alberta Society of Petroleum Geology, p. 150-168.
- Sarjeant, W.A.S., 1974, *Fossil and living dinoflagellates*; Academic Press, New York, p.
- Schlumberger Limited, 1972, *Log interpretation - principles*; Schlumberger Limited, New York, 113 p.
- Schlumberger Limited, 1974, *Log interpretation - applications*; Schlumberger Limited, New York, 116 p.
- Schlumberger Limited, 1979, *Log interpretation charts*; Schlumberger Limited, New York, 97 p.
- Scholle, P.A., 1979, A color illustrated guide to constituents, textures, cements, and porosities of sandstones and associated rocks; *American Association of Petroleum Geologists, Memoir No. 28*, 201 p.
- Seilacher, A., 1967, Bathymetry of trace fossils; *Marine Geology*, Vol. 5, p. 413-428.
- Selley, R.C., 1978, *Concepts and methods of subsurface facies analysis*; American Association of Petroleum Geologists, Education Course Notes Series, No. 9, 86 p.

- Serra, O. and Sulpice, L., 1975, Sedimentological analysis of shale-sand series from well logs; Society of Professional Well Log Analysts, Sixteenth Annual Logging Symposium, No. 16, 23 p.
- Shurr, G.W., 1984, Geometry of shelf sandstone bodies in the Shannon Sandstone of southeastern Montana in Siliciclastic Shelf Sediments (Tillman, R.W. and Seimers, C.T., Eds.); Society of Economic Paleontologists and Mineralogists, Special Publication No. 34, p. 63-83.
- Slater, R.D., 1984, Prediction of tides in epeiric seas with a numerical model: The Cretaceous seaway of North America (Abstr.), in Program and Abstracts, Research Symposium: Sedimentology of Shelf Sands and Sandstones; Society of Economic Paleontologists and Mineralogists, Calgary, p. 63.
- Smith, J.D., 1969, Geomorphology of a sand ridge; Journal of Geology, Vol. 77, p. 39-55.
- Stelck, C.R., 1975, Basement control of Cretaceous sand sequences in western Canada in The Cretaceous System in the Western Interior of North America (Caldwell, W.G.E., Ed.); Geological Association of Canada, Special Paper No. 13, p. 427-440.
- Stride, A.H., 1963, Current-swept sea floors near the southern half of Great Britain; Quarterly Journal of the Geological Society of London, Vol. 119, p. 175-199.
- Swift, D.J.P., 1969, Evolution of the shelf surface and the relevance of modern shelf studies to the rock record in The New Concepts of Continental Margin Sedimentation (Stanley, D.J., Ed.); American Geological Institute, Short Course Lecture Notes, p. DS-7-1-DS-7-19.
- Swift, D.J.P., 1969, Outer shelf sedimentation: processes and products in The New Concepts of Continental Margin Sedimentation (Stanley, D.J., Ed.); American Geological Institute, Short Course Lecture Notes, p. DS-7-1-DS-7-19.
- Swift, D.J.P. and Rice, D.D., 1984, Sand bodies on muddy shelves: a model for sedimentation in the western interior Cretaceous seaway, North America in Siliciclastic Shelf Sediments (Tillman, R.W. and Seimers, C.T., Eds.); Society of Economic Paleontologists and Mineralogists, Special Publication No. 34, p. 43-62.
- Tilley, B.J. and Last, W.M., 1980, Upper Mannville fluvial channels in east-central Alberta (Abstr.) in Lloydminster and Beyond: Geology of Mannville Hydrocarbon Reservoirs (Beck, L.S., Christopher, J.E. and Kent, D.M., Eds.); Saskatchewan Geological Society, Special Publication No. 5, p. 217.
- Tillman, R.W. and Martinsen, R.S., 1984, The Shannon shelf-ridge sandstone complex, Salt Creek antidune area, Powder River basin, Wyoming in Siliciclastic Shelf Sediments (Tillman, R.W. and Seimers, C.T., Eds.); Society of Economic Paleontologists and Mineralogists, Special Publication No. 34, p. 85-142.

- Tixier, M.P., Alger, R.P. and Doh, C.A., 1959, Sonic logging; *Petroleum Transactions, A.I.M.E.*, Vol. 216, p. 106-114.
- Tixier, M.P., Morris, R.L. and Connell, J.G., 1968, Log evaluation of low resistivity pay sands in the Gulf coast; *Society of Professional Well Log Analysts, Ninth Annual Logging Symposium, Transactions*, 26 p.
- Triplehorn, D.M., 1966, Morphology, internal structure and origin of glauconite pellets; *Sedimentology*, Vol. 6, p. 247-266.
- Truman, R.B., Alger, R.P., Connell, J.C. and Smith, R.L., 1972, Progress report on interpretation of the dual-spacing neutron log (CNL) in the U.S.; *Society of Professional Well Log Analysts, Thirteenth Annual Logging Symposium*, 33p.
- Vigrass, L.W., 1968, Geology of Canadian heavy oil sands; *Bulletin American Association of Petroleum Geologists*, Vol. 52, No. 10, p. 1984-1999.
- Vigrass, L.W., 1977, Trapping of oil at intra-Mannville (Lower Cretaceous) disconformity in Lloydminster area, Alberta and Saskatchewan; *Bulletin American Association of Petroleum Geologists*, Vol. 61, No. 7, p. 1010-1028.
- Vincent, C.E., Swift, D.J.P. and Hillard, B., 1981, Sediment transport in the New York Bight, North American Atlantic shelf; *Marine Geology*, Vol. 42, p. 369-398.
- Walker, R.G., 1979a, Facies and facies models, general introduction in *Facies Models* (Walker, R.G., Ed.); *Geological Association of Canada, Reprint Series 1*, p. 1-7.
- Walker, R.G., 1979b, Shallow marine sands in *Facies Models* (Walker, R.G., Ed.); *Geological Association of Canada, Reprint Series 1*, p. 75-89.
- Webber, H.J., 1967, The oil sands of Alberta; *Journal of Canadian Petroleum Technology*, October-December, p. 146-149.
- Wenneker, J.H.N., Ryckborst, H., Abougoush, M.S., McCreary, R.K.V. and Letkeman, J.P., 1979, Heavy oil, tar sands play key role in Alberta, Saskatchewan production, part 1; *Oil and Gas Journal*, Vol. 77, No. 46, p. 290-304.
- Wickenden, R.T.D., 1948, Lower Cretaceous of the Lloydminster oil and gas area, Alberta and Saskatchewan; *Geological Society of Canada, Paper 48-21*, 15 p.
- Williams, G.D., 1963, The Mannville Group (Lower Cretaceous) of central Alberta; *Bulletin of Canadian Petroleum Geology*, Vol. 11, p. 350-368.

- Williams, G.D. and Stelck, C.R., 1975, speculations on the Cretaceous palaeogeography of North America in *The Cretaceous System in the Western Interior of North America* (Caldwell, W.G.E., Ed.); Geological Association of Canada, Special Paper No. 13, p. 1-20.
- Wilson, M.D. and Pittman, E.D., 1977, Authigenic clays in sandstones: recognition and influence on reservoir properties and paleoenvironmental analysis; *Journal of Sedimentary Petrology*, Vol. 47, No. 1, p. 3-31.
- Woodhouse, R. 1976, Athabasca tar sand reservoir properties derived from cores and logs; *Society of Professional Well Log Analysts, Seventeenth Annual Logging Symposium*, No. 17, 13 p.
- Wyllie, M.R.J. and Rose, W.D., 1950, Some theoretical considerations related to the quantitative evaluation of the physical characteristics of reservoir rock from electrical log data; *Petroleum Transactions A.I.M.E.*, Vol. 189, p. 105-118

## Appendices

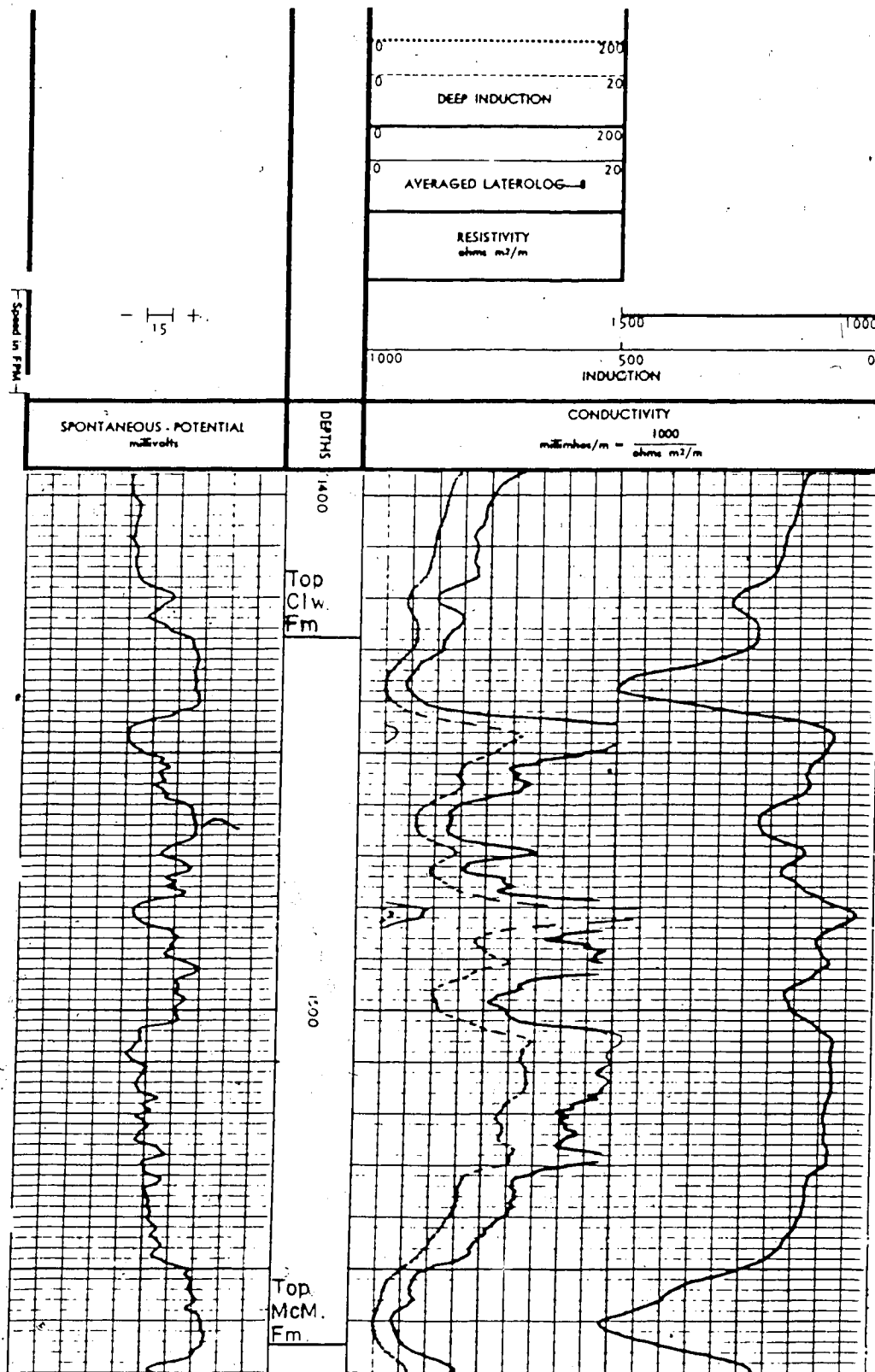
**Appendix I: Geophysical Well Logs for well 10-17-66-5W4**



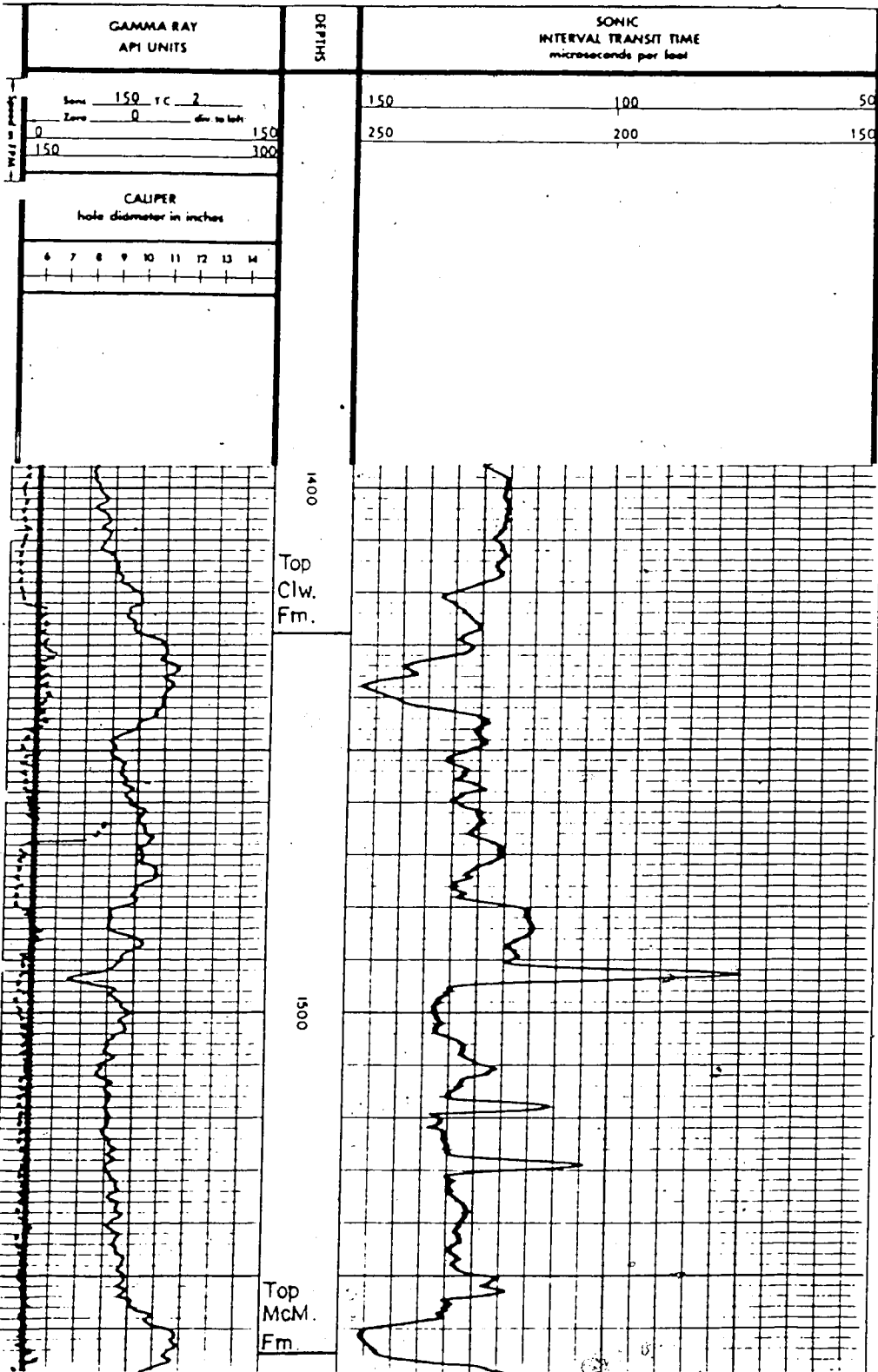
Geophysical Well Log Response of Stratigraphic Units

Strat. Unit	Bulk Density (gm/cc)	Neutron Porosity (%)	Density Porosity (%)	Sonic Porosity (%)	Density Gamma Ray (API units)	Sonic Gamma Ray (API units)	Sonic travel time (microsec/ft)	Spontaneous Potential (millivolts)	Laterolog 8 (Ohms m <sup>2</sup> /m)	Averaged Laterolog 8 (Ohms m <sup>2</sup> /m)	Induction Log Medium (Ohms m <sup>2</sup> /m)	Induction Log Deep (Ohms m <sup>2</sup> /m)	Conductivity 1000 (Ohms m <sup>2</sup> /m)
A	2.150 - 2.200	46.00 - 60.00	22.00 - 30.00	40.32 - 52.99	096.0 - 117.0	078.0 - 097.5	125.5 - 147.5	48.0 - 66.5	03.00 - 07.10	03.60 - 07.20	02.10 - 04.80	01.95 - 04.40	230.0 - 502.0
B	2.070 - 2.150	44.00 - 49.00	30.00 - 34.50	39.17 - 40.32	082.5 - 100.5	059.0 - 080.0	123.5 - 125.5	59.0 - 89.0	07.00 - 11.75	08.00 - 28.00	03.00 - 10.45	04.00 - 12.60	082.0 - 270.0
C	2.050 - 2.110	45.00 - 54.00	33.00 - 35.50	38.59 - 43.49	082.0 - 089.0	060.0 - 071.5	122.5 - 131.0	65.0 - 89.0	09.20 - 11.50	11.70 - 22.76	08.00 - 10.45	07.50 - 11.40	087.0 - 133.0
D <sub>1</sub>	2.100 - 2.245	45.00 - 50.00	24.00 - 32.75	38.02 - 43.20	084.0 - 107.0	068.5 - 087.0	121.0 - 130.5	48.0 - 61.0	06.25 - 11.10	06.90 - 13.50	04.60 - 10.40	04.45 - 07.60	132.0 - 220.0
D <sub>2</sub>	2.215 - 2.225	47.00 - 48.00	25.00 - 28.50	37.73 - 38.59	102.0 - 106.5	077.0 - 078.5	121.0 - 122.5	51.0 - 68.0	07.25 - 10.90	08.00 - 13.70	04.75 - 09.20	05.20 - 07.65	190.0 - 235.0
E	2.120 - 2.250	46.50 - 50.50	24.00 - 32.00	37.15 - 42.62	092.5 - 107.0	067.0 - 086.5	120.0 - 129.5	51.0 - 65.5	07.00 - 10.25	08.30 - 12.00	05.50 - 07.95	05.60 - 09.00	112.0 - 180.0
F <sub>1</sub>	2.130 - 2.210	45.92 - 52.85	28.50 - 31.00	34.27 - 34.85	077.5 - 093.0	059.5 - 069.0	115.0 - 116.0	60.0 - 85.0	08.20 - 15.50	15.20 - 53.00	06.80 - 12.50	10.00 - 28.00	035.0 - 107.0
F <sub>2</sub>	2.065 - 2.280	39.00 - 54.50	26.75 - 35.00	28.51 - 44.64	077.5 - 096.0	061.0 - 080.0	105.0 - 133.0	54.5 - 75.0	08.25 - 12.80	10.40 - 25.00	06.00 - 11.35	06.00 - 15.00	068.0 - 170.0
F <sub>3</sub>	2.060 - 2.150	39.50 - 54.00	26.75 - 35.75	32.26 - 44.93	073.5 - 088.0	055.0 - 071.0	111.5 - 133.5	57.0 - 87.0	09.00 - 11.40	12.00 - 27.00	07.00 - 10.55	07.50 - 13.70	075.0 - 135.0
G	2.039 - 2.220	41.50 - 50.00	24.50 - 36.25	37.15 - 43.49	074.0 - 089.0	058.5 - 068.5	120.0 - 131.0	63.0 - 81.0	10.00 - 12.10	12.25 - 20.00	08.70 - 10.60	08.25 - 12.25	080.0 - 122.0
H	2.075 - 2.180	45.92 - 51.00	31.00 - 34.25	37.15 - 42.62	081.5 - 096.0	062.0 - 073.0	120.0 - 129.5	62.0 - 74.5	07.75 - 10.25	08.00 - 10.25	04.90 - 08.70	04.80 - 08.20	122.0 - 220.0
I	2.220 - 2.320	40.50 - 54.00	20.00 - 29.00	36.29 - 52.13	091.0 - 125.0	069.0 - 103.0	118.5 - 146.0	40.5 - 60.0	03.00 - 07.75	03.40 - 06.70	02.15 - 05.00	02.00 - 04.60	225.0 - 475.0
Calc. Cement	2.108 - 2.503	24.50 - 50.00	07.25 - 33.75	11.23 - 50.11	059.5 - 116.0	037.5 - 090.0	075.0 - 142.5	43.0 - 83.5	03.50 - 12.10	04.00 - 22.00	02.60 - 10.50	02.25 - 13.00	076.0 - 115.0

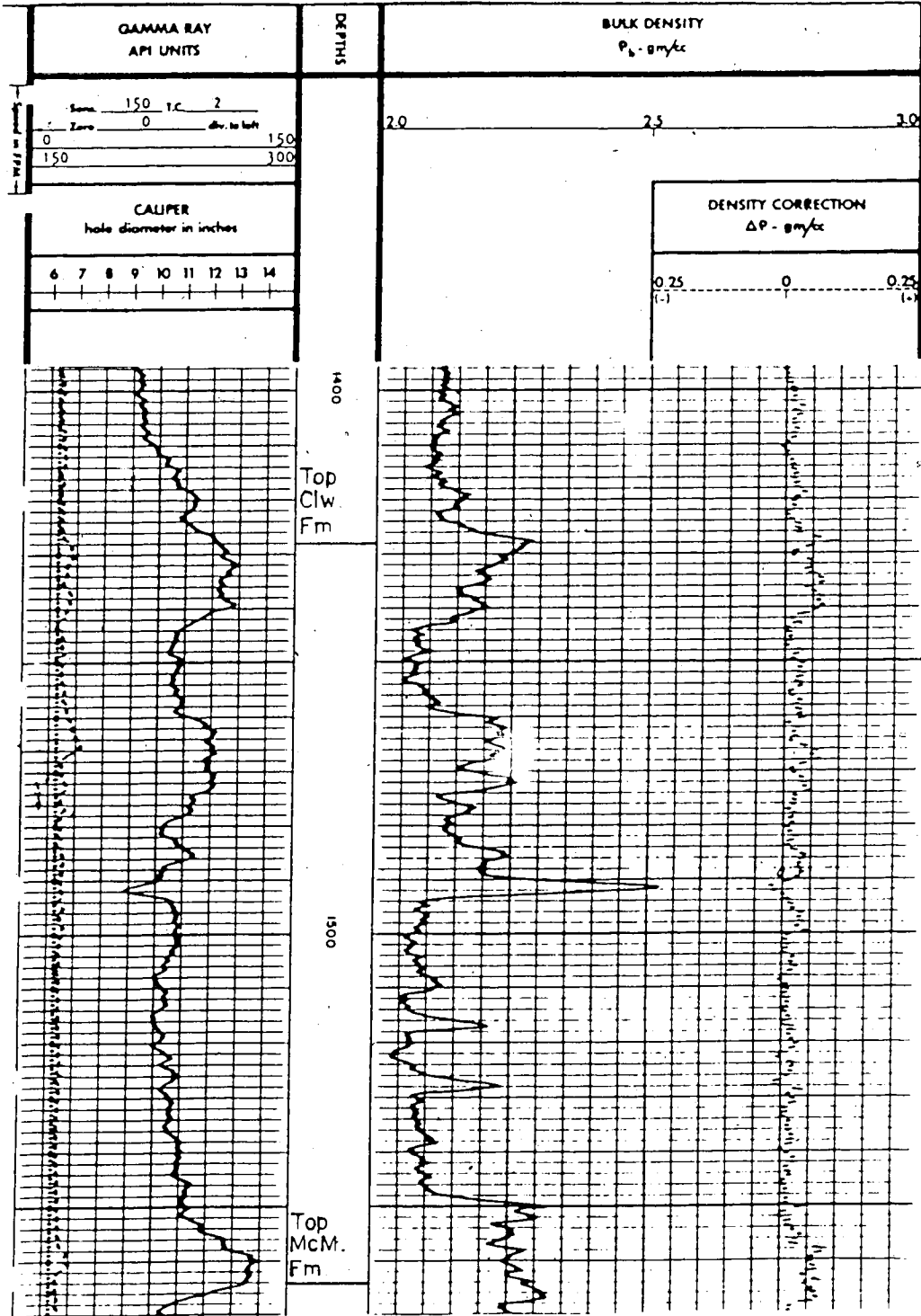
DUAL INDUCTION LATEROLOG



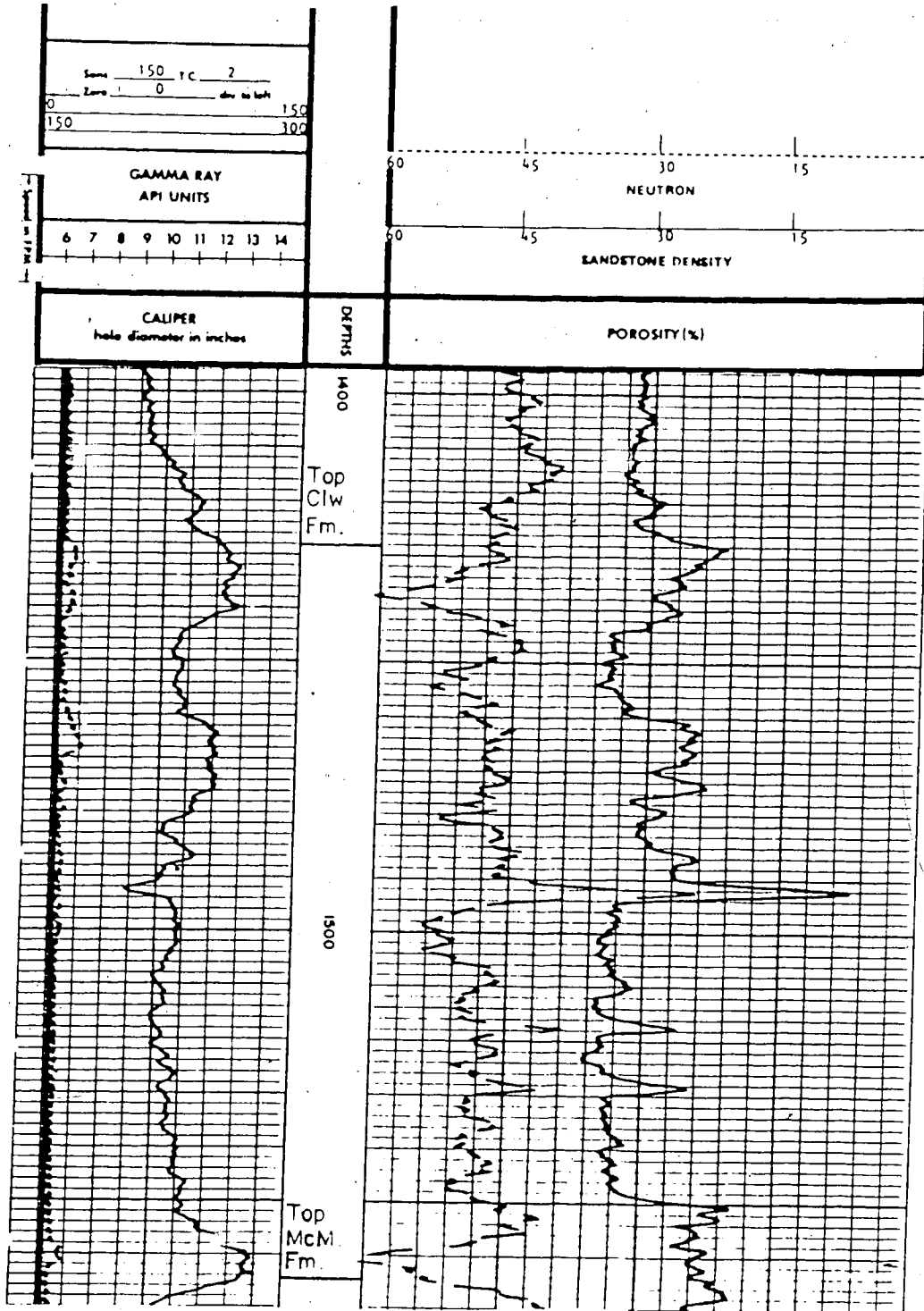
BOREHOLE COMPENSATED SONIC LOG



COMPENSATED NEUTRON — FORMATION DENSITY



COMPENSATED NEUTRON - FORMATION DENSITY: APPARENT SANDSTONE POROSITY



**Appendix II: Point Count and Grain Size Data for Well 10-17-66-5W4**

SAMPLE	DEPTH (feet)	ELEVATION	ROCK FRAGMENTS									
			Un-crystalline Quartz	Chert	Feldspar	Igneous	Volcanic	Metamorphic	Polycrystalline Quartz	Sedimentary	Clastic Carbonates	
80-9-1	1442.0	657.0	16.33	2.33	3.67	6.00	5.33	7.33	10.00	1.67	2.67	
80-9-2	1444.3	654.7	16.33	1.67	5.00	13.33	7.67	4.67	9.33	2.67	0.00	
80-9-3	1447.5	651.5	17.00	3.67	8.33	11.33	4.00	6.33	9.33	1.00	1.00	
80-9-4	1449.5	649.5	14.00	5.67	3.67	0.00	3.33	3.33	11.33	0.67	2.00	
80-9-5	1451.7	647.3	12.33	1.33	2.00	5.33	4.67	4.67	7.67	1.33	1.33	
80-9-6	1452.0	647.0	19.00	6.00	7.33	9.00	8.00	4.33	11.33	1.33	1.67	
80-9-7	1454.2	644.8	14.00	2.00	7.00	7.67	6.67	7.67	7.33	2.33	1.67	
80-4-25	1461.0	638.0	23.33	3.00	2.33	3.67	2.67	9.67	9.33	3.00	4.00	
80-9-11	1467.9	631.1	19.33	5.33	4.33	4.67	3.00	7.33	4.00	4.33	4.00	
80-9-13	1471.2	627.8	6.00	4.33	4.33	1.33	2.00	6.33	5.00	0.67	0.33	
80-9-14	1475.3	623.7	13.67	4.00	4.00	3.00	5.00	8.00	5.67	2.00	2.67	
80-9-16	1478.0	621.0	16.33	3.67	2.67	4.00	2.00	8.33	4.00	4.67	21.00	
75-1-1	1478.5	620.5	22.00	6.67	1.00	3.00	0.67	8.67	10.00	2.33	15.33	
80-9-17	1481.0	618.0	22.67	1.33	3.00	2.33	2.33	9.33	6.33	2.33	24.00	
80-9-18	1484.0	615.0	15.67	5.00	4.00	1.67	2.00	13.67	9.67	3.33	17.00	
80-9-21	1487.8	611.2	23.00	2.33	2.00	2.67	1.00	8.33	7.67	3.33	20.00	
80-9-22	1489.0	610.0	15.00	4.00	4.67	6.00	4.00	9.33	5.00	3.00	10.00	
80-9-23	1490.4	608.6	22.67	6.00	8.67	2.33	3.33	5.00	5.67	2.00	5.67	
75-1-2	1491.0	608.0	12.67	5.33	0.67	0.00	0.00	0.33	6.67	0.00	0.00	
75-1-3	1491.5	697.5	1.33	0.67	0.33	0.00	0.00	0.00	3.33	0.33	0.67	
75-1-4	1492.7	606.3	24.00	4.33	4.67	0.33	1.33	2.00	12.33	0.67	0.33	

SAMPLE	DEPTH (feet)	ELEVATION	Unicrystalline Quartz	Chert	Feldspar	ROCK FRAGMENTS					
						Igneous	Volcanic	Metamorphic	Polycrystalline Quartz	Sedimentary	Clastic Carbonates
80-9-24	1495.8	603.2	18.67	4.00	5.33	2.00	3.67	7.00	5.33	2.67	0.67
80-9-25	1501.2	597.8	21.00	6.33	4.67	3.00	6.33	8.00	10.00	1.67	1.67
80-9-26	1505.0	594.0	21.67	3.33	5.67	6.33	3.33	8.00	5.00	2.00	1.67
75-1-5	1510.0	589.0	18.33	6.33	4.00	0.67	4.33	4.67	18.67	2.67	0.00
75-1-6	1510.1	588.9	15.67	6.00	2.33	0.33	1.00	4.00	22.00	1.33	0.33
80-9-27	1511.8	587.2	18.67	6.00	4.67	5.67	6.33	12.00	10.67	2.67	2.33
80-9-28	1515.0	584.0	19.67	5.33	9.00	1.67	3.00	7.33	7.33	1.67	3.67
75-1-7	1517.0	582.0	14.67	5.33	1.33	2.33	2.67	2.67	6.67	5.00	0.67
80-9-29	1518.4	580.6	13.00	2.33	7.33	5.67	4.33	9.33	6.00	2.00	1.33
80-9-30	1522.0	477.0	17.33	3.00	9.00	6.67	2.67	7.67	10.33	3.33	0.67
80-9-31	1526.0	573.0	19.67	4.67	5.67	1.67	3.00	6.33	11.67	0.67	0.67
80-9-32	1527.5	571.5	15.33	2.33	4.33	2.00	1.67	3.00	7.33	2.67	1.00
80-9-33	1532.5	566.5	21.33	6.33	8.33	3.33	6.00	6.67	12.33	0.67	2.00
80-9-34	1534.0	565.0	18.67	4.33	5.00	1.67	1.33	5.00	11.33	1.67	2.00
80-9-35	1542.5	556.5	23.33	3.67	7.33	3.00	4.00	6.67	9.00	1.67	5.00
80-9-36	1549.1	549.9	16.33	2.00	7.33	2.67	4.00	7.00	10.33	1.67	1.33
80-9-37	1550.1	548.9	18.33	2.67	8.67	4.00	2.00	9.33	11.67	0.67	1.67
80-9-38	1551.3	547.7	18.33	4.33	4.67	0.33	2.67	1.00	6.33	3.00	0.00
80-4-27	1552.3	546.7	6.33	1.67	2.00	0.00	1.33	0.67	5.33	0.67	1.00
80-9-39	1555.8	543.2	10.67	2.33	4.33	0.33	1.00	3.00	2.67	1.00	0.00



SAMPLE	Glauconite	Calcareous Cement	Organics	Mica and Chlorite	Zircon	Oil and/or Clay	Opagues (Pyrite)	Undifferentiated Matrix	Quartz Overgrowths	Pore Space	Unidentified Rock Fragments
80-9-1	2.00	0.00	6.33	1.00	2.00	23.67	1.00	0.67	1.33	6.67	0.00
80-9-2	1.67	0.00	6.67	1.33	2.33	19.00	1.00	0.33	1.67	4.67	0.67
80-9-3	2.67	0.00	5.67	0.67	3.67	18.33	0.00	2.00	0.67	4.33	0.00
80-9-4	0.33	0.00	8.33	0.67	0.33	0.33	0.00	43.67	0.00	2.00	0.33
80-9-5	1.33	0.00	32.67	1.33	0.00	4.00	15.00	0.33	0.33	4.33	0.00
80-9-6	1.00	0.00	4.00	0.67	2.33	14.00	0.67	4.67	0.00	4.00	0.67
80-9-7	1.67	0.00	2.00	0.00	0.33	33.67	1.00	0.00	0.67	3.67	1.00
80-4-25	2.33	0.00	9.67	4.33	0.33	5.00	5.67	2.67	1.00	7.00	1.00
80-9-11	10.00	0.00	7.33	1.00	0.67	10.33	1.00	2.00	2.00	7.67	0.00
80-9-13	3.33	0.00	2.00	2.00	0.00	0.33	1.67	57.33	0.00	2.00	0.00
80-9-14	6.00	0.00	4.33	1.00	2.67	7.67	1.00	2.67	0.33	8.00	0.33
80-9-16	4.67	0.00	4.00	0.33	1.00	11.67	0.33	0.00	1.00	9.33	0.67
75-1-1	2.00	0.00	9.00	0.67	0.33	12.67	0.00	0.33	1.00	3.33	0.33
80-9-17	4.33	0.00	2.00	1.33	0.33	12.67	0.33	1.00	1.00	3.00	0.00
80-9-18	4.00	0.33	2.00	2.00	0.33	14.00	0.33	0.33	1.33	3.33	0.00
80-9-21	5.00	0.00	7.67	0.67	0.00	3.33	0.33	6.67	0.33	5.67	0.33
80-9-22	7.33	0.00	5.67	0.67	0.33	15.67	1.33	1.00	0.00	7.00	0.00
80-9-23	4.00	0.00	3.67	2.33	0.33	12.00	1.00	5.67	0.33	7.67	0.67
75-1-2	0.33	61.33	10.33	0.67	0.00	0.00	0.67	0.00	0.00	1.00	0.00
75-1-3	0.00	62.67	28.67	0.00	0.00	0.00	2.00	0.00	0.00	0.00	0.00
75-1-4	0.67	24.67	8.33	0.00	0.33	12.00	0.00	0.00	0.00	4.00	0.00

SAMPLE	Glauconite	Calcareous Cement	Organics	Mica and Chlorite	Zircon	Oil and/or Clay	Opagues (Pyrite)	Undifferentiated Matrix	Quartz Overgrowths	Pore Space	Unidentified Rock Fragments
80-9-24	0.67	0.00	20.00	2.00	1.00	4.00	0.33	17.00	0.33	5.33	0.00
80-9-25	0.33	0.00	0.67	1.67	3.33	22.00	0.00	3.67	0.00	5.00	0.67
80-9-26	2.67	0.00	2.67	1.33	2.33	26.00	0.00	0.00	1.67	6.33	0.00
75-1-5	2.67	23.67	1.67	0.67	0.33	9.67	0.33	0.00	0.33	0.33	0.67
75-1-6	1.00	36.33	2.00	1.00	0.33	4.67	0.00	0.00	0.67	1.00	0.00
80-9-27	1.33	0.00	1.33	1.67	1.00	17.67	0.00	0.33	0.00	7.33	0.33
80-9-28	1.33	0.00	3.33	0.33	6.33	20.33	0.00	4.33	0.33	4.67	0.33
75-1-7	1.67	54.00	1.00	0.67	0.00	0.00	1.00	0.00	0.33	0.00	0.00
30-9-29	2.00	0.00	24.67	1.00	0.00	6.00	0.00	7.00	1.00	6.67	0.33
80-9-30	2.00	0.00	5.00	0.67	0.67	19.67	0.00	6.33	1.33	3.33	0.33
80-9-31	1.00	0.00	9.67	1.67	0.00	3.00	0.00	29.67	0.00	1.33	0.00
80-9-32	2.67	32.33	13.33	2.33	0.67	5.33	0.67	0.67	0.33	2.00	0.00
80-9-33	1.67	0.00	3.00	2.33	1.33	16.33	0.67	4.33	0.00	3.33	0.00
80-9-34	3.33	1.00	1.67	0.67	2.00	21.33	0.33	7.67	0.67	9.33	1.00
80-9-35	3.00	0.00	9.33	1.33	0.00	8.67	0.00	5.00	1.67	7.00	0.33
80-9-36	1.33	0.00	4.67	2.67	0.33	4.33	0.00	27.67	1.00	6.33	0.00
80-9-37	1.33	0.00	4.33	0.00	0.67	24.00	0.00	4.67	1.67	4.00	0.33
80-9-38	1.33	43.33	5.00	0.67	0.00	3.67	0.00	0.00	1.00	4.33	0.00
80-4-27	0.33	0.00	5.67	0.00	0.00	0.00	0.00	74.67	0.00	0.33	0.00
80-9-39	1.00	56.67	12.33	1.33	0.00	0.33	1.67	0.00	0.00	1.33	0.00

SAMPLE	Mode	Median	Mean	Standard Deviation	Skewness	Kurtosis	Percent Sand	Percent Silt	Percent Clay
80-9-1	3.25	3.85	3.16	1.10	0.42	1.86	90.72	8.60	0.68
80-9-2	3.25	2.80	3.25	1.54	0.06	3.77	91.47	6.23	2.30
80-9-3	3.75	3.16	3.36	1.31	0.23	2.22	92.18	6.18	1.65
80-9-4	4.25	3.76	4.75	2.85	0.59	1.51	58.24	30.76	11.00
80-9-5	3.75	3.36	3.81	1.74	0.51	2.47	74.93	22.99	2.02
80-9-6	3.75	3.21	3.44	1.39	0.24	2.03	88.61	9.52	1.87
80-9-7	3.25	3.07	3.48	1.76	0.07	9.27	88.51	8.75	2.74
80-9-11	3.75	3.29	3.91	1.97	0.59	2.23	74.40	21.69	3.92
80-9-13	9.75	6.83	6.64	3.57	0.05	0.62	43.98	22.50	33.52
80-9-14	3.75	3.44	4.20	2.07	0.71	5.87	79.66	14.46	5.88
80-9-16	4.25	3.75	3.98	1.09	0.34	3.94	83.02	16.00	0.98
80-9-17	4.25	3.72	3.91	1.06	0.34	2.64	81.76	17.40	0.84
80-9-18	4.25	3.66	3.67	0.95	-0.05	2.22	88.16	11.34	0.50
80-9-21	7.00	5.22	5.72	3.10	0.33	1.09	42.89	40.94	16.17
80-9-22	3.75	3.16	3.43	1.56	0.20	1.60	86.55	11.61	1.84
80-9-23	7.25	4.43	5.76	2.89	0.60	0.84	46.04	37.72	16.24
80-9-24	3.75	4.17	5.40	2.77	0.66	1.07	46.66	40.52	12.82
80-9-25	3.75	3.23	3.46	1.34	0.35	3.22	88.16	10.21	1.63
80-9-26	3.75	3.21	3.39	1.14	0.21	2.13	91.85	7.31	1.02
80-9-27	3.75	3.30	3.77	1.56	0.56	2.65	78.50	19.30	2.20

SAMPLE	Mode	Median	Mean	Standard Deviation	Skewness	Kurtosis	Percent Sand	Percent Silt	Percent Clay
80-9-28	3.75	3.43	3.79	1.33	0.44	2.17	82.45	15.78	1.77
80-9-29	3.75	3.32	3.71	1.34	0.52	2.60	85.57	12.78	1.66
80-9-30	3.75	3.31	3.86	1.62	0.66	3.16	32.73	14.52	2.75
30-9-31	3.75	3.64	4.78	2.72	0.69	1.39	62.67	26.67	10.66
80-9-32	4.25	4.22	4.97	2.60	0.46	0.69	45.52	46.06	8.42
80-9-33	3.75	3.29	3.58	1.22	0.42	2.19	85.02	13.80	1.18
80-9-34	3.75	3.41	3.95	1.85	0.57	3.05	81.66	14.18	4.16
80-9-35	3.75	3.42	4.15	1.87	0.26	3.09	76.16	19.40	4.45
80-9-36	3.75	3.50	4.42	2.05	0.79	2.14	64.64	29.48	5.88
80-9-37	3.75	3.31	4.06	1.88	0.73	3.10	77.42	18.46	4.12
80-4-27	3.75	7.04	7.20	4.01	0.25	0.64	37.37	23.71	38.92

**Appendix III: Calculation of Parameters Generated from Geophysical Well Log Data**

The values obtained from the digitization of the geophysical well logs were used to generate parameters for shaly sand analysis.

The equations used to obtain these values are as follows:

$$(1) \quad M = \frac{\Delta_{tf} - \Delta_t}{\rho_b - \rho_f} \times 0.01$$

$$(2) \quad N = \frac{\phi_N - \phi_{Nf}}{\rho_b - \rho_f}$$

$$(3) \quad \phi_S = \frac{\Delta_t - \Delta_{ma}}{\Delta_{mf} - \Delta_{ma}} \times C_p$$

$$(4) \quad \text{Gamma Ray Index} = \frac{GR - GR_{cl}}{GR_{sh} - GR_{cl}}$$

$$(5) \quad \text{Bulk Volume Clay Fraction} = \phi_c - \phi_e$$

$$(6) \quad \text{Calculated Effective Porosity} = (1 - q) \phi_c$$

$$(7) \quad q = \frac{\phi_S - \phi_D}{\phi_S}$$

$$(8) \quad \text{Bulk Volume Oil} = \left( \frac{\text{wt. \% oil}}{\text{wt. \% oil} + \text{wt. \% water}} \right) \cdot \phi_c$$

$$(9) \quad \text{Bulk Volume Water} = \left( \frac{\text{wt. \% water}}{\text{wt. \% oil} + \text{wt. \% water}} \right) \cdot \phi_c$$

where:  $\Delta_{tf}$  = sonic travel time for fluid (assumed 189 microsec/ft)

$\Delta_t$  = sonic travel time for point in question

$\rho_b$  = bulk density for point in question

$\rho_f$  = bulk density of the fluid (assumed 1.0 gm/cc)

$\phi_N$  = neutron porosity of point in question

$\phi_{Nf}$  = neutron porosity of fluid (assumed 100.0 percent)

$\phi_S$  = corrected sonic porosity of point in question

$\Delta_{ma}$  = sonic travel time for matrix: clean quartz sand  
(assumed 55 microsec/ft)

$\Delta_{mf}$  = sonic travel time for mud filtrate  
(assumed 189 microsec/ft)

$C_p$  = Compaction Correction:  $\frac{\text{sonic travel time of formation shale}}{100} =$

$$\frac{130}{100} = 1.3$$

GR = gamma ray value for point in question

$GR_{cl}$  = gamma ray value for clean quartz sand (assumed 20 API units)

$GR_{sh}$  = gamma ray value for shale (132 API units)

$\phi_c$  = core porosity

$\phi_e$  = effective porosity

q = volume of dispersed shale

$\phi_D$  = density porosity of point in question